

arXiv:1906.05111v2 [cs.RO] 17 Jun 2019

---

---

# Co-modelling of Agricultural Robotic Systems

---

---

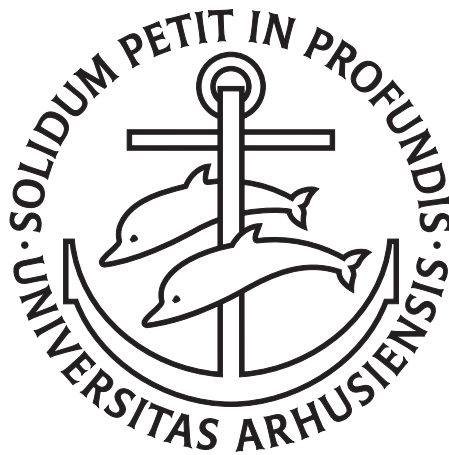
PhD Dissertation  
Martin Peter Christiansen  
June, 2015



AARHUS  
UNIVERSITY  
DEPARTMENT OF ENGINEERING



# Co-modelling of Agricultural Robotic Systems



A Dissertation  
Presented to the Faculty of Science and Technology  
of the University of Aarhus  
in Partial Fulfilment of the Requirements for the  
PhD Degree

by  
Martin Peter Christiansen  
June 17<sup>th</sup>, 2015





---

## Abstract

---

Automated and robotic ground-vehicle solutions are gradually becoming part of the agricultural industry, where they are used for performing tasks such as feeding, herding, planting, harvesting, and weed spraying. Agricultural machinery operates in both indoor and outdoor farm environments, resulting in changing operational conditions. Variation in the load transported by ground-vehicles is a common occurrence in the agricultural domain, in tasks such as animal feeding and field spraying. The development of automated and robotic ground-vehicle solutions for conditions and scenarios in the agricultural domain is a complex task, which requires input from multiple engineering disciplines. This PhD thesis proposes modelling and simulation for the research and development of automated and robotic ground-vehicle solutions for purposes such as component development, virtual prototype testing, and scenario evaluation. The collaboration of multiple engineering disciplines is achieved by combining multiple modelling and simulation tools from different engineering disciplines. These combined models are known as co-models and their execution is referred to as co-simulation. The results of this thesis are a model-based development methodology for automated and robotic ground-vehicles utilised for a number of research and development cases. The co-models of the automated and robotic ground vehicles were created using the model-based development methodology, and they contribute to the future development support in this research domain. The thesis presents four contributions toward the exploration of a chosen design space for an automated or robotic ground vehicle. Solutions obtained using co-modelling and co-simulation are deployed to their ground-vehicle realisations, which ensures that all stages of development are covered.



---

## Resume

---

Robotkøretøjs-løsninger, som har til opgave at forbedre effektiviteten og produktiviteten, er gradvist ved at blive en del landbrugssektoren. Disse køretøjer bliver anvendt til driftsopgaver inden for husdyrshold som dyrefodring og hyrdeopgaver samt markarbejde såsom såning, og høst og ukrudtsbekæmpelse. Landbrugskøretøjerne har forskellige driftsbetingelser da de opererer både indenfor og udenfor. I mange driftsopgaver der udføres af et køretøj i landbrugssektoren, transporteres der en last der ændrer sig undervejs, så som dyrefodring hvor der bliver mindre foder efterhånden som der udfodres eller marksprøjtning hvor tank-indholdet løbende fordeles over marken. Udvikling af robotkøretøjs-løsninger til forholdene i landbruget er en kompliceret opgave, der kræver samspil imellem flere forskellige ingeniørdiscipliner.

Til forskning og udvikling af robotkøretøjer til landbruget foreslår denne ph.d.-afhandling modellering og simulering, som kan anvendes til komponentudvikling, test af virtuelle prototyper og evaluering af scenarier. Til samarbejdet imellem ingeniørdisciplinerne kombineres modellerings- og simuleringsværktøjer fra de forskellige discipliner. Disse kombinerede modeller er kendt som co-modeller og deres udførelse co-simulering.

Resultatet af denne afhandling er en model-baseret udviklingsmetode til robotkøretøjs-løsninger til landbruget og en række co-modellerede forsknings- og udviklingsprojekter inden for dette domæne. De co-modellerede projekter er blevet til ved hjælp af den model-baserede udviklingsmetode som bidrager og yder support til effektiv videreudvikling af robotkøretøjer til landbruget. Der præsenteres fire forskellige metode-bidrag til udforskningen af et brugerdefineret designrum for co-modeller af et givet robotkøretøj. Løsninger fundet ved brug af co-modellering og co-simulering er blevet implementeret på de reelle køretøjer, så alle trinene fra koncept til endelig løsning er dækket.



---

## Acknowledgments

---

This PhD research project would not have been possible without the financial funding provided by the Danish Ministry of Food, Agriculture, and Fisheries, which is gratefully acknowledged. A great number of people were important to the completion of this dissertation, as their support, guidance, and assistance made this research project possible. I would like to thank my supervisors, Senior Researcher Ole Green, Professor Peter Gorm Larsen, and Senior Researcher Rasmus Nyholm Jørgensen. Each of these individuals has acted as my main supervisor at different stages of my PhD research project. Their different approaches to supervision have had a significant impact on both my research and my personal development.

I would like to acknowledge current and former colleagues at the Department of Engineering, Aarhus University, who provided me with aid, support and knowledge. Special thanks are due to Kenneth Lausdahl, Kim Steen, Morten Stigaard Laursen, Morten Larsen, José Antonio Esparza Isasa, Peter W. V. Jørgensen, and Sune Wolf for their camaraderie and discussions on various scientific subjects. I also wish to thank Søren Hansen for introducing me to academic instruction and teaching, Ole Balling for discussing the topic of vehicle dynamics, and Michael Nørremark for discussions on automation in agriculture. Thanks are due to all of you for your assistance.

For their collaboration on joint work described in this thesis, I thank my co-authors: Rasmus Nyholm Jørgensen, Peter Gorm Larsen, Ole Green, Gareth Edwards, Morten Larsen, Kim Bjerre, Dionysis Bochtis, and Claus Aage Grøn Sørensen.

I wish to express my gratitude to Christian Kleijn, Paul Weustink, Frank Groen, and Marcel Groothuis from the company, Controllab Products B.V., for providing me with the opportunity to visit them in Enschede, Netherlands, to gain further insight into the 20-sim modelling technology. I also wish to thank Tom Simonsen and Han Knutson from Conpleks Innovation in Struer, Denmark, for allowing me to work on the FixiRobo Mink-feeder project in my half-year leave period from my PhD studies.

On a more personal level, I would like to thank my girlfriend, Mette Fredsted Gram, for all her support, love, encouragement, and understanding throughout my PhD studies. She provided continual motivation and encouragement for me to challenge myself academically, along with support when the research work became too overwhelming. Thanks are also due to my sister and brother, Anja Elisabeth Søndergaard Christiansen and Holger Erik Christiansen, for their support and encouragement.

*Martin Peter Christiansen*  
Aarhus, June 2015

---

## Abbreviations

---

The abbreviations used in this thesis are listed below.

<b>Abbreviation</b>	<b>Full Term</b>
ASuBot	Aarhus and Southern Denmark University robot
ACA	Automated co-model analysis
CT	Continuous-time
CG	Center of Gravity
DE	Discrete event
DEST ECS	Design support and tooling for embedded control software
DOF	Degrees of freedom
DSE	Design space exploration
EKF	Extended kalman filter
FMI	Functional mock-up interface
GNSS	Global navigation satellite system
GPS	Global positioning system
ID	Identification data
IMU	Inertial measurement unit
ODE	Ordinary differential equation
RFID	Radio frequency identification
RSSI	Received signal strength indicator
ROS	Robot operating system
RTK-GPS	Real time kinematic GPS
SDP	Shared design parameter
VDM	Vienna development method
QR	Quick response
XTE	Cross track error





---

## Contents

---

<b>Abstract</b>	<b>i</b>
<b>Resume</b>	<b>iii</b>
<b>Acknowledgments</b>	<b>v</b>
<b>Abbreviations</b>	<b>vii</b>
<b>I Summary</b>	<b>1</b>
<b>1 Introduction</b>	<b>3</b>
1.1 Automated and Robotic Agricultural Ground Vehicles . . . .	5
1.2 Modelling and Simulation . . . . .	9
1.3 Motivation . . . . .	11
1.4 Research Objectives . . . . .	12
1.5 Research Methods . . . . .	13
1.6 Evaluation Criteria . . . . .	14
1.7 Academic Work . . . . .	15
1.8 Outline and Reading Guide . . . . .	17
<b>2 Modelling and Simulation of Automated and Robotic Agricultural Vehicles</b>	<b>19</b>
2.1 Approaches to Co-modelling and Co-simulation . . . . .	19
2.2 Extended Development Methodology . . . . .	21
2.3 Case Study: The LEGO Micro-Tractor Platform . . . . .	24
2.4 Case Study: Common Agricultural Ground-vehicle Platforms.	29
2.5 Case Study: Animal Feeding System . . . . .	34
2.6 Deployment . . . . .	38
2.7 Summary . . . . .	40

<b>3</b>	<b>Design Space Exploration</b>	<b>41</b>
3.1	Design Space Exploration Concepts . . . . .	42
3.2	Alternative Design Configurations . . . . .	43
3.3	Derivation of a New Design Idea from the Creative Process .	47
3.4	Exploring Controller Solutions . . . . .	52
3.5	Obtaining a Multidisciplinary Solution Overview using DSE	58
3.6	Summary . . . . .	62
<b>4</b>	<b>Concluding Remarks</b>	<b>63</b>
4.1	Research Contributions . . . . .	63
4.2	Evaluation of Contributions . . . . .	67
4.3	PhD Project Hypothesis Validation . . . . .	70
4.4	Future Work . . . . .	71
	<b>Bibliography</b>	<b>79</b>
<b>II</b>	<b>Publications</b>	<b>87</b>
<b>1</b>	<b>Towards a Methodology for Modelling and Validation</b>	<b>89</b>
<b>2</b>	<b>Adaptive Controller Settings for a Load-carrying Vehicle</b>	<b>99</b>
<b>3</b>	<b>Planned Field Operations using LEGO Mindstorms NXT</b>	<b>109</b>
<b>4</b>	<b>Patent Application</b>	<b>125</b>
<b>5</b>	<b>Candidate Overview using Co-model Driven Development</b>	<b>161</b>
<b>6</b>	<b>Multidisciplinary Robotic Design Space Exploration</b>	<b>169</b>

# **Part I**

## **Summary**



# 1

---

## Introduction

---

The development of complex systems regularly involves many project stakeholders from different disciplinary backgrounds. The project stakeholders are the group of individuals who are actively involved in the project and who may exert influence over the project development, objectives, and outcome. These stakeholders typically have different points of view on the problem they are addressing, the system being developed, and the process by which it is being developed. In this context, a system is a group of interacting or independent components forming a coherent whole. The development of such a system is, therefore, a highly interactive process involving overlapping problems, along with the collaboration of stakeholders designing interrelated components and making coupled decisions [36]. The well-known tree-swing illustration shown in Figure 1.1 demonstrates the dangers and failures that can be encountered if stakeholders do not communicate with each other and their customers when developing a product.

Even different engineering disciplines, such as software, electrical, and mechanical engineering, have different perspectives or points of view on a system design. Further, the engineering disciplines have developed different concepts and theories to approach product and system development. In general, however, an engineer will try to determine the purpose behind a task, to help ensure that the development process is on target. Focusing on a single engineering discipline or skill area will not meet future needs for product development. Engineering disciplines should be perceived as overlapping and interconnected rather than constituting separate fields of knowledge [69].

Industry demand exists for engineers who can collaborate with project stakeholders outside of their own discipline. Development involving multidisciplinary teams are intended to provide innovative new solutions and to improve the multidisciplinary thinking of developers. Multidisciplinary collaboration also allows product design to be understood from multiple viewpoints

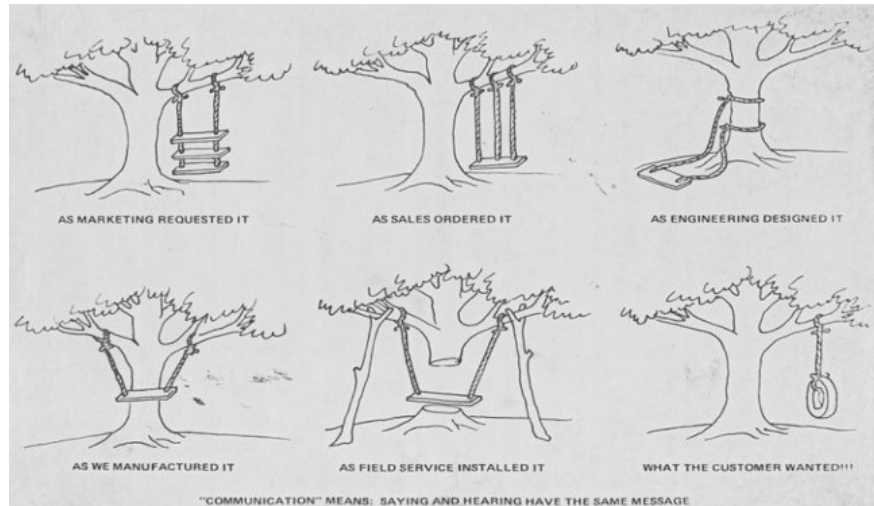


Figure 1.1: 1970's tree swing picture concerning communication<sup>1</sup>

and provides team members with the ability to understand the significant design constraints affecting the other disciplines [59].

### Mechatronics and Robotics

Mechatronics is an engineering field that is heavily dependent on skills from multiple disciplines. The word mechatronics was coined by Tetsuro Mori in 1969, and is a combination of the words “mechanics” and “electronics” [8, Foreword]. Today, mechatronics combines the areas of control, computer, mechanical and electrical engineering [7, 51]. Mechatronics contains sub-fields such as automation, consumer products, machine vision, and robotics, where the former and latter are the focus here. The term “robot” was first used in 1923 in a play entitled R.U.R [13],[74, Preface] by Karel Capek. Here, R.U.R. represents Rossum’s Universal Robots.

The areas of automation and robotics tend to overlap, with robotics systems having the ability to perform similar tasks that may differ in terms of objects, distances and other variables. Automation and robotics engineering projects can be found in most areas of industry and related academic areas. The examples in Figure 1.2 illustrate the broad application of automation and

<sup>1</sup> Source: <http://www.businessballs.com/treeswing.htm>. Last accessed: 08-06-2015.



Figure 1.2: Multidisciplinary automated and robotic engineering system examples from various industry areas: prototyping (a); marine conservation (b); and space exploration (c).

robotics. They show use in prototype production (Cartesian plotter), material dredging from the seabed, and exploration of the Mars surface. Robotics systems are diverse in their applications, but all such systems share three similarities, in the form of electronic components, mechanical constructs and software code.

To narrow the scope of this project on multidisciplinary automation and robotics development, it was decided to focus this thesis on applications in the mobile agricultural ground-vehicle domain. The intention is to accommodate the multidisciplinary view when developing an agricultural ground-vehicle system. Note that the concepts presented in this PhD thesis may be applicable to other industry areas involving multidisciplinary mechatronics development.

## 1.1 Automated and Robotic Agricultural Ground Vehicles

The introduction of robotics and automated precision agriculture machinery provides a means of improving efficiency and productivity. Research and development to improve machine efficiency and production output has been on-going for several decades [54, 60, 67, 71, 91], and such development efforts have resulted in various commercial products for industry [26, 40]. The automated and robotic vehicles use localisation systems such as Global navigation satellite system (GNSS) for automated steering in the environment and perform tasks such as field spraying and animal feeding. Partially and

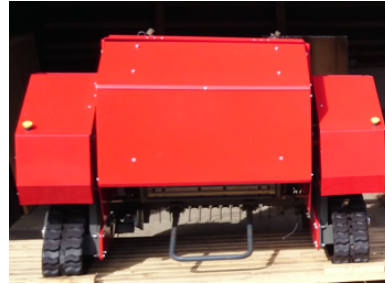
<sup>2</sup> Source: Picture by Marcel A. Groothuis [41].

<sup>3</sup> Source: [34].

<sup>4</sup> Source: [34].



(a) Robotic mink-feeding system<sup>5</sup> mounted on a manually operated vehicle.



(b) Grass-collector robot<sup>6</sup> from the Grassbots EU FP7 project.

Figure 1.3: Examples of robotics systems in the agricultural industry.

fully automated systems have been developed for most phases of agricultural operation, from feeding to herding, planting to harvesting, and for packaging and boxing.

Today, one can encounter automated and robotic agricultural systems that are either add-ons to manually operated vehicle systems or fully robotics-focused redesigns. Figure 1.3 illustrates two examples of robotics systems intended for the agricultural industry. The use of fully robotic platforms is a direct leap towards robotic and autonomous automation, which is intended to provide new approaches to overall design and utilisation. In contrast, the add-on approach to development of an already operational mobile vehicle aims to provide incremental system improvements by gradually adding automation functionality. The concept here is that greater functionality can be obtained by adding control and software intelligence, rather than by improving on well-known mechanical designs. For example, agricultural machines such as tractors are used with several various implements for different operational tasks, yielding highly modular systems that may require online changes of their control parameters. Implementing controllers for these modular systems is a complex task, as they are used for a number of specific purposes.

### Development and Testing

Like the tree-swing illustration in Figure 1.1, different stakeholders can have different points of view on the automated or robotic agricultural system they

<sup>5</sup> Source: Picture of a Minkpapir A/S vehicle solution, Conpleks Innovation.

<sup>6</sup> Source: Picture of a Kongskilde Industries A/S vehicle solution, Conpleks Innovation.



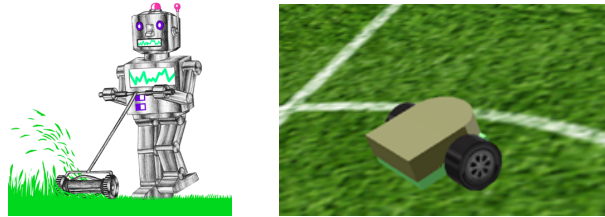


Figure 1.4: Examples of different stakeholder perceptions<sup>7</sup> of robots for cutting grass.

are developing. Even the overall envisaged concept of a specific agricultural robotic system can differ between stakeholders in a development team that is communicating internally. When a project team is assigned the task of developing a robot for grass cutting, the different members might envision solutions such as those illustrated in Figure 1.4. The above example is an extreme case, but it illustrates some of the problems stakeholders can encounter when they are collaborating on developing a system. Visual imagery can provide a means of establishing an improved common understanding between different stakeholders in a project, and also provide clarification of the intended direction of the project.

One of the main obstacles developers must overcome is comparison between different system setups. Various testing methods for development and evaluation have been proposed in the literature for sensors [25, 38] and control system operation [28, 75]. Reproducible scenarios are difficult to obtain in an agricultural setting, because of the semi-controlled outdoor environment, which is in contrast with the controlled surroundings of the manufacturing industry. Geographical conditions influence operation and vary in response to weather and terrain conditions [29, 43]. Prior history from weather and farm operation influences the terrain and soil conditions [64, 78]. However, the focus of the developers is to produce the desired machinery response in these semi-controllable conditions.

Robotic and automated systems can perform operations that are both open- or closed-loop in nature. Compared to open-loop control, a closed-loop control utilises feedback to compare the actual output to the desired response. Many control tasks in agriculture are closed-loop in nature, as the input/outputs of the system are tightly coupled; making it a challenge to

<sup>7</sup> Source: Robot illustration by Mette Fredsted Gram.

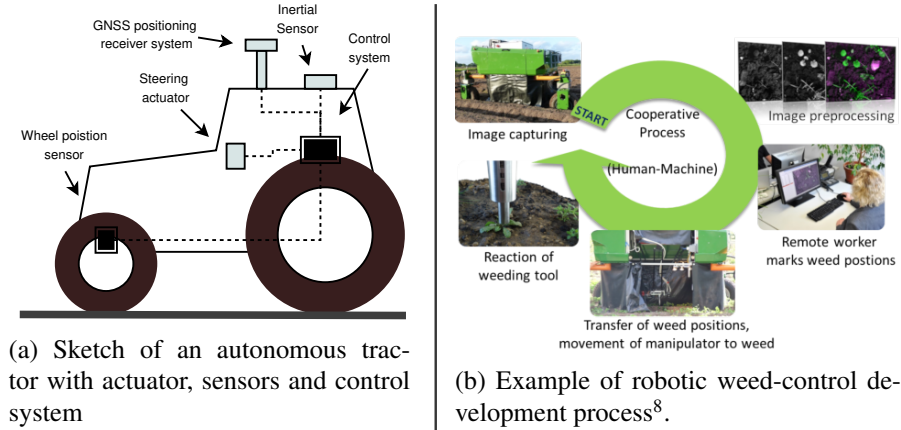


Figure 1.5: Illustration of two automated or robotic agricultural ground-vehicle systems, where coupling between the control components differ.

develop components independently. An example of closed-loop control is the GNSS-based steering system for a tractor illustrated in Figure 1.5a, where the movement in the environment is managed by the controller, based on sensory feedback. Evaluating different control strategies for the intended automated or robotic ground vehicle requires field testing to compare their effectiveness. Because of the semi-controllable outdoor environment testing conditions, the control responses differ between field runs, making direct comparison a challenge.

Robotic weed control in farming is based on sensory input from vision systems [77, 79]. In Figure 1.5b, a remote worker marks the positions of weeds in the captured images and transmits them to the weeding tool. In this case, a vision sensor is used for detection meaning that the overall process is open-loop. The remote worker's marking of weed positions is stored as a base reference and used to evaluate updates to the automated weed-detection algorithms. The illustrated robotic weed-control development process allows for decoupled development between the sensory input processing and the actuation system intended to handle the treatment of weeds. The system decoupling and remote worker setup allows the system to be developed gradually with an increasing level of automation. Having a similar decoupled development process for the control of closed-loop automated or robotic agri-

<sup>8</sup> Source: Figure by Fabian Sellmann [79].

cultural ground-vehicle systems would allow developers to develop subtasks independently.

## 1.2 Modelling and Simulation

A model provides the developer with a tool to experiment with system design parameters and configurations. The concepts of modelling and simulation are present in one form or another in all engineering disciplines. Essentially, modelling and simulation are used to represent a specific system with a certain level of fidelity. They also provide a means of representing the physical world for purposes such as component development, prototype testing (virtual prototype), and evaluation of dangerous or cost-demanding scenarios. Visualisation of simulation results can be a means to address the problem illustrated in Figure 1.4.

Engineers and other developers can use modelling and simulation to divide a system into subparts that can be analysed separately and, thus, allow for decoupled development of components. This approach to development is similar to the method presented for robot weed-removal development, in which subcomponents are developed independently. By dividing the system into subcomponents one can achieve a similar development advantage to that illustrated in Figure 1.5b.

Modelling and simulation have been utilised in automated and robotic agricultural ground-vehicle development. In [81], the authors provide a comparison between commercial and open-source robotic simulation software and tools ranging from MATLAB/Simulink to the Robot operating system (ROS). A 2D kinematic model of the tractor and implement was used in [3] to test nonlinear model predictive control, while a dynamic model of a tractor system was developed in [32], based on measurements from Real time kinematic GPS<sup>9</sup> (RTK-GPS) and wheel-encoders. In [53] the authors developed a model implementing back- and front-wheel cornering stiffness and turned model parameters, based on sample data from RTK-GPS. In all these cases, a single tool was used to perform the modelling and simulation of a specific project. The single tool approach creates a need for project engineers and other developers to collaborate using this specific tool.

---

<sup>9</sup> Global positioning system (GPS) is one of the satellite system types under the international common GNSS.

### Collaborative modelling and co-operative simulation

Domain-specific modelling software tends to focus on a subset of the engineering disciplines. Modelling and simulation across multiple disciplines and domains represent a design challenge in the development of a single tool. Collaborative modelling (co-modelling) combines separate domain-specific models to create a full model of the intended system, by collaboratively exchanging information between the tools. Co-modelling allows system components to be developed using different development tools and then run simultaneously using co-operative simulation (co-simulation) [10, 66]. The exchanged information concerns simulation parameters, control signals, or system events.

The Crescendo co-simulation technology provides a model-based approach to the engineering of embedded and robotic systems [33]. The Crescendo tool is an open-source tool originally developed in the EU FP7 DESTECs research project. Crescendo models are built in order to support various forms of analysis, including simulation. The Crescendo technology supports models where the controller and plant or environment are modelled using different specialised tools. Co-simulation is intended to allow for multidisciplinary modelling with input from domain experts from the different disciplines.

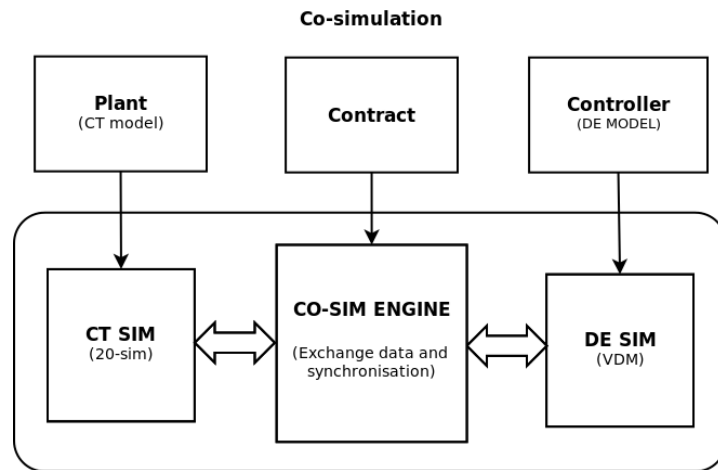


Figure 1.6: Crescendo co-simulation engine and synchronisation of the CT and DE simulation.

The Crescendo tool uses a combination of discrete-event (DE) modelling of a digital controller and Continuous-time (CT) modelling of the plant/en-

vironment for co-simulation. The Overture tool [48] and Vienna development method (VDM) formalism models the DE controllers, and the 20-sim tool [55, 56] models the CT components. 20-sim is a modelling and simulation tool that can model complex multi-domain dynamic systems, such as combined mechanical, electrical, and hydraulic systems. VDM Real Time (VDM-RT) [85] is the VDM dialect used for DE models in Crescendo, and has the capability to describe real-time, asynchronous, object-oriented features. VDM and 20-sim are well-established formalisms with stable tool support and a record of industry use.

The Crescendo co-simulation engine coordinates the 20-sim and VDM simulation by implementing a protocol for time-step synchronisation between the tools. Crescendo binds the domain models together using the Crescendo contract and is responsible for information exchange between the tools. The contract contains the parameters and variables CT and DE developers must be aware of when developing a combined model (a co-model).

The developers can use co-simulation to explore the solution design space, so as to determine viable candidate solutions. This kind of viable candidate search using co-simulation is known as Design space exploration (DSE). Crescendo provides a feature called Automated co-model analysis (ACA), with the means to perform automated DSE of a co-model [73]. ACA provides the ability to test different system configurations, by running all combinations chosen by the user. Such alternative system configurations can, for example, involve different actuators, controllers, filters, platforms, and sensor combinations in the design space the developers intend to explore.

The current state-of-art for co-modelling and co-simulation focuses on embedded and robotic system design in general. Automated and the robotic ground vehicle has a number of design challenges that is not addressed in the current co-model co-simulations, such as localisation, operation in semi-controllable outdoor environments and load transportation.

### 1.3 Motivation

Co-simulation performed in the agricultural domain has been documented previously in the literature [70, 86]. However, this research field is still in the early stages of development and further research is required to achieve a systematic development methodology. Such a methodology would allow developers to move from project start-up through co-modelling to finish with a product that can be deployed on a system realisation.

Model development is normally constrained by resources such as time and money. The developers' primary goal is to achieve a system model that is viable for controller development. One should remember that modelling is not an attempt to replicate the full reality into a model, but rather an attempt to focus on the parts relevant to the developers' current case [31]. To support development using co-modelling and co-simulation, there is a need for general modelling building blocks that can be reused to kickstart development projects.

The ability to divide the development of new automated or robotics systems into subtasks that can be developed independently will increase efficiency, by allowing independent subtasks to be completed in parallel by a development team. Here, co-modelling and co-simulation can facilitate development of different parts of the system independently and allow developers from different disciplines to collaborate.

Using co-modelling and co-simulation for the development of automated and robotic agricultural ground-vehicle systems can allow developers to address the problem of comparing different system setups that are intended to operate in a semi-controllable environment. Ground vehicles are dependent on solutions for variable sensory conditions, such as GNSS and visual input based on landmarks, when the ground vehicle is automatically moving between indoor and outdoor operational conditions on a farm. Scenarios in which the load transported by the ground vehicles varies also occurs in agricultural operational task, such as animal feeding and field spraying. Addressing changing operational conditions for automated and robotic agricultural ground vehicles is an ongoing area of research that has been fully developed. Here co-simulation has the capacity to allow developers to explore these changing operational conditions and to compare alternative solutions.

#### **1.4 Research Objectives**

This PhD project deals with the problems encountered during the design and deployment of an automated or robotic mobile ground vehicle in the agricultural domain. The overall aim of the project is to have co-models and a methodology that support the design and deployment of robotic and automated agricultural vehicles. The focus is on co-models, combining DE models of the control elements with CT modelling of the physical elements and the surrounding environment. We believe that better system configurations can be selected by utilising a co-simulated model of an automated or robotic agricultural ground vehicle. The intended approach is to model the

significant factors influencing a specific scenario. For instance, steering performance has a higher impact than motor vibrations on the vehicle ground movement. Part of the intended development process is to determine the influential factors for a given model. The project hypothesis can be divided into the following two statements:

- **Collaborative models can support multidisciplinary collaboration and system development.**

Model-based development can support collaboration between different engineering disciplines throughout the development process. A model can provide insights into the multidisciplinary development design of an automated or robotic agricultural ground vehicle. Collaborative models of different vehicle solutions can also be used to understand the controller interactions with the vehicle and its dynamics. The candidate solutions found using co-modelling and co-simulation can be deployed in the system realisation.

- **A collaborative model of a robotic or automated agricultural ground-vehicle can be utilised to explore alternative design configurations.**

Co-simulation can be used to test and evaluate developer-defined virtual prototype solutions of robotic or automated agricultural ground-vehicles. The design space can be rather large and real-world testing can be a costly and time-consuming task. The goal of prototype testing in co-simulation mode is to diminish the amount of prototype solutions that require testing in the real world. Developers can also use the co-model to obtain an overview of a design space they have defined, to allow them to select viable candidate solutions.

The two components of the hypothesis should not be regarded as separate entities, but rather as different aspects of the PhD research objectives. The hypothesis division is intended to allow for improved evaluation of the contributions of this PhD thesis, based on the evaluation criteria described in section 1.6 below.

## 1.5 Research Methods

To facilitate understanding of the approach and results of this PhD project, a description of the applied research methods is given in this section.

The approach adopted in this PhD project focuses on co-model design and the application of co-simulation in the development of robotic and automated agricultural vehicles. A robotics engineering perspective on the development of co-models for the agricultural domain is assumed. This research focuses on designing co-models using input from a combination of external case studies, domain specialists, literature surveys, and collaboration with companies in the agricultural industry. Additional input is gained through observations and analysis of academic and industrial case studies in the DESTECs project.

In the early research stages, time was spent on identifying relevant academic and industrial development cases that were deemed to benefit from co-modelling and co-simulation. The selected development cases are used as case studies in this PhD project and should be regarded as a significant part of this study's contribution to the wider field. For each case study, the existing literature for multi disciplines is consulted to identify similar problems with related solutions. Model elements found in different domains are evaluated and coupled into a working co-model. Models from the domains of mechanical vehicle modelling, software structuring, control theory, and optimisation are adapted and extended to fit the demands of the project. The experience obtained from these case studies is collected to derive a methodology for the development of co-models for automated and robotic agricultural ground vehicles.

## 1.6 Evaluation Criteria

The individual contributions made by this PhD project are numbered sequentially in Chapters 2 and 3. There is a total of 9 contributions, each of which is evaluated using the evaluation criteria described below:

**Multi-disciplinary collaboration support** Improved support for intercommunication between different types of developers and other stakeholders in a project concerning agricultural robotic or automated vehicle development. This evaluation criterion focuses on contributions that have value for project collaboration or that allow stakeholders the ability to grasp concepts that are not inherent in their own disciplines.

**Model Deployment** Evaluation of the ability to deploy a component from a co-modelling scenario to a system realisation. The intent is to verify that a solution is applicable in an actual system setting.



**Determination of candidate solutions** The use of co-simulation to determine prototype and parameter solutions automatically in both the DE and CT domains.

**Support for modelling of different vehicle solutions** Different types of vehicle solution exist in the agricultural industry; the ability to model these different types will aid in expanding the co-modelling base.

**Virtual prototype development support** The ability to support system development using virtual prototypes based on co-modelling and co-simulation. The virtual prototypes are used to evaluate the impact of changes and to test new system designs.

The evaluations of the research contributions are described in Section 4.2, where the level of fulfilment of the individual criteria is assessed. The extent

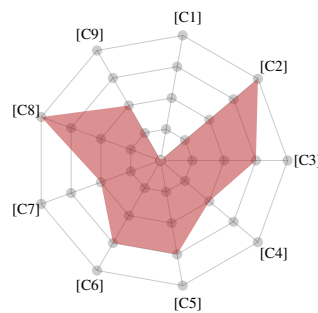


Figure 1.7: Sample comparison chart.

to which the criteria are fulfilled is illustrated using a chart, as exemplified in Figure 1.7, which shows the research contributions and the fulfilment of the criteria. We use the natural number range 0–4 as the value set used to judge the contribution relevance for each evaluation criterion. Thus, the value “2” should be seen as 50% of the maximum evaluation value.

## 1.7 Academic Work

This section presents the academic work produced during this PhD project, which primarily focuses on the topics of co-simulation and DSE of automated agricultural vehicles.

### 1.7.1 Publications

The publications listed here are all included in Part II of this thesis.

- [P17] Martin Peter Christiansen, Kim Bjerge, Gareth Edwards, and Peter Gorm Larsen. Towards a Methodology for Modelling and Validation of an Agricultural Vehicle's Dynamics and Control. In Sergio Junco, editor, *The 6th International Conference on Integrated Modeling and Analysis in Applied Control and Automation*, IMAACA, pages 112–119, September 2012
- [P20] Martin Peter Christiansen, Morten Larsen, and Rasmus Nyholm Jørgensen. Collaborative Model Based Development of Adaptive Controller Settings for a Load-carrying Vehicle with Changing Loads. In Dionysis D. Bochtis and Claus Aage Grøn Sørensen, editors, *CIOSTA XXXV Conference*, July 2013
- [P30] Gareth Edwards, Martin P. Christiansen, Dionysis D. Bochtis, and Claus G. Sørensen. A Test Platform for Planned Field Operations Using LEGO Mindstorms NXT. *Robotics*, 2(4):203–216, 2013

### 1.7.2 Submitted work

- [P19] Martin Peter Christiansen and Rasmus Nyholm Jørgensen. Method for recording and predicting position data for a self-propelled wheeled vehicle and delivery or pick up system comprising a self-propelled, self-guided wheeled vehicle, Submitted 19-12-2014 Patent application, DP 14870, Filing number: PA 2014 70803
- [P23] Martin Peter Christiansen, Peter Gorm Larsen, and Rasmus Nyholm Jørgensen. Agricultural Robotic Candidate Overview using Co-model Driven Development. In *IEEE/RSJ International Conference on Intelligent Robots and Systems*, 3 Submitted 4-3-2015
- [P22] Martin Peter Christiansen, Peter Gorm Larsen, and Rasmus Nyholm Jørgensen. Robotic Design Choice Overview using Co-simulation and Design Space Exploration. *Robotics*, pages 398–421, October 2015

### 1.7.3 Other publications

The publications listed here have not been selected for inclusion in this thesis but are all available from their publishers.

- [P18] Martin Peter Christiansen and Ole Green. Utilizing DESTECS co-modelling in agricultural testing. In Nils Bjurstad, Eskill Nilsson, and Gints Birzietis, editors, *NJF Seminar 452 - Testing and certification of agricultural machinery*, NJF - Nordic Association of Agricultural Scientists, pages 74–75, October 2012
- [P24] Martin Peter Christiansen, Morten Stiggaard Laursen, Rasmus Nyholm Jørgensen, and Ibrahim A. Hameed. Collaborative model based design of automated and robotic agricultural vehicles in the Crescendo Tool. In *NJF Seminar 477 - Agromek and NJF joint seminar: Future arable farming and agricultural engineering*, November 2014
- [P21] Martin Peter Christiansen, Peter Gorm Larsen, and Rasmus Nyholm Jørgensen. Robotic design choice overview using co-simulation. In *NJF Seminar 477 - Agromek and NJF joint seminar: Future arable farming and agricultural engineering*, November 2014

## 1.8 Outline and Reading Guide

The dissertation is divided into two parts: Part I contains an introduction and provides a summary of the research performed during the PhD project. This part also provides an overview of the research contributions on the basis of the publications that were produced during the project. Part II contains a subset of publications by the author with co-authors, on which the research contributions are based.

In addition to an introduction to the research field, Part I provides an overview of the research performed, on the basis of the abovementioned publications. For clear identification, contributions are numbered, e.g., [C1], and framed:

Contribution 1: Description
-----------------------------

The purpose of Part I is to provide an overview of the publications produced during this project and their contributions to this topic, while also introducing relevant background material and related work. It was decided to rewrite formulas differently to their representation in the papers included in Part II, to provided consistent parameter terminology throughout Part I. Part I introduces a total of six publications, three of which have been published

and three of which have been submitted. To allow these publications to be distinguished from other references, they are prefixed with “P”, e.g., [P17].

Part I is structured as follows: Chapter 1 contains a short introduction to the PhD thesis. Chapter 2 presents the agricultural automated and robotic co-modelling cases and the developed co-modelling methodology, while Chapter 3 introduces work regarding DSE. Chapter 4 concludes Part I of this thesis by summarising the work produced within the PhD project and discusses the contributions made. The contributions are evaluated based on the set criteria and compared to similar or related work. The conclusion also contains a discussion of how the contributions meet the research aim and hypothesis, and outlines possible future work.

Part II presents a selection of scientific papers written by the author of this PhD thesis in collaboration with others. Each chapter presents a publication and starts by listing the bibliography entry for the publication. This is followed by the publication in its original form.

## 2

---

### **Modelling and Simulation of Automated and Robotic Agricultural Vehicles**

---

This chapter presents the research and resultant contributions regarding the co-model based development of automated and robotic agricultural ground-vehicles and the derived extended agricultural development methodology. The extended methodology is dependent on co-simulation to evaluate the co-models and to allow for model deployment. This chapter begins with a literature survey of the state-of-art in co-modelling development methodologies. The chapter then moves on to the extended agricultural development methodology, derived from the development of co-models for agricultural ground vehicles. The extended agricultural development methodology is derived based on key case studies co-modelled in this PhD project, which we present in this chapter. We conclude the chapter with an overview of the projects in which the co-modelling technology has been applied and deployed to the actual ground-vehicle realisations.

The publications [P17, P20, P22, P23, P30] are related to this chapter. A total of five contributions are derived from these publications, which are framed in each section discussing a specific publication.

#### **2.1 Approaches to Co-modelling and Co-simulation**

The approach to mechatronic system design using modelling and co-simulation is intended to improve cross-discipline design dialogue and to reduce development cost and time. This modelling approach provides designers with the ability to explore candidate solutions virtually using co-simulation from a possible candidate design space. In indoor industrial robotics design applications, research indicates that a model-driven co-design approach incorporating co-simulation improves cross-disciplinary design dialogue [11, 12]. For example, co-simulation has been used in the development of several robotics manipulator systems, where no development methodology seems to be defined and the focuses are on the structure of the specific model. All of these

models use a combination of Matlab Simulink and Adams tools, where the Simulink model is the controller and ADAMS operates the robot body and environment dynamics [9, 14, 84]. A tomato-harvesting robot manipulator using the ADAMS/Simulink combination and with a similar development focus has also been designed [49].

In the CODIS framework, a design methodology has been used in which the gradual definition of the simulation interface functionality between continuous/discrete model components drove the development. A single case study of an optical network on a chip was used to verify the model components [37]. Based on published literature, the MODELISAR project focus was on developing the Functional Mock-up Interface (FMI) and defining a tool independent standard for model exchange and co-simulation [5, 6]. Later, a methodology for use of FMI for development in the automotive industry was published, which was related to the product life-cycle [58]. In the DESTECs project, the design approach could be DE-first, CT-first, or contract-first. This flexibility allowed the developers to either begin modelling the DE or CT side or to begin defining the co-model based on what should be shared knowledge between the disciplines.

These observations clearly indicate that, in order to address design challenges, a design methodology for the development of automated and robotic agricultural ground vehicles should be capable of:

- *Ensuring a methodical movement from idea/problem to actual implementation of the automated or robotics ground-vehicle. Co-modelling should be a stepping-stone to bridge the gap between project initialisation and the final product.*
- *Providing the project stakeholders with guidelines to aid in the selection of the relevant aspects of the project that is being co-modelled. Providing the development team with improved capabilities to address the various design and implementation challenges in the multiple subsystems contained within an automated or robotic agricultural ground-vehicle system.*
- *Providing engineers with varying degrees of experience with the agriculture domain with an understanding of development cases and permitting inter-disciplinary collaboration with project stakeholders using co-modelling. The intention behind this approach is to allow the project stakeholders to obtain a combined overall project view and to gain confidence in the system design.*

## 2.2 Extended Development Methodology

The proposed co-model development methodology and process workflow are illustrated in Figure 2.1, and are designed to encompass the full process from problem definition to deployment of a useable system. The co-modelling development methodology addresses model-based development for automated and robotics agricultural ground vehicles operating under the changing operational conditions described in Sections 1.1 and 1.3. Therefore, one contribution of this thesis is:

**Contribution 1.** An extended co-modelling and co-simulation methodology for the development of automated and robotic agricultural ground-vehicle systems.

The work in [33, 89] has partly inspired the proposed methodology used for the co-model development conducted in this study. Where these methods primarily focus on movement from controller requirements and environment assumptions to a complete system co-model, we extend this approach to include deployment to the actual system realisation. In this thesis, the new methodology is called an extended development methodology, as it extends previously described work.

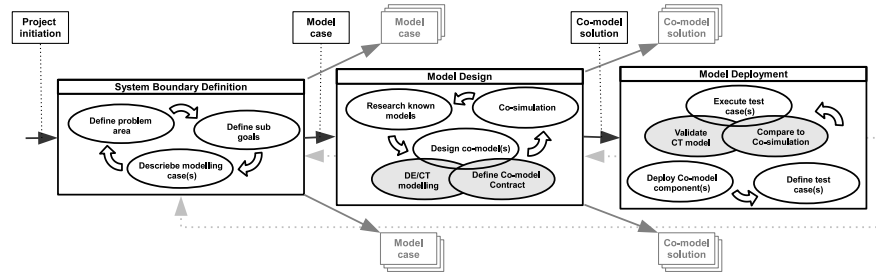


Figure 2.1: Proposed co-modelling process workflow, from initial problem definitions to model deployment. Depending on the project, each stage can result in one or more branches of the next stage.

The extended methodology is intended to be used in the design of new product solutions and as an approach to updating currently available products such as tractors. The motivation for developing this extended methodology is to gradually move towards automated or robotic agricultural ground-vehicles

and the intended semi-controllable operational environment. The proposed extended methodology allows the development team to validate their co-model solution against a developed product solution.

The extended development methodology is structured to produce the intended system gradually, with a finer level of granularity being achieved in each stage. The development process incorporates both the model developers and the remaining project stakeholders, to ensure input from the related partners. The development process divides the workflow into three main stages through which the co-model development iterates: *System Boundary Definition*, *Model Design* and *Model Deployment*. The main focus of the extended methodology is the given concrete objective of the developers for a particular system. The extended methodology provides guidelines to aid in the selection of the relevant aspects being co-modelled.

The extended development methodology is designed to provide agile development from initial concept to product solution. Process iterations occur both internally and through movement between the development stages, based on the input from the project stakeholders. In Figure 2.1, movement forward to the next main stage is indicated by black arrows and occurs when the project developers initiate the next stage in agreement with the stakeholders. Each successive main stage can branch into multiple instances as different aspects of the system may be developed separately. We do not claim that the output of the development process at each stage in our approach is necessarily a refinement of its predecessors. If the project stakeholders discover the need to redefine a model case or co-model solution, backward movement in the development process to revisit an earlier stage can be initiated.

Each main stage in the extended development methodology contains three substages that are cycled between during development of the intended system. The developers should expect to run through the substages multiple times and advance based on the previous iteration. The stakeholders should continually update the project timeframe based on the progress achieved using the extended methodology. Here, we provide a description of the three main stages of the extended development methodology:

**System Boundary Definition:** The initial decision in the development process is the definition of the boundaries of the problem area. Boundaries can be defined based on current standards in the domain area, the demands of the stakeholders, and the limitations of the system. The stakeholders decide their aim regarding the model, in terms of controller type and operating vehicle/environment.



Based on the problem area definition, the stakeholders then define the subgoals the system modelling must help realise. For a grass-cutting robot, the subgoals might be to achieve in-field automated navigation, controlled grass-cutting operation, and field management in relation to fuel consumption. For a manually driven ground vehicle used for animal feeding, the subgoals might be to achieve automated feeding operation and selection of robot arm solution for the feeding process. The stakeholders should rank the development subgoals based on their deemed importance to the deployment of the product.

The task of the developers is to determine if the subgoals can be developed into separate co-modelling cases, or if several subgoals should be grouped into a single case. A co-modelling case focuses on specific parts of the system relevant to the selected subgoals and abstracts all other parts. The development team achieves a form of decoupling that ensures a lower level of interdependence, by allowing subgoals to be developed in separate co-modelling cases.

**Model Design:** New co-models should not be reinvented by the developers for each project. In the design of viable model components that can effectively represent the modelling case, we recommend legacy domain knowledge from DE and CT modelling. In the majority of cases, one can find related case studies from agriculture or other industry domains, aspects of which can then be implemented in the project in question. The task is to select model components that the developers deem most likely to fit the demands of the co-model case.

The co-model design is comprised of two parts: the co-model structuring and implementation of the CT/DE models. The co-model structuring results in the co-model contract, which defines the communication between the models and is known to both DE and CT developers. When the initial version of the co-model contract has been designed, the DE and CT developers can start implementing their individual co-model parts. A CT- or DE-first modelling-based approach can still be used, but co-modelling cannot commence until the co-model contract is defined.

When a new revision of the co-model has been produced, co-simulation can be executed to analyse and verify the model response. Different candidate solutions can also be compared and analysed using co-simulation, as they can be easily run for the same scenario. The objective is to meet the goals

set by the stakeholders, so that the solution can be deployed onto the actual platform realisation.

**Model Deployment:** The first step to deploying the co-model is porting the CT or DE components to the actual platform. CT deployment could be the implementation of actuators or mechanical constructs. Co-simulation can be used to select a viable mechanical solution, for example an arm for animal feeding operations, which is implemented and tested on the actual platform. DE deployment converts the model into software code that can be directly executed on the intended platform.

To validate that the solution obtained from the co-model has been implemented correctly, the development team should define a number of test cases, which are intended to validate that the predictions from the simulation are sufficiently close to the actual realisation.

The intended final internal state is the execution of the test case(s), which should verify that the co-model solution is implemented in the design of the automated or robotic ground vehicle. When the implementation of the co-model solution has been verified, the focus can move to other aspects of the project.

Development using this extended methodology should never be viewed as complete, as a system can be moved in a new direction or new uses can be found. Lessons learned from the deployment can be used to initiate the development of the next generation of product solution. A deployed system solution can be adapted to related areas through further development. For example, a robotic system that can feed pigs may be adapted to feed cows, sheep, or other farm animals. The light grey arrow from *Model Deployment* to *System Boundary Definition* in Figure 2.1 indicates that a finished system can be used to initiate new systems development.

In the following sections, the main modelling cases that have been used to define the extended development methodology are described.

### 2.3 Case Study: The LEGO Micro-Tractor Platform

The lack of reported automated and robotic ground-vehicle co-models when this PhD project was initiated, made it clear that movement towards these model types needed to be conducted gradually. Many of the parts for such systems are not realised, making it difficult to completely verify a co-model

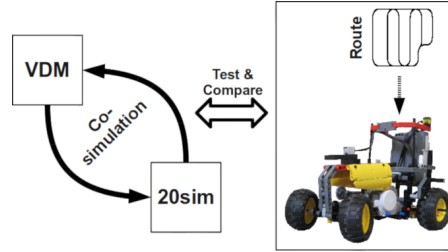


Figure 2.2: Overview of the Lego@Mindstorm@NXT tractor and the co-modelling method. 20-sim models the vehicle/environment and VDM models the control part of the micro-tractor. Comparisons are made between real and simulated systems to determine errors and shortcomings in the model.

based on testing and analysis. LEGO Mindstorms is an example of a common framework that has been used in other scientific disciplines related to robotics, e.g., robotic exploitation [57] and team intelligence [80]. LEGO Mindstorms provides a proven, versatile framework for prototyping mechanical robotic systems that are programmed with a high degree of complexity. It also provides a system that has the ability to add and remove functionalities, as well as to reconfigure its architecture.

### 2.3.1 Co-modelling

A co-model based on a LEGO Mindstorms NXT tractor (micro-tractor) was developed, to simplify the initial co-modelling design process. The micro-tractor is intended to be a representative scaled model of agricultural machinery used to test and demonstrate operations. This prototype co-model of an automated vehicle is intended to provide an abstraction with key components in autonomous vehicle steering. Therefore, a contribution of this thesis is:

**Contribution 2.** A kinematic co-model of an automated LEGO tractor platform.

The DE controller models the NXT's steering of the micro-tractor and is modelled using VDM-RT. A pre-planned route is given to the autonomous system, which is used when the micro-tractor commences its task in a given field area. The route is based on a collection of continuous curve elements. Each continuous path element is either a line segment or circular arc with

constant radius, containing a start and stop waypoint [4]. The micro-tractor is aware of its current position and can use this information when following the route. A route-manager ensures that each route segment is performed in the order described in the route. The VDM model uses invariants and pre- and post-conditions to ensure that only a viable route and route segments are commenced.

A similar methodology is applied when modelling the CT components in 20-sim. A combination of bond graphs and iconic diagrams are used to model the CT part of the micro-tractor co-model. The bond-graph model motor and environmental dynamics and the iconic diagram are used for differential equations and sensor models.

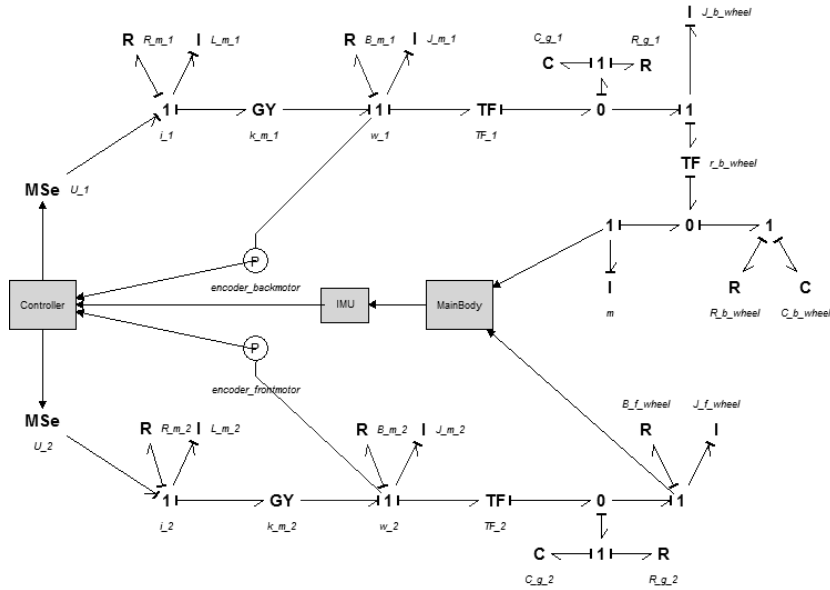


Figure 2.3: Micro-tractor model in 20-sim. A combination of bond graphs and iconic diagrams are used to model the micro-tractor.

The controller is connected to the DC-motor implementations, providing the interface for communication with the VDM model. Interactions between the wheels and ground plane are only considered for a smooth surface to reduce the complexity of the model. Only the longitudinal effects on the wheel are considered, since the tyre-road normal effort [63] is expected to be minimal.

To combine the dynamic effects of the back and front wheels, a first-order bicycle model was chosen. The resultant first-order bicycle model is a pure kinematic model [76] of the chassis movements, without regard for the forces acting on the body. The speed  $u$  of the back wheels in combination with the rotational speed  $\delta_f$  of the front steering system are used as the model inputs. Then, the chassis movement is modelled as:

$$\dot{x} = \cos(\psi)u \quad (2.1)$$

$$\dot{y} = \sin(\psi)u \quad (2.2)$$

$$\dot{\psi} = \frac{\tan(\delta_f)}{L}u \quad (2.3)$$

Equations (2.1), (2.2), and (2.3) are used to calculate the vehicle rotation  $\psi$  and speed  $\dot{x}, \dot{y}$  in the x-y direction in a global reference frame.  $L$  represents the distance between the front and back wheels and  $\delta_f$  is the orientation of the front wheels.

The experience obtained by modelling of the LEGO Mindstorms micro-tractor described above was used to refine the concept of the extended development methodology, indicating that legacy models and related case studies should be researched before co-modelling is commenced. Even though the extended development methodology was updated based on the lessons learned from the modelling case study, the structure illustrated in Figure 2.1 was followed.

### 2.3.2 Testing operational management techniques

In order to quickly test operational management techniques, a test platform utilising a LEGO Mindstorms micro-tractor was developed, allowing for easily replicable results that can be evaluated while interpreting collected data. Compared to a Hardware-In-the-Loop solution, the micro-tractor allows for the evaluation of software components using actual sensory input. This test platform is seen as an intermediary step between simulation and full-scale testing, rather than a replacement of either.

The micro-tractor is equipped with a drawbar suitable for connecting implements. In this research, an indoor GPS (iGPS) was used to test the accuracy of the micro-tractor position determination. The iGPS system (Nikon Metrology, NV Europe) combined a transmitter sensor placed at the center

of the rear axle of the micro-tractor (Figure 2.4a) with six beacon posts (Figure 2.4b) located around the working area.



(a) Micro-tractor with mounted iGPS sensor.



(b) iGPS beacon.

In the related paper [P30], the test platform was described in terms of its hardware and software components. The performance of the platform was demonstrated and tested in terms of its capability for supporting decision making on field operation planning using indoor environment simulations. Further the micro-tractor was equipped with a drawbar suitable for connecting implements. Therefore, another contribution of this thesis is:

**Contribution 3.** Deployment of a co-model solution to a LEGO tractor to allow for two-step gradual verification and movement from simulation to an actual system.

A series of navigation accuracy tests were performed in a “virtual” field. Figure 2.5 presents the three paths (off-line planned, on-line estimated and actual measured) on a “virtual” field for the case of a 0.250 m working width and  $0^\circ$  driving direction. Based on the tests, for a basis driving distance of 71.43 m (corresponding to a 1 km full-scale distance), including straight line driving (operating on a field-work track) and  $180^\circ$  maneuvering (headland turnings), the average cross-track error between the estimated path and the iGPS path executed by the micro-tractor was 0.028 m, corresponding to a 0.39 m full-scale Cross-track error (XTE).

The lessons learned from the testing using the micro-tractor were used to define the model deployment development stage to achieve actual realisation using the extended methodology in Section 2.2. Note that the goal is not

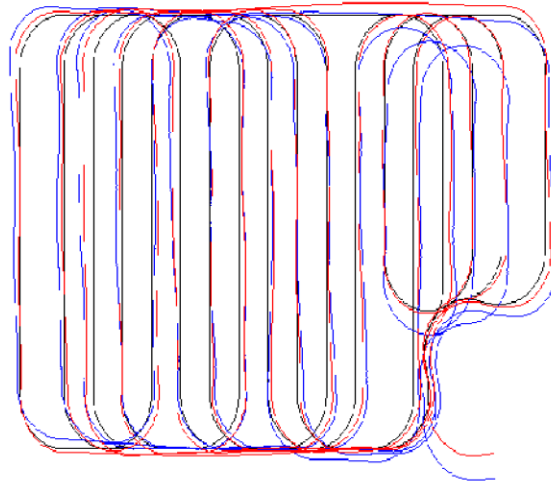


Figure 2.5: Planned path (black line), path estimated by micro-tractor internal sensors (red line), and actual path recorded by iGPS (blue line).

be the co-model in itself, but rather the realisations one can derive from the model-based development methodology.

The micro-tractor system example encapsulates the basic measures necessary for developing a complete test platform for field operations, where route plans, mission plans, and multiple-machinery cooperation strategies can be simulated and tested in the laboratory. The execution of coverage plans was chosen to demonstrate the capabilities of the test platform to implement agricultural operation management techniques. The demonstration examples also show that it is possible to evaluate coverage plan scenarios involving various operational features (e.g., working widths, driving angles, and number of headland passes) in terms of various operational efficiency measures, e.g., the measured non-working travelled distance, overlapped or missed area, and the operational time.

## 2.4 Case Study: Common Agricultural Ground-vehicle Platforms.

The LEGO case study demonstrated the need to develop a base co-model that takes more aspects of a normal agricultural vehicle platform into account. In the current market, a significant number of agricultural vehicles are based on front- or back-axle-operated steering, like tractors or combine harvesters.

Skid steering, also known as differential steering, four-wheel steering, and other steering schemes are becoming more common [92, Ch. 2]. In this study, it was decided to focus the modelling development on front- or back-axle-operated steering, as this is still the most common platform and developers can utilise this approach in automated or robotics projects. Therefore, another contribution of this thesis is:

**Contribution 4.** A dynamic co-model of a front- or back-axle-steered automated agricultural ground-vehicle platform.

The base co-model for a front- and back-steered vehicle is complementary to the extended development methodology presented in Section 2.2, designed to support future model-based development projects. The base co-model illustrated in Figure 2.6 is implemented in agricultural development cases where automated path following is of interest.

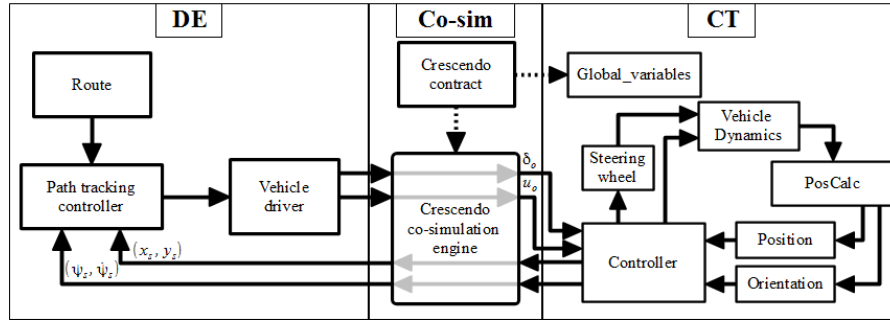


Figure 2.6: Communication between the CT and DE models of the envisioned automated and robotic vehicle base co-model using the Crescendo co-simulation engine.

This co-model allows multiple views and permits the developers to focus on six shared variables. This simplification is intended to allow DE and CT developers to focus on their own domains and only requires them to be aware of the Crescendo interface. Both the DE and CT model parts are well-known components; the strength here is that a developer can utilise a development tool related to their domain [2, 3, 4, 52]. The idea is to have a base agricultural vehicle co-model structure that can be used in a number of different development cases to complement the extended development methodology. Other



shared design parameters (**sdp**) or variable extensions may be implemented in a specific project, to allow for analysis of the concrete problem on which the developers are working.

Two **controlled** ( $u_o, \delta_o$ ) variables are used to operate the actuators for vehicle speed and steering axle angle. In some cases,  $u_o$  is assumed to be constant for specific co-simulation and is instead a **sdp**; this simplifies both the DE and CT parts of the co-model. With an update to the vehicle driver block on the DE side, the DE-model can be reused for differential and four wheeled vehicle steering. In the case of a differentially steered vehicle, the controlled variables to the CT side would instead be the left- and right-side rotational speeds of the wheels.

On the CT side of the co-model, all communication with the co-simulation engine is performed through the controller interface, which contains local versions of **controlled** and **monitored** variables. The **monitored** variables ( $x_s, y_s, \phi_s, \dot{\phi}_s$ ) are sensor measurements that the DE controller receives, which concern the current vehicle position and rotational speed in the yaw plane. Compared to the actual automated or robotic solution, one is not required to implement aspects of sensor fusion to obtain reliable vehicle state information for the DE side of the co-model. Using abstractions of system components such as sensor-fusion, the developers on the DE side can focus directly on the ground-vehicle steering algorithm. The intention is not to model the full reality, but rather to provide a base model that allows us to analyse automated and robotic agricultural ground-vehicle design problems.

#### 2.4.1 DE modelling

The DE part of the base co-model assumes that the developers intend the robot to follow a pre-planned or updated infield route. The DE-mode utilises a route based on a waypoint sequence and path tracing methods that can select the waypoints the ground vehicle must follow at a given instance in time. The model utilises the method given in Listing 2.1 to retrieve the current and next waypoint from the sequence. The VDM variables *current\_waypoint* and *next\_waypoint* are nominated  $P_k$  and  $P_{k+1}$ , respectively, where  $k$  represents the current element in the sequence.

To ensure that the update method for the route is not called for an empty waypoint sequence, a precondition is set for the minimum length. When running a co-simulation, the precondition functionality can be used to warn the developer if the condition is met and the update method is, therefore, being called under the wrong pretences.

```

public NextWayPoint: () ==> WayPoint
NextWayPoint() == (
    -- Goto next waypoint in sequence
    current_waypoint := (hd waypoints);
    -- Remove waypoint from sequence
    waypoints := (tl waypoints);
    -- Get next waypoint in sequence
    next_waypoint := (hd waypoints);
    return(current_waypoint);
)pre (len waypoints > 1);

```

Listing 2.1: VDM-RT method for updating to the next waypoint in the sequence contained in the route.

The three different path-tracking controller methods that have been implemented as DE model components and utilised as single or mixed solutions to steer ground-vehicles are illustrated in Figure 2.7. One should note that the path tracking controller methods use either one or two waypoints to calculate the vehicle steering response.

The look-a-head distance  $l_d$  is used to determine both the current waypoints for the vehicle to follow and when the vehicle control should move to the next waypoint in the sequence. The magnitude of  $l_d$  is dependent on the vehicle type and the speed of the controlled vehicle. Different path-tracking methods are utilised depending on the operational task the vehicle must per-

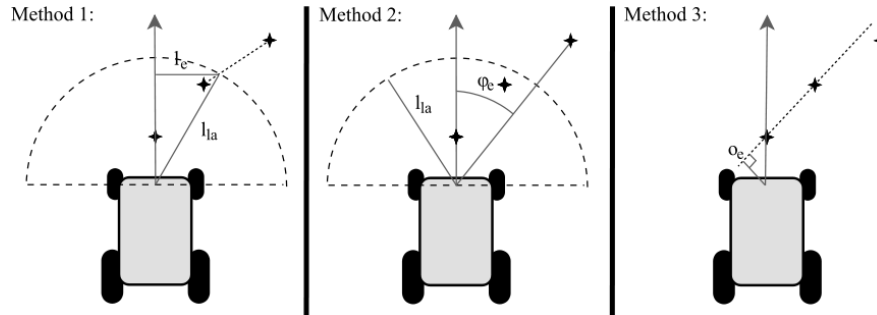


Figure 2.7: Three waypoint path-tracking methods: Method 1: Heading error path-following based on look-a-head distance  $l_d$  and a single waypoint. Method 2: Lateral error path-following based on  $l_d$  and two waypoints. Method 3: Line segment path-following based on  $l_d$  and two waypoints.

form. Examples of the utilisation of different path tracking controllers can be found in [P20], [P23], and [P22].

### 2.4.2 CT modelling

The CT part defining the vehicle is a non-linear model with three Degrees of freedom (DOF), i.e., the longitudinal, lateral, and yaw directions, irrespective of the suspension and described in [P23]. The model of the vehicle utilises the bicycle approach, meaning that the lateral forces on the left and right wheels are assumed to be equal and summed together. This assumption holds for typical agricultural vehicle operation velocities ( $<7.5$  m/s) [52]. The bicycle structure is also known as a half-vehicle (Figure 2.8). The model allows for yaw and lateral motion through adjustment of the front wheel angle  $\delta_f$ .

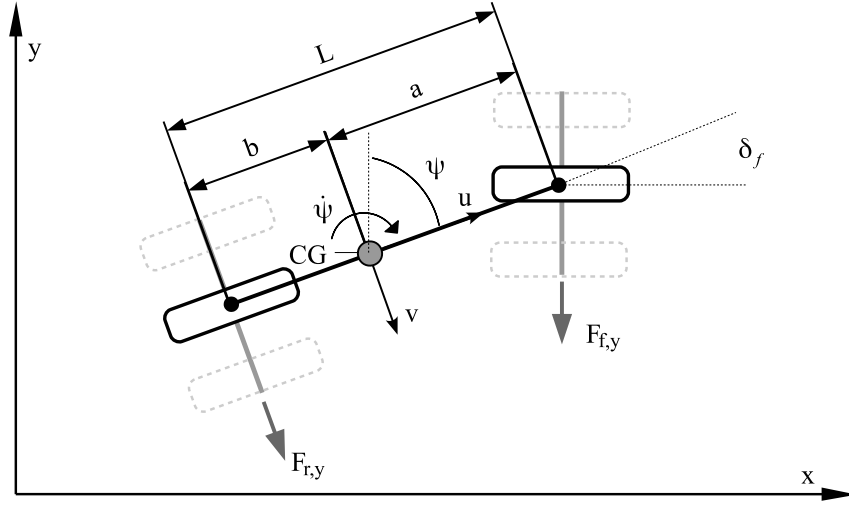


Figure 2.8: Dynamic bicycle model of the vehicle part of the robot system.

The velocities  $u, v$  are at the Center of gravity (CG) of the vehicle.  $L$  is the wheelbase, where  $a$  is the longitudinal distance to the front wheel, and  $b$  is the longitudinal distance to the rear wheel. For a constant forward velocity, the vehicle motion is given by

$$m(\dot{v} + u\dot{\psi}) = F_{f,y}\cos(\delta_f) + F_{r,y} \quad (2.4)$$

where  $r$  is the angular rate about the yaw axis. Similarly, the vehicle yaw motion is expressed by

$$I_{zz}\ddot{\psi} = aF_{f,y} - bF_{r,y} \quad (2.5)$$

where  $I_{zz}$  is the moment of inertia along the yaw axis.

A similar solution can be used for a back-axle-steered vehicle solution, where steering wheel angle  $\delta$  impacts the forces from the rear wheel. The ability to change the co-model to back-axle steering allows the solution to be used for combine harvesters and similarly steered vehicles.

## 2.5 Case Study: Animal Feeding System

The base co-model case study is intended to provide a base co-model that is applicable to a large number of agricultural cases. However, this model cannot be applied in the study of aspects relevant to a special case. For example, the base co-model cannot be used to model aspects of sensor-fusion or other operational vehicle dynamics directly, and more specialised modelling solutions are needed to satisfy the requirements of these kinds of co-modelling cases. A specialised co-model solution allows the development team to analyse unique aspects of the given system, but this new co-model's levels of re-usability in other projects is also reduced. In this research project, a robotic ground-vehicle for mink feeding was used to study of specialised co-modelling solutions, and was developed using the extended development methodology presented in Section 2.1. Therefore, a further contribution of this thesis is:

**Contribution 5.** A specialised co-modelling solution for automated and robotic agricultural ground-vehicle solutions related to mink feeding.

The chosen robot is a four-wheeled vehicle with front-wheel steering and rear-wheel drive equipped with a differential gearing. The robot receives sensory input from a vision system, a Radio frequency identification (RFID) tag reader, Inertial measurement unit (IMU), and rotary encoders installed on the back wheels and front wheel kingpins. The vision system is used to detect the entrance to the feeding area, when the robot is still outside. The RFID tags are placed along the rows of mink cages to act as fixed location reference points, as illustrated in Figure 2.9. Fused sensory data are used to determine the current location and to enable the robot to perform its required actions in

the environment. A feeder arm mounted on the robot is used to dispense the fodder on the cages at the predetermined locations. When the robot moves into the feeding area, it stops to deploy the feeding arm and then begins the feeding procedure.

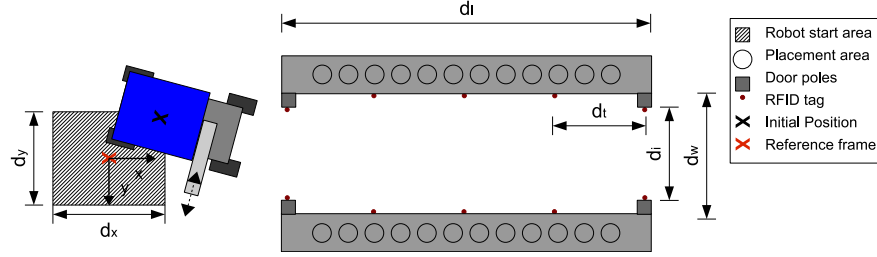


Figure 2.9: Sketch of the load-carrying robot and the mink feeding area.

Sensor fusion concepts and load distribution dynamics were co-modelled for this robotic vehicle solution. The robotic vehicle solution is described in additional detail in Section 3.2 and 3.5, where the base co-model and this co-model are used for DSE. The main focus here is the model extension of the base co-model using the extended methodology. We here present the vehicle dynamics and sensor fusion parts of the co-model, which were developed based on the base co-model.

### 2.5.1 Vehicle body dynamics

The generated tyre forces interact with the robot to produce the output response in the environment. To take the front steer angle into consideration, the CT-model rotates the front tyre forces into the coordinate system of the robot vehicle.

Based on the trigonometric relationships illustrated in Figure 2.10a, the steer angle was transformed using the rotation matrix at the front of the left-hand side of Equation (2.6) [4]. The robot utilises Trapezoid- steering, which produces equal steering angles on the right and left sides, making the transformation the same for both sides. Thus,

$$\begin{bmatrix} F_{xlf} \\ F_{y lf} \end{bmatrix} = \begin{bmatrix} \cos(\delta_f) & -\sin(\delta_f) \\ \sin(\delta_f) & \cos(\delta_f) \end{bmatrix} \begin{bmatrix} F_{xwlf} \\ F_{ywlf} \end{bmatrix} \quad (2.6)$$

The CT side models the dynamic yaw  $\psi$ , pitch  $\phi$ , lateral  $u$ , and longitudinal  $v$  motion responses of the robot vehicle. The yaw motion is modelled by

Equation (2.7). Variables  $a$  and  $b$  are respectively the longitudinal distances from the front and rear wheels to the CG,  $I_{zz}$  is the yaw moment of inertia, and  $T_c$  is the tyre base track width. Then,

$$I_{zz}\ddot{\phi} = a(F_{ylf} + F_{yrf}) - b(F_{ylr} + F_{yrr}) + \frac{T_c}{2}(F_{xlf} - F_{xrf} + F_{xlr} - F_{xrr}) \quad (2.7)$$

Similarly, the robot roll motion is given by equation (2.8), where  $K_r$  and  $C_r$  represent a combined rotational spring-damper based on tyre values, with  $\sum F_y$  being the sum of the forces in the longitudinal direction. The variable  $H$  represents the current CG height above grounds,  $M$  is the current total mass of robot  $m$  and transported load, and  $g$  is the Earth's gravity.

$$I_{xx}\ddot{\psi} = -\left(H \sum F_y + (K_r - MgH)\psi + C_r\dot{\psi}\right) \quad (2.8)$$

The load shift from the right to the left of the robot is assumed to be proportional to the current pitch angle. The longitudinal motion output of the robot is given by

$$\sum F_y = M(\dot{u} - v\dot{\phi}) \quad (2.9)$$

The lateral motion of the feeder robot is determined by the sum of the lateral forces, the roll acceleration, and the longitudinal speed, such that

$$\sum F_x = M(\dot{v} + u\dot{\phi} + H\ddot{\psi}) \quad (2.10)$$

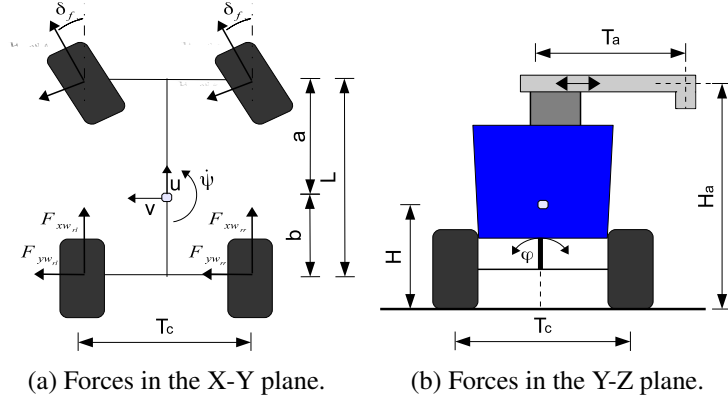


Figure 2.10: Free-body diagrams of the robot in the x-y and y-z coordinate frames.

### 2.5.2 Sensor fusion

The concept behind sensor fusion is that more accurate estimates of a physical phenomenon can be obtained by combining different sensor-data sources [42]. The combined sensor data can better accommodate uncertainty and noise in measurements [82]. The sensor fusion solution adopted in this study uses an Extended kalman filter (EKF) [83] to estimate the current position of the robot. The process is represented by the following velocity motion model:

$$f(\hat{x}_{k-1}, \mu_k, 0) = \begin{bmatrix} x_k \\ y_k \\ \psi_k \end{bmatrix} = \begin{bmatrix} x_{k-1} \\ y_{k-1} \\ \psi_{k-1} \end{bmatrix} + \begin{bmatrix} -\frac{u_{e_k}}{\dot{\psi}_{s_k}} \left( \sin(\psi_{k-1}) - \sin(\psi_{k-1} + \dot{\psi}_{s_k} T_k) \right) \\ \frac{u_{e_k}}{\dot{\psi}_{s_k}} \left( \cos(\psi_{k-1}) - \cos(\psi_{k-1} + \dot{\psi}_{s_k} T_k) \right) \\ \dot{\psi}_{s_k} T_k \end{bmatrix} \quad (2.11)$$

The process input  $\mu_k$  at interval  $k$  in time is used to predict the next state and is based on the monitored variables  $\dot{\psi}_s$  and estimated speed  $u_e$  based on rotary encoder values.

The EKF utilises an event-based correction stage that is dependent on the inputs from the vision system and RFID. The vision system provides updates when the door poles of the entrance and exit are in view, and compares them against a pole landmark map. The chosen landmark  $(m_{x,j}, m_{y,j})$  are converted into polar coordinates  $(r, \theta)$  to allow for direct comparison with the sensor input:

$$h_{vision_{out}}(x_{k,j}, 0) = \begin{bmatrix} r_{k,j} \\ \theta_{k,j} \end{bmatrix} = \begin{bmatrix} \sqrt{(m_{x,j} - x_k)^2 + (m_{y,j} - y_k)^2} \\ \arctan2(m_{y,j} - y_k, m_{x,j} - x_k) - \psi_k \end{bmatrix} \quad (2.12)$$

where  $(m_{x,j}, m_{y,j})$  is the position of the door-pole in the local map and  $(x_k, y_k, \psi_k)$  is the estimated position of the robot.

When the robot is moving inside the feeding area the vision input can be used to update the vehicle orientation and distance to the side wall [45].

$$h_{vision_{in}}(x_{k,j}, 0) = \begin{bmatrix} d_m \\ \theta_m \end{bmatrix} = \begin{bmatrix} \frac{A_m y_k + B_m x_k + C_m}{\sqrt{A_m^2 + B_m^2}} \\ \arctan2(A_m, B_m) - \psi_k \end{bmatrix} \quad (2.13)$$

where  $A_m$ ,  $B_m$  and  $C_m$  are the parameters for the general form of the line equation representing the mapped position of the side wall. The sensory update does not provide the robot with information about its current position along the side wall and, therefore, position correction is needed.

The positions of the RFID tags can also be seen as points along the sidewall  $(m_{x,i}, m_{y,i})$ . When the RFID tag reader first detects the tag we can use this to provide a position estimate  $(\Delta x_{e,i}, \Delta y_{e,i})$  relative to this tag by combining the detection event with input from the vision sensor. In these co-modelling scenarios, we assume it to be at the centre of the detection zone (i.e. at zero), making the relative position measurement output correspond the intersection point between the line (sidewall) and ellipse (detection zone). The relating landmark of the RFID tag is then:

$$h_{rfid}(x_{k,j}, 0) = \begin{bmatrix} \Delta x_{k,i} \\ \Delta y_{k,i} \end{bmatrix} = \begin{bmatrix} m_{x,i} \cos(-\psi_k) - m_{y,i} \sin(-\psi_k) - x_k \\ m_{x,i} \sin(-\psi_k) + m_{y,i} \cos(-\psi_k) - y_k \end{bmatrix} \quad (2.14)$$

The Jacobian matrices utilised in the EKF localisation method are not presented, but can be calculated based on equations (2.11), (2.12), (2.14) and (2.13).

## 2.6 Deployment

In this section, we summarise the different modelling cases that have been deployed on agricultural automated or robotic ground-vehicle platforms. The development of models for the sake of modelling and simulation only is not the intended focus of this thesis. Rather, the use of co-models to analyse and solve actual design cases in the agricultural domain and the application of the acquired knowledge to ground-vehicle realisation (deployment) is the primary aim. This approach is also in accordance with the extended agricultural development methodology presented in Section 2.2.

This chapter has primarily focused on cases involving front- or back-axle-steered ground vehicles, but a solution for differentially steered vehicles has also been deployed. In the majority of scenarios, DE components were moved from the Crescendo co-modelling environment and developed into executable code for the different solutions illustrated in Figure 2.11. The arrows between the co-models indicate how the previous co-models were utilised to develop the next generation.



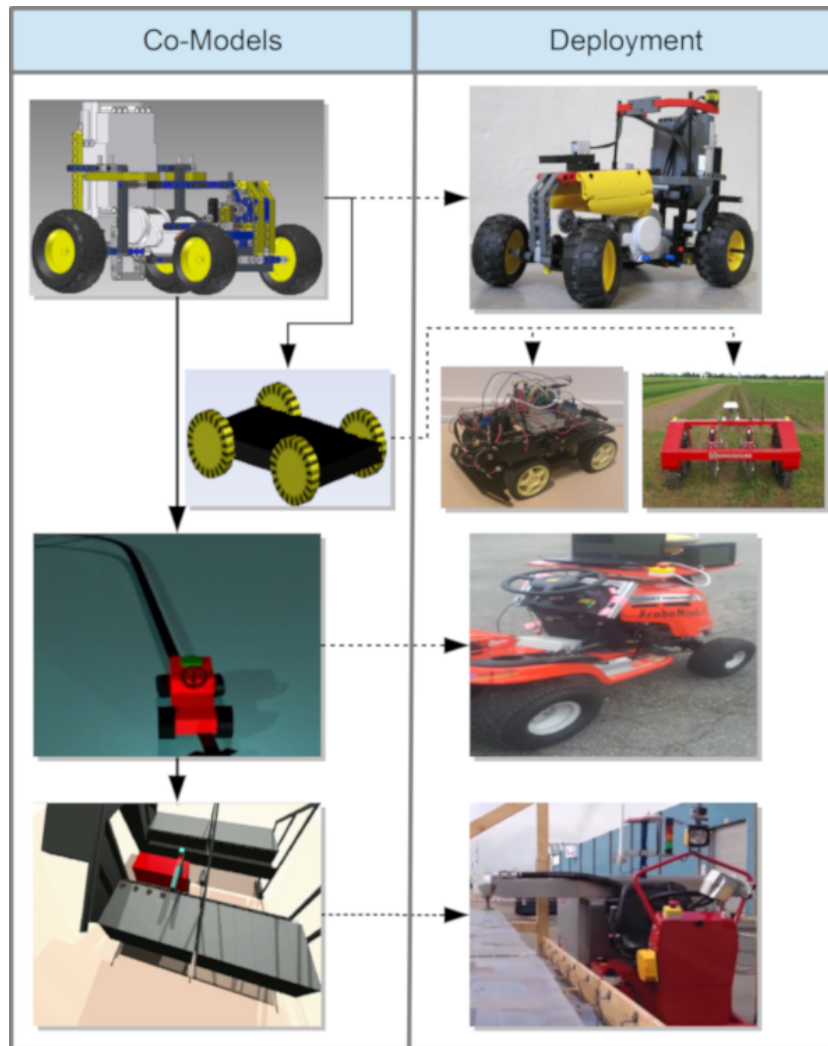


Figure 2.11: Co-models that have been developed and deployed to actual ground-vehicle system platforms.

The LEGO case study was the first to be deployed onto an actual platform for testing and demonstration purposes [P17, P30]. The LEGO tractor should be regarded as an intermediate step between modelling, simulation and deployment to an agricultural ground-vehicle platform to provide gradual verification. The four-wheeled differentially steered co-model was utilised

in a master's thesis project and was deployed to a prototype platform [47]. The same co-model was used in the modelling of noise encoder feedback on the KongsKilde Vibro Crop Robotti platform [P24, 39]. Deployment of the ASuBot<sup>1</sup> vehicle platform allowed us to confirm the functionality of the path-following control system developed in the VDM formalism [P20], and actual verification allowed the path following functionality to be reused in the remaining presented co-models.

The feeding system discussed above extended the DE model controller functionality to the operation of an animal feeding system for mink [P22, P23]. The feeding operation was tested in a mink farm environment with a vehicle matching the co-model structure.

## 2.7 Summary

This chapter has presented extended methodology guidelines to address the development of automated and robotic agricultural ground vehicles, based on the state-of-the-art in this field, along with summaries of the three primary co-modelling case studies described in this thesis. The deployment results show how co-modelling has been used in the development of a number of different automated and robotic agricultural ground-vehicle solutions. The results indicate that co-modelling and co-simulation can strengthen the future development of automated and robotic solutions in the agricultural domain.

---

<sup>1</sup> An acronym for Aarhus and Southern Denmark University Robot. Source: [http://www.frobomind.org/index.php/FroboMind\\_Robot:ASuBot](http://www.frobomind.org/index.php/FroboMind_Robot:ASuBot)

# 3

---

## Design Space Exploration

---

This chapter presents the research and contributions of this thesis to the area of DSE in relation to co-modelling and co-simulation. The chapter begins by introducing the basic concepts of DSE and their use in other projects. Figure 3.1 provides an overview of the research conducted using DSE and outlines the four contributions presented in this chapter. This chapter discusses experimentation with alternate design solutions based on DSE, in order to discover product solutions that can be implemented on actual platform realisations and to provide insight into alternative solutions to a problem. The chapter describes ACA of two case studies for single- and multi-domain design problems. This approach was used to find potential viable candidate solutions.

The publications [P19, P20, P22, P23] are related to this chapter. A total of four contributions are derived from these publications, which are presented in separate sections.

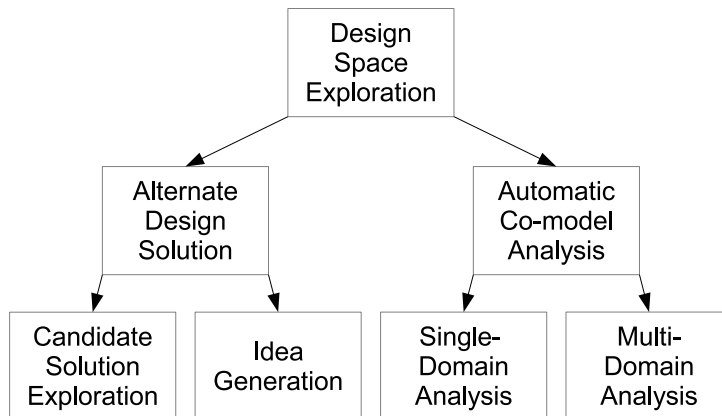


Figure 3.1: Overview of the different design space search approaches

### 3.1 Design Space Exploration Concepts

The aim of Design Space Exploration is to provide the project stakeholders with the ability to conduct experiments in the search for solutions that can meet the system requirements within the defined design space. The stakeholders manually define the design space for the system, from which they wish to determine viable candidate solutions, using the co-simulation response surface of the design space [35]. The design alternatives in a design space can be a continuous parameter range, discrete value ranges, or distinct mode alternatives. One could, for example, use the different path tracking-methods (modes) in Figure 2.7 and their configurations to define a design space for the operation of an automated vehicle in a specific set of scenarios. The point is that the stakeholders must select which aspects of a co-model they find of interest and wish to explore.

The motivation for using DSE in combination with co-simulation is to find candidate solutions for a specific aspect of a system, such as the actuation, controller, or sensor operation of a robotic system [65]. The use of DSE relates to the design problem illustrated in Figure 1.4, since the method can be used to allow the different stakeholders to compare candidates and to use the co-simulation response to select a solution. Co-simulation can be used to explore alternate solutions for specific design aspects which would be too costly to test in the real world. An informed discussion can then be conducted on which solution should be developed into an actual product and deployed into a platform solution, by allowing the stakeholders to visualise the response of the system.

One candidate solution might be deemed to be optimal, based on the output response of a specific co-model and a specific design space. The intention in this thesis was to avoid focusing on identifying the best or optimal solution within a certain design space, as factors not considered by the stakeholders might influence the outcome in the real world. One could still determine the minima or maxima responses of a defined design space, but this does not mean that the stakeholders have found the best or optimal solution under all conditions.

The design space is explored either automatically, manually, or using a combination mode, to determine viable candidate solutions. The different overall design space search approaches are related to the DSE structure illustrated in Figure 3.1. Manually experimenting with a co-model can have two purposes: to aid the developer in better understanding the co-model response and to determine if an alternative design solution the stakeholders have pro-

posed is viable. Research has shown that examples of how a desired system should perform are beneficial for the creative process [46]. An idea developed through such a creative process could result in an alternative design solution outside the initially defined design space. The potential for idea-generated candidate solutions outside the stakeholder's well-defined design space is one of the reasons why we do not refer to the "best" or "optimal" design solution for a system.

The Crescendo technology provides an automatic functionality to search a defined design space called ACA. The line-following robot in [72] was developed through the first ACA-based search for a candidate solution. The intention was to determine a solution for the placement of the robot light sensors utilised for line-following. A candidate solution based on preselected evaluation metrics was found by rerunning the same scenarios for different sensor-position candidates. The ACA functionality is designed to provide automatic search and optimisation methods in order to determine viable candidate solutions. The idea is to provide a cost function [16] for the ACA functionality to categorise and compare candidate solutions, so as to automatically select the most promising candidates. Automatic parameter sweeps using ACA are one such approach to finding viable candidate solutions, when little is known about the system configuration. The parameter sweep search methods can be somewhat calculation intensive if a larger design space must be examined, making input from optimisation methods relevant.

Academic research has been conducted in the area of optimisation methods for multi-disciplinary systems [27, 68]. Current publications concerning multi-disciplinary optimisation have focused on identifying solutions in cases where the system model has been developed using a single tool and the design space is based on a bounded continuous parameter range. When new automatic search methods is developed for ACA functionality, one should attempt to adopt optimisation methods that have been used for single- or multi-domain problems.

### **3.2 Alternative Design Configurations**

Manually experimenting with alternative solutions using co-simulation helps exemplify the type of system the developers intend to produce. Visualisation of the co-simulation can be used to convey the type of system the developers have in mind to the other project stakeholders. Visualisation also allows domain experts with knowledge in the project area to provide input on the solutions and to identify any faulty assumptions that have been made by the

developers. Figure 3.2 illustrates such a visualisation of the first co-model version of the mink-feeding robot, where the intention was to obtain input on how and where the mink-feeding robot should dispense fodder.

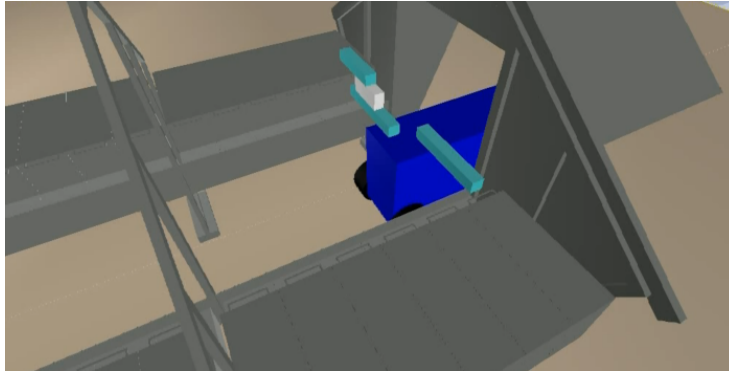


Figure 3.2: Exploring feeding-arm solutions for the mink robot.

Feeding mink is a high-precision task compared to that of other domesticated animals used in livestock production. The farmer chooses the amount of fodder each cage receives, based on personal experience and knowledge concerning demands for mink gender, age, and species. Based on feedback from mink-farmers, the author determined that each mink cage would receive a portion of fodder in the range of 80–300 g. In all mink-feeding cases, the total weight of the vehicle changes gradually throughout the feeding process. With vehicle fodder tanks that can transport maximum loads in the range of 500–2500 kg, a machine would theoretically be able to feed 1500–30 000 cages. Automatically placing the fodder in these specific areas requires an on-board localisation system that can determine the current vehicle position. Examples of ground-vehicle solutions for automated mink feeding can be found in Figures 1.3a and 3.4a.

In the case illustrated in Figure 3.2, it was unclear whether the feeding should be performed on the upper or lower part of the mink cages on each side of the robot vehicle. The intention was to have the capacity to switch feeding between the upper and lower parts of the mink cages without moving the feeding-arm system by using two feeding outputs for one side. The feedback from the stakeholders determined that food is placed at one level for an entire row of mink cages and that the cage heights can vary between rows. In addition, the feedback from the stakeholders made it clear that analysis

of the different solutions to this problem was required. Therefore, a sixth contribution of this thesis is:

**Contribution 6.** Manual analysis of alternative design solutions using DSE for a robot where different candidates exist.

The co-modelling methodology extensions defined in Section 2.2 were used to model the system solutions. This co-modelling case also clarified the need for the ability to branch into multiple modelling cases when applying the co-modelling methodology extensions. This branching ability was added to the co-modelling extensions, to facilitate the exploration of multiple solutions to a problem.

### 3.2.1 Robotic mink-feeding-arm solutions

Feeding mink is a high precision task compared to that of cows and pigs, because the normal feeding area has been empirically determined to be between 0.2-0.35 m for each cage. Each mink cage must be dosed with a predetermined amount of fodder, which is placed on top of the cage. A co-model was therefore designed for a robot system to dispense mink food along a row of cages at predetermined locations. The robot co-model was evaluated according to the overall system performance demands for the different system configurations.

We considered solutions with single- and double-sided feeding-arm outputs with two prismatic or revolute joints. The goal of this analysis was to determine the most viable candidate for development into an actual system. Double-sided feeding was considered based on the idea of better utilisation of the feeding robot. Feeding on both sides would double the output placement of fodder at the same vehicle speed. Further, shifting the arms by half a cage length would allow the same pump system to be used for both sides, while still permitting individual amounts of fodder to be output.

### 3.2.2 Results

Each solution was modelled for evaluation based on the DSE co-simulation response. The DSE functionality was used to evaluate each co-simulation robot system through collision checking and in relation to placement of the mink fodder. Throughout the model development, we ran the same scenarios using DSE on the four different candidate solutions. The DSE results were

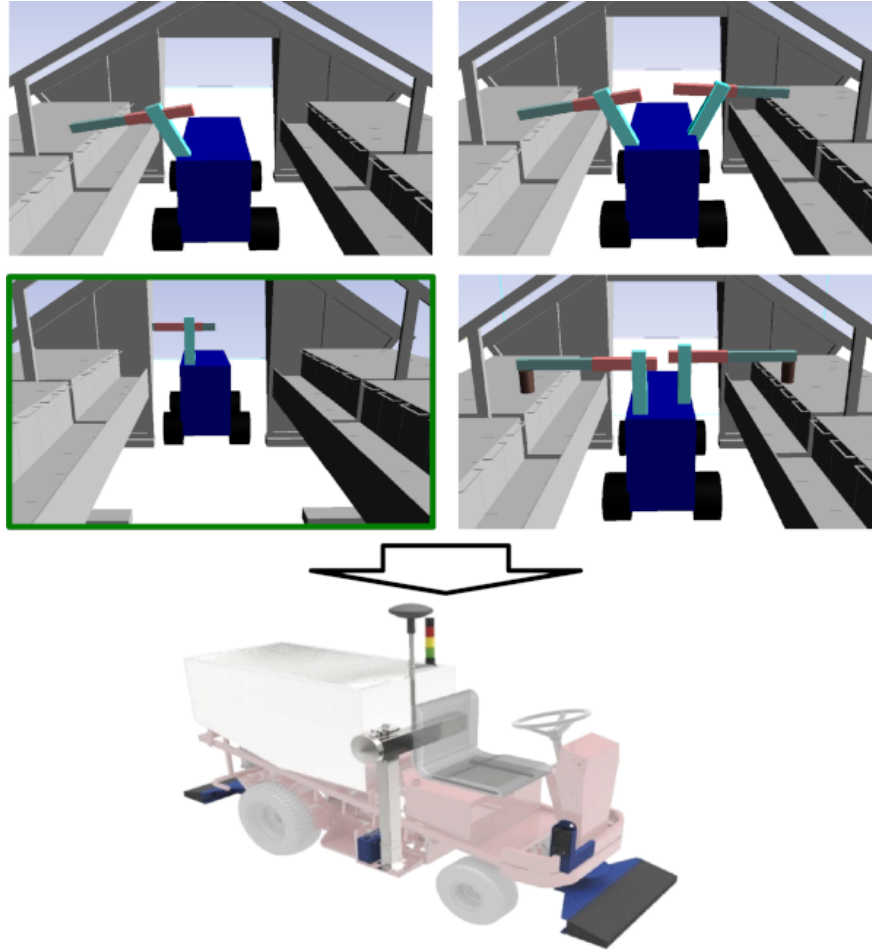


Figure 3.3: Feeding-arm candidate solutions experimentally examined to determine a viable candidate solution.

used to determine when the co-model was working as intended and to allow the project stakeholders to compare the solutions.

In the final version, all four candidate solutions successfully fulfilled the stakeholder requirements. The four candidate solutions for the four different arm and feeding systems are illustrated in Figure 3.3. The single-sided feeding-arm solution with prismatic joints was selected for feed-arm operation, as the prismatic solution was deemed simpler to operate manually should



this be necessary. The single-side feeding-arm solution was chosen over a double-sided feeding-arm solution, because the stakeholders deemed it to be a better first prototype design for the actual robot. The double-sided solution can be easily applied as an upgrade of the same prototype platform at a later stage, because no major software upgrades are required.

### 3.3 Derivation of a New Design Idea from the Creative Process

Identification tags such as RFID have been used in the last decade to provide local and global positioning information for a vehicle [15, 61, 93]. Examples of other identification tags that have been used for localisation are bar-codes, Quick response (QR), or other visual identification code tags, such as those illustrated in Figure 3.4. In the illustrated cases, the designed vehicle was equipped with a tag reader at a known position on the vehicle. Identification tags with known positions were placed along the vehicle's path to provide fixed position references (landmarks). Using an a priori map of the identification tag locations, the vehicle could obtain absolute positioning estimates in relation to its surroundings. Positioning estimates from the identification tags were provided to the vehicle, when the tag reader was within the detection zone of each tag.



(a) Bar-code localisation solution<sup>1</sup>.

(b) RFID localisation solution.

Figure 3.4: Example of different identification-tag-based localisation systems, which allow the robotic vehicle to automatically distribute fodder along the cage rows.

<sup>7</sup> Source: Image from Maach Technic video.

Sensory information from other sensor sources can be used to reduce the required number of identification tags. By combining the identification tag locations with other on-board positioning sensors, for example, wheel rotary encoders and an IMU, the vehicle can continually update the current position estimate [62]. The required distance between identification tags is dependent on the user-defined position accuracy and available data from other sensor sources.

### 3.3.1 Idea motivating the invention

A vehicle with mink fodder transports a varying load over time, which affects the steering and operational performance. When a wheel rotary encoder is used to estimate the distance travelled, one normally assumes an a priori known effective wheel radius  $R_{ee}$ . By measuring the number of wheel rotations using the wheel rotary encoders, the vehicle computer can provide an estimate of the distance travelled  $d_e$ , with

$$d_e = 2\pi R_{ee} \frac{G_k}{G_o} \quad (3.1)$$

where  $G_k$  is the current count of the encoder and there are  $G_o$  counts per revolution. The wheel speed can be calculated using the estimate of the rotational speed

$$u_e = R_{ee}\omega_e \approx R_{ee} \frac{2\pi G_k}{G_o T_k} \quad (3.2)$$

where  $\omega_e$  is the estimate of the wheel rotational speed and  $T_k$  is the sample time.

When operating a load-transporting vehicle, the effective radius of the wheel will vary dependent on the current load transported. Following equation 3.1, if the  $R_e$  is compressed by 0.01 m compared to normal operation, this corresponds to an estimated difference of  $\approx 0.0628$  m for each rotation, not accounting for other influencing factors. The changing load conditions makes it relevant to provide a means of estimating  $R_e$  online, i.e., during operation. Therefore, another contribution of this thesis is:

**Contribution 7.** A method for online estimation of wheel and vehicle parameters for a load-carrying ground vehicle using two or more identification tag readers.

The patent application for this device is given in [P19], while an introduction to the concept is given in this section. The concept was devised by working with virtual prototypes of the robotic mink-feeding vehicle using the co-modelling and co-simulation methodology extensions presented in Section 2.2. The solution to the wheel rotary encoder problem was devised by working with the example from the previous section and by developing the virtual prototype solution illustrated in Figure 3.5.

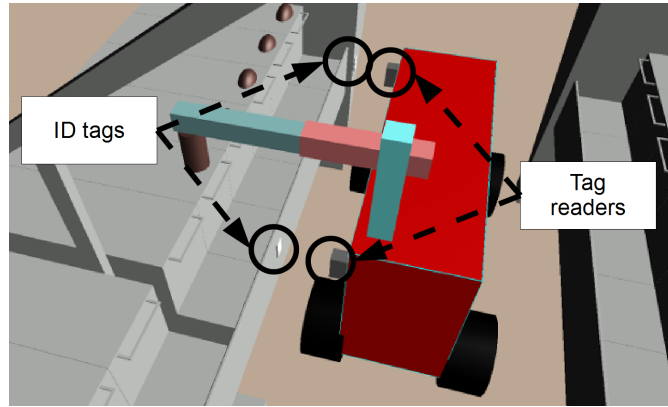


Figure 3.5: General invention concept. The vehicle uses two or more identification tag readers for the localisation process.

This invention is intended to improve localisation of load-changing automated ground-vehicles where the tyre experiences deformation, e.g., in the case of pneumatic tyres, depending on the load distribution at a given instant. A vehicle for feeding mink could utilise this invention to improve localisation estimates. Both a fully automated version and a version driven by a human driver with automatic feeding could benefit from this invention.

### 3.3.2 Envisioned system configuration

The envisioned standard system illustrated in Figure 3.6 is composed of a load-changing vehicle with sensory input from two tag readers, wheel rotary encoders, and an IMU. The design concept is to utilise the tag readers on the vehicle with a fixed distance in the known driving direction, to provide a reference distance and time measurement so that online calibration of the wheel rotary encoder values and vehicle parameter estimation can be performed. Online calibration of the wheel rotary encoder values can be used

to increase the distance between the identification tags. By increasing the distance between the identification tags, the number of tags needed to cover the same area can be diminished. Each tag has the potential to be read by both tag readers, which in itself increases the number of position updates using the same number of tags.

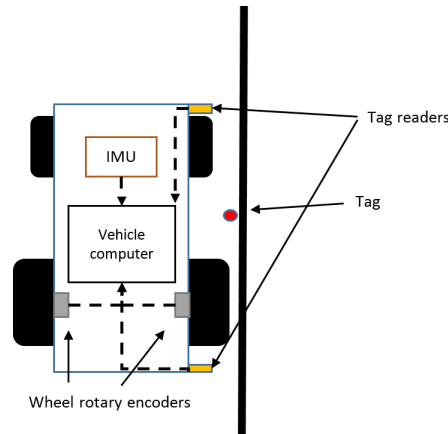


Figure 3.6: Sample configuration of envisioned invented system.

The envisioned system has two or more tag readers of the same or different types. Both tag readers mounted on the vehicle must be able to read the same tag. A tag could, for example contain both a bar-code string and RFID information, making it possible to utilise a combination of tag readers.

The time required for the tag reader to pass the same identification tag can be used as a speed estimate source. Compared to the IMU and the wheel rotary encoder sensor measurements, the tag-reader based vehicle speed estimates are not based on a derived measurement in terms of wheel rotational speed or acceleration measured by the IMU. The precision of the speed estimate can influence the placing of the load in the surroundings, as the systems may have a reaction time that affects the placement position.

The combined information from the tag readers in combination with the IMU and the wheel rotary encoders can indicate whether each tag reader is working properly and whether the identification tags can be read. If the vehicle passes a predefined number of tags but only one of the readers is detecting the tags, the operator will receive a warning about the non-inputting tag reader. Combined information from two tag readers can also be used to evaluate whether an identification tag is placed correctly according to the

identification tag map. In cases where both tag readers are unable to read an identification tag over multiple runs, the system could warn the operator that the identification tag needs replacement.

### 3.3.3 Detection method

Figure 3.7 illustrates an example of tag detection using RFID readers. The RFID reader has a detection zone in which it can receive identification information from an RFID tag, such as Identification data (ID). The vehicle computer receives the RFID reader information at a specific periodic time interval. When there is no tag inside the RFID-reader receiving zone, the reader either transmits no data or no tag in range to the computer. When one of the RFID reader detection zones moves within range of the RFID tag, the computer logs a tag event. When a bar-code, QR, or visual tag reader

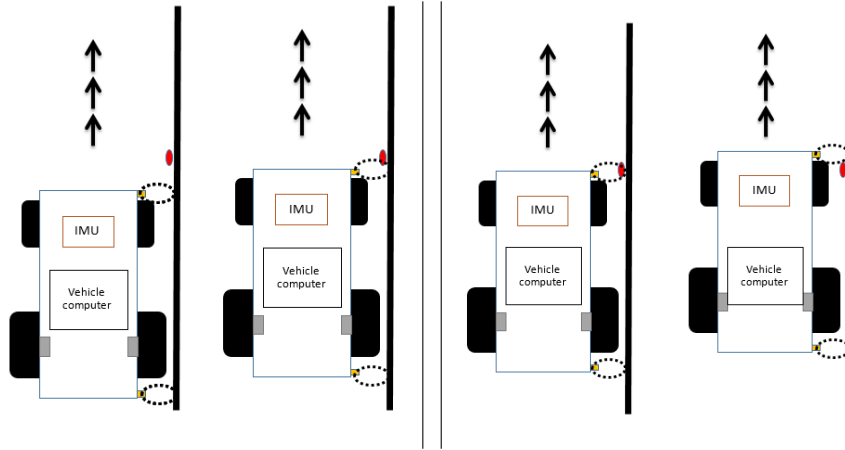


Figure 3.7: Method used in the calibration procedure.

is utilised, the principle remains the same in terms of detection edges, even though the readers have different types of detection zones. The next event occurs when the tag reader moves outside the logged tag's detection zone. Both tag events are defined as specific events in time and used as time interval references when both readers have passed the tag.

The edges of the tag readers' receiving ranges can be perceived as known positions in the lateral direction of the vehicle movement. In terms of the vehicle movement direction, we denote the two readers as the front and rear tag-reader units. Using two of these points, we can define a length distance,

with a total of four length distances ( $d_{ii}, d_{oo}, d_{io}, d_{oi}$ ) for the two tag readers. Here,  $d_{ii}$  denotes the distance between the points for activation of the front and rear tag readers via an ingoing tag event.

The movement direction determines when we should start the parameter estimation procedure. Until the expected event has been triggered at the rear tag reader, the computer continues to log data from the wheel rotary encoders. The flow diagram for the detection procedure is documented in the patent application [P23] illustrated in internal Figures 6 and 7. When the vehicle has passed a single tag, it produces four encoder measurements and four time intervals in total, which can be matched to the known length distances.

### 3.3.4 Parameter estimation processing example

Multiple methods can be used to estimate the relevant parameters related to the vehicle. A number of these methods are mentioned below:

- Direct calculation for single sample based on equation 3.1
- Least squares estimation [16, Chapter 12]
- Kalman filtering [50, 87]

Based on equation 3.1, the least squares method can be implemented in order to estimate the current rolling wheel radius  $R_{ee}^*$  for a single tag, where

$$R_{ee}^* = \frac{2\pi(d_{ii}G_{ii_k} + d_{io}G_{io_k} + d_{oi}G_{oi_k} + d_{oo}G_{oo_k})}{(d_{ii}^2 + d_{io}^2 + d_{oi}^2 + d_{oo}^2)G_o} \quad (3.3)$$

The intention here is to use the combined measurements to estimate  $R_{ee}^*$ . The above case is for a single encoder on a flat surface. If two encoders are available, as depicted above, one can calculate the average the value for matching samples.

## 3.4 Exploring Controller Solutions

In industrial projects, components can be produced by different producers; this includes software components. Parts of the software components comprising a system may be locked against modification by the external developers making the component black box [44]. Locked software components pose a design and modification challenge for both farmers and external developers in the agriculture industry [88]. Scenarios involving locked software

components mean that it is important to explore whether alternative solutions in other parts of the system design space, might be modified to obtain the intended result. Co-modelling can constitute a means of modelling these agriculture systems using approximations of the locked software components, allowing developers to identify alternative solutions within the design space that they can manipulate.

#### 3.4.1 Agricultural vehicles transporting loads

Load-carrying agricultural vehicles can experience load changes during operation. Changes in load occur in operational tasks where animal food is dispensed, sprayer tanks are emptied, or operational implements change position over time. Load changes affect the weight distribution of the vehicle and, consequently, the steering and driving performance. The surface conditions the vehicle traverses also vary in response to the environment. As a consequence, automated guidance controllers for such agricultural vehicles should have the ability to adapt to changes in load and surface conditions.

Commercial steering controller solutions can be locked, i.e., external developers cannot make direct changes to the software. Such locked software solutions render it necessary to explore solutions in other areas of the system when adjustments to the functionality need to be made. Therefore, another contribution of this thesis is:

**Contribution 8.** Automated design space exploration to determine adaptive settings for a steering controller solution.

Here, the co-modelling methodology extensions defined in Section 2.2 were used to model an auto-steering solution for an agricultural vehicle. The auto-steering solution was based on an early version of method 1 described in Section 2.4, which ensures a one-to-one consistency between the co-model and the actual implementation. A pre-modelled auto-steering solution was utilised instead of attempting to use measurements to develop an estimated model of a commercial auto-steering system. Such a pre-modelled auto-steering solution ensures correct modelling of these system parts and allows the project to focus on the exploration of alternative system changes. The auto-steering software is assumed to be a locked module, and the search for alternative solutions is therefore relevant. The design concept here was to use an adaptive vehicle drive speed as the alternative solution, to facilitate

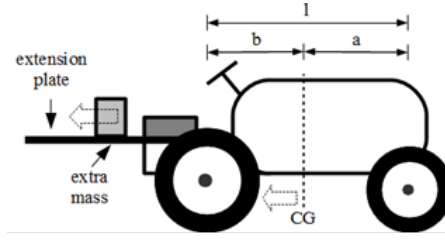
auto-steering performance interaction with changing vehicle weight distribution and surface conditions.

### 3.4.2 Co-model setup

The co-modelled case for autonomous steering operation discussed here uses the ASuBot vehicle platform. The ASuBot vehicle used in the modelling is a Massey Ferguson MF 38-15SD garden tractor. The garden tractor is also



(a) Visualisation of the ASuBot co-simulation for the load-change test case.



(b) Sketch of the garden tractor equipped with a load displacement mechanism controlling the load distribution between the front and rear wheels.

Figure 3.8: Virtual setup for the DSE search.

equipped with the mechanical load displacement mechanism illustrated in Figure 3.8b, which enables experiments with the CG placement. The co-model of the garden tractor is used to describe the different CG placement scenarios when the garden tractor is set to follow a pre-planned route. The shift of the CG is intended to model load changing that affects the operation of the garden tractor. The change in the load distribution is performed in the co-model, by adjusting the values of  $a$  and  $b$  for the garden tractor, with

$$a = a_0 + \Delta cg \quad (3.4)$$

$$b = L - (a_0 + \Delta cg) \quad (3.5)$$

where  $a_0$  is the normal distance from the front wheel to the CG,  $\Delta cg$  is the shift in the CG, and  $L$  is the wheelbase. The current position of the CG determines the load ratio ( $N_f, N_r$ ) placed on the back and front wheels. For the front wheels, the load can be calculated from

$$N_f = \frac{b}{L} N_{tot} \quad (3.6)$$



where  $N_{tot}$  is the total normal force.

The co-model utilises the parameter  $\mu$  in the CT model to describe the vehicle wheel-surface interaction in terms of wheel slip (see Section 2.4 for a description of the differential equations). The change in surface condition is intended to co-simulate the garden tractor solution for different environments.

The pre-planned route consists of a sequence of waypoints with relative Cartesian coordinates, which describe the path the vehicle must follow. A complete route for an agricultural vehicle consists of a number of distinct segments with the possibility of repetition throughout the path. All intended path scenarios are encompassed into the single looped path illustrated in Figure 3.8a, so as to reduce the length of the test scenario. The selected route is intended to represent a realistic scenario that the vehicle could encounter in the field. The route for the project consists of straight lines in opposite parallel directions, with circle arc turns in the clockwise and anticlockwise directions and two lane changes in the opposite direction.

### 3.4.3 Automatic Co-model Analysis

The ACA implementation utilised in this project is used to select a viable candidate setup based on DSE. The ACA is set to perform a DSE for a backwards shift in CG between 0 and 0.4 m. The ACA explores the drive speed  $u$  in the range 1–2 m/s representing the intended operational vehicle speed area. Note, that 1–2 m/s is the speed range at which the garden tractor is expected to operate within under normal conditions. Throughout each co-simulation, the drive speed is kept constant, so the evaluation is not based on specific parts of the route; this allows an overall estimate of the steering performance for the route to be obtained.

The ACA also explores tyre-surface friction  $\mu$  coefficients between 0.55 and 0.7, representing asphalt/concrete, soil, gravel, and sand conditions [90]. A variety of surface conditions are used in order to determine their impact on the auto-steering operation performance. In Crescendo, the ACA functionality is used to automatically run all the different surface conditions for the chosen drive speeds.

The DSE is used in a mode that combines automatic and manual execution. In this case, the automatic mode is applied, which involves parameter sweeping of the complete drive speed range with a 0.2 m/s interval. The new search drive speed range is manually selected when the border between the viable and unviable solutions is found. The ACA process is then repeated with a 0.1 m/s step interval to increase the precession. This process is in-

tended to first provide a rough overall view and then to zoom in on the areas of relevance. The process can be repeated for even smaller drive-speed step intervals, but from experience, it was determined that 0.1 m/s was the controllable limit for this garden tractor.

To evaluate the results from the ACA runs, a cost function was used to compare the vehicle movement against the evaluation route. Starting from the first waypoint in the route sequence, the direct distance between the GNSS-receiver and the relative route, which is also known as XTE [28], was determined. The viable candidate settings were determined based on a maximum criterion of 0.3m XTE for each simulation. The evaluation criterion for this case study is the acceptable deviation from the route which was chosen as a sample value to demonstrate selection of viable solutions. Note that, if the described ACA are to be rerun for a specific operational task intended for the garden tractor, the evaluation criteria value should be chosen to fit these demands.

#### 3.4.4 Results

The ACA was run for the chosen design space to produce the output path for each co-simulation. Each co-simulation was run until the vehicle had

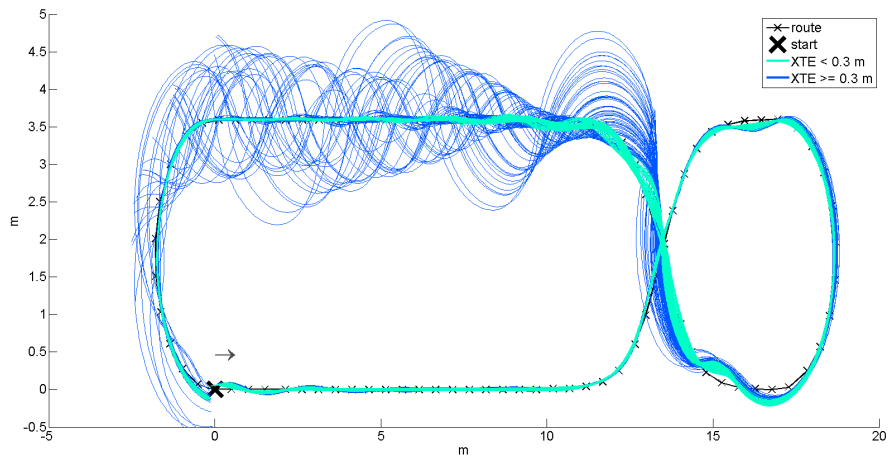


Figure 3.9: Simulated paths from ACA plotted in relation to the route. The simulation path results are coloured based on a 0.3m maximum XTE criterion.

traversed the route or the controller was unable to steer towards any remain-

ing route waypoints. The results are illustrated in Figure 3.9 and 3.10, and the simulations are coloured based on the evaluation criteria. The data in both Figure 3.9 and 3.10 are plotted for  $\mu = 0.55$ , which represents the tyre-surface contact for wet soil. The automated vehicle may be unable to determine the specific surface it is traversing at any given time; therefore, it is helpful to assume the vehicle is always moving on wet soil.

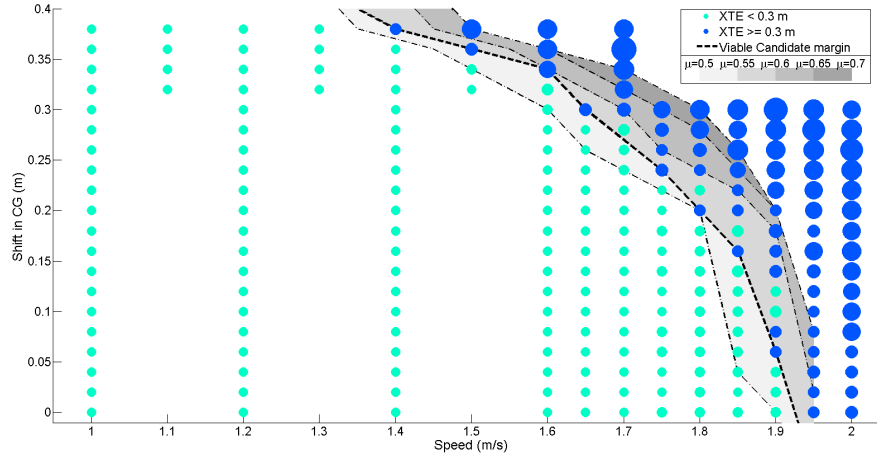


Figure 3.10: The full set of ACA results. Blue represents the non-viable speed setting candidates for  $\mu = 0.55$ . The safety margins are plotted for  $\mu = 0.5$ – $0.7$ . The  $\mu = 0.5$  scenario is plotted to illustrate the conditions outside the worst-case range.

The results from the ACA provide the developer with the ability to design an adaptive solution regulating the speed in relation to the current vehicle CG. The final runs of the ACA produce a smaller subset of the total explored design space that indicates the margin between viable and non-viable control setting candidates.

### 3.4.5 Remarks on results

The results obtained here indicate that the simulation and DSE method can be used to improve the performance, of classical guidance controller systems on load-changing vehicles. A small number of instances have been successfully tested on the actual garden tractor, but further testing is required in order to cover the full range of CG positions. Future DSE analysis in this area

should also incorporate a combination of different load distributions and load amounts, to encompass a broad range of scenarios.

This DSE case study should be viewed as an approach to determining a solution for the circumvention of locked components of a software solution using co-modelling and co-simulation. If developers had access to the locked components, they could simply implement a yaw-rate controller in the steering solution to compensate for the load-change problems.

### 3.5 Obtaining a Multidisciplinary Solution Overview using DSE

In some instances, candidate solution for the same design problem can be found in multiple disciplines. An overview of these solutions should then be provided, so the stakeholders can make an informed choice between the different disciplinary solutions. As an illustration of this type of analysis, the co-model in Section 2.5 was intended to give an overview of a multi-disciplinary engineering design problem. Here, we revisit the problem scenario from Section 3.3 for solutions to the tyre  $R_e$  and transported load. We assume that the invention solution has not been considered and other approaches are explored instead. Therefore, the final contribution of this thesis is:

**Contribution 9.** A multi-domain design space exploration analysis has been illustrated, involving evaluation of solutions from different engineering disciplines for the same design problem.

These estimation problems require cross-disciplinary analyses, because multiple factors affect the outcomes and possible solutions can be found in different engineering disciplines. Here, we demonstrate the approach to analysing the problem by modelling a load-carrying robot used for dispensing mink fodder at predetermined locations along rows of cages.

#### 3.5.1 System performance demands

The system performance demands define the task robot must complete in order to be considered effective. The system performance required by the project stakeholders includes the following:

- A maximum vehicle speed of 0.25 m/s (conforming to ISO-10218 [1])
- No collisions with surroundings as illustrated in Figure 2.9.

- The distance between the RFID tags  $d_t$  should be between 0.3 m and 20 m.
- Feeding with a precision of  $\pm 0.08$  m inside the placement areas.

It should be noted that the performance requirements are non-domain-specific and focus on the overall performance of the robot. Here, the maximum distance between the RFID tags represents the length of the feeding area and sets the limit for the minimum number of tags. The lower limit for  $d_t$  is chosen based on the mink cages length used in the co-modelling, resulting in one RFID tag for each cage.

### 3.5.2 Modelling cases

The co-model describes the vehicle and its sensor, actuators, steering controller, feeding system, and sensor-fusion components. The goal was to achieve the maximum possible distance between the RFID tags without compromising the pre-set system constraints. The question here was whether the loading of the vehicle should be accounted for by reducing the maximum compression of the tyre, implementing a compensation method in the DE controller, or a combination of both. The following DE controller conditions were applied:

- <**Static**> The estimated effective tyre radius was considered to be the mean of the values for the unloaded and fully loaded robot. This is based on the assumption that the mean value will produce the least overall error in the estimate.
- <**Pre-calibration**> A pre-measured estimate of the current rear tyre wheel radius in relation to the transported load is used in the DE part of the co-model. The estimates of the effective radius were obtained through the MATLAB bridge and directly passed from 20-sim with an accuracy of  $\pm 0.001$  m.
- <**Estimator**> The input data obtained by the vision sensor were used to estimate the current effective radius before entering the feeding area. This estimate was based on the distance travelled between the updates, with an accuracy of  $-0.005$  m.

Rather than simulating a single scenario, the test set shown in Table 3.1 is designed to evaluate the expected min-mean-max operational values. The DSE was used to evaluate the configuration solutions shown in Table 3.1

in different development domains, so as to account for the load-carrying effects. The operational values represent the expected range of transported load values and the surface-wheel and initial robot position conditions. The initial position was of interest in this case because a human operator may inaccurately place the robot at its starting point. The models of the tyre radius on the CT side were varied between low and fully loaded conditions. The tyre-surface friction was of interest here as the vehicle must stop in order to deploy the feeding arm before beginning the feeding process.

Table 3.1: Candidate solution sets used for the system evaluation and min-mean-max test set used for the DSE of the feeding robot.

System configurations		Min-mean-max test set		
Rear tyre radius change	Vehicle state estimate	Load mass	Surface-tyre $\mu$ friction	Initial Position $x_{init}, y_{init}, \psi_{init}$
0.001 m	<Static>	1% (6 kg)	0.3	$x_{init} = \{-0.5 \text{ m}, 0 \text{ m}, 0.5 \text{ m}\}$
0.02 m	<Pre-calibration>	50% (300 kg)	0.5	$y_{init} = \{-0.1 \text{ m}, 0 \text{ m}, 0.1 \text{ m}\}$
0.04 m	<Estimator>	100% (600 kg)	0.7	$\psi_{init} = \{-15^\circ, 0^\circ, 15^\circ\}$

### 3.5.3 Automatic co-model analysis

To select the value of  $d_t$  parameter that for the ACA co-simulation, an output cost-function is defined. The result of each co-simulation is evaluated based on the success-rate in placing the fodder at the correct positions between two tags.

$$f_{d_t} = -\frac{b_{suc}^2}{b_{tot}} \quad (3.7)$$

where  $b_{tot}$  is total placement positions between two RFID-tags and  $b_{suc}$  is the number of successfully fodder placements. The output of the cost-function ensures largest  $d_t$  with the highest number of successful fodder placements is the minima for the searchable range. In mathematics, by convention optimization problems are usually stated in terms of minimization, thus the minus sign. ACA uses the golden section search method [16, Chapter 7] in combination with the cost-function in Equation (3.7), to determine the best candidate within the design space. To use golden-section search it is assumed that the cost-function is unimodal function, meaning that there is only a single local minimum.

### 3.5.4 Results

The result of the ACA is illustrated in Figure 3.11 using boxplots. In each box-plot, the central line marks the median, the edges of the box are the 25th and 75th percentiles and the whiskers marks to the two most extreme data points. Each system configurations box-plot, represents the determined max RFID  $d_t$  distance values, for each instance in the min-mean-max test set from Table 3.1.

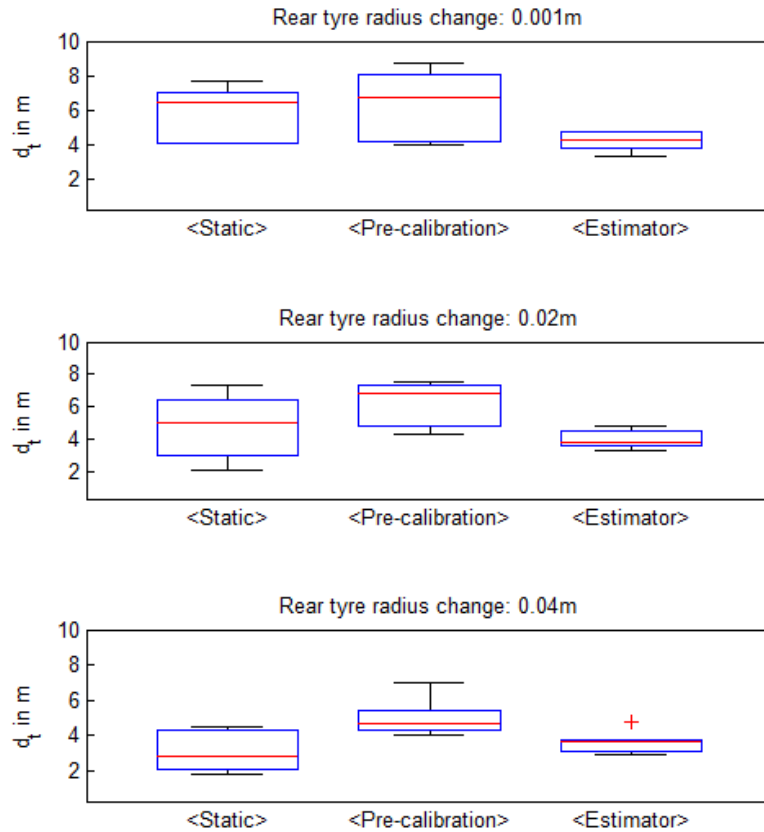


Figure 3.11: Result of the ACA run for the feeding farming co-model in terms of determined  $d_t$ , for the nine different system configurations in Table 3.1.

### 3.5.5 Discussion of results

The results provide an overview of the candidate system configurations based on the estimated RFID tag distance. Developers can use the candidate overview to select configurations for testing on the an actual platform. The intention here is to provide the stakeholders in the project with an overview of the different candidate solutions.

From the box plots, it can be seen that <Pre-calibration> method provides the best overall results for all tyre solutions. This is to be expected since the value  $R_{ee}$  used matches reality with a high degree of accuracy. The candidate with the best results in terms of largest overall  $d_t$  for all co-simulation cases is not necessarily the one that will be chosen for implementation on the actual robot. Factors such as material, development, implementation, and maintenance costs affect the final configuration selection. The 0.001 m tyre compression solution requires adjustment by an operator before start-up. The pre-calibrated solution must be updated periodically to account for changes in the robot setup. The vision solution is calibrated for a specific set of farm configurations and requires adjustments for new conditions. Nevertheless, this overview provides a means of evaluating the external costs with respect to the expected distance between the RFID tag and affords a more educated configuration selection.

Note, that the co-model can be reused to explore other aspects of this robotic system, such as the invention described in Section 3.3. The time saved by the co-modelling and ACA could be invested in other areas of the project. The overview obtained by ACA does not guarantee optimal solutions, but it does facilitate the analysis of multiple candidate solutions.

## 3.6 Summary

This chapter has presented four different search approaches to DSE using co-modelling and co-simulation. The results show how DSE can be used for both automated and manual exploration of a design space. The four different approaches illustrate that DSE can be used for virtual prototype development support and the determination of candidate solutions.



# 4

---

## Concluding Remarks

---

This chapter summarises the results achieved in this thesis and presents the conclusions to the research hypothesis. In this thesis, a model-based approach to the development of automated and robotic agricultural ground vehicles was proposed. The hypothesis and objectives of the thesis defined in Chapter 1 are related to the chapters on automated and robotic ground-vehicle co-modelling (Chapter 2) and Design Space Exploration (Chapter 3).

The purpose of this chapter is to evaluate the outcome of the thesis, and to assess the extent to which the evaluation criteria, objectives, and hypothesis have been met. Section 4.1 summarises the research contributions; this is followed by an evaluation of research contributions in Section 4.2 and an assessment of how the contributions have fulfilled the PhD project hypothesis which is given in Section 4.3. Finally, future work is described and presented in Section 4.4. Some of these areas will be addressed in the follow-up research project INTO-CPS<sup>1</sup>, which will be conducted using industrial case studies. Other topics discussed in the future work section are also related to a possible future postdoctoral research project.

### 4.1 Research Contributions

This PhD thesis has presented nine research contributions in the previous chapters. The research contributions are collected into three different categories: *Methodological extensions*, *Co-modelling of automated and robotic ground vehicles* and *Methods to perform Design Space Exploration*. An overview of the contributions and the relations between them is provided in Figure 4.1. The contributions have been given individual short-form names for easier identification (C1, C2, C3, etc.). The methodological extensions represented using Contribution 1 (blue block) have been applied in the modelling of dif-

---

<sup>1</sup> The INTO-CPS project website can be found at: <http://into-cps.au.dk/>.

ferent automated and robotics agricultural ground-vehicle case studies. The contributions that are related to the implementation of co-modelling of various automated and robotic agricultural ground-vehicle systems (using green blocks) are categorised by the green dashed border marking. The green block contributions comprise 2 to 5. The remaining contributions (6 to 9) which are related to DSE (using yellow blocks), are categorised by the light yellow dot-dashed border marking. Individual contributions that are interconnected are marked with dashed arrows, to clarify their influences upon each other during their derivation.

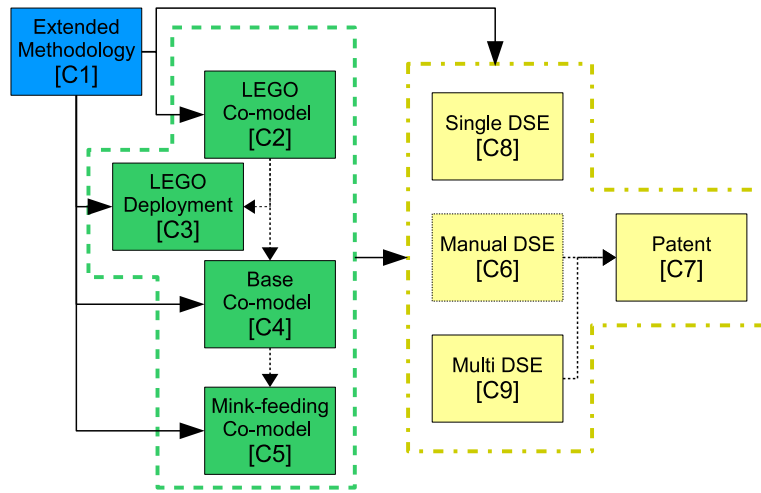


Figure 4.1: Overview of the research contributions presented in this PhD thesis and how their categorisation in relation to each other.

The interconnection between the automated or robotic agricultural ground-vehicle modelling cases illustrates the gradual expansion of the co-modelling of these systems. The invention concept was derived through research related to contributions 7 and 9.

#### 4.1.1 Methodological extensions

The literature survey of co-simulation in the agriculture domain presented in Section 2.1 revealed the lack of a defined development methodology for this area of research. The base development methodologies from [89, 33] focused on model-based development of embedded and cyber physical systems. This constituted the first contribution, which was formulated as:

**Contribution 1.** An extended co-modelling and co-simulation methodology for the development of automated and robotic agricultural ground-vehicle systems.

Section 2.2 introduced the extended model-based methodology for the development of automated and robotics agricultural ground vehicles, which was developed based on the three presented case studies.

#### 4.1.2 Co-modelling of automated and robotic ground vehicles

The second group of contributions are related to modelling case studies, which have contributed to the definition of the current extended development methodology for the model-based design of automated and robotic agricultural ground-vehicles. The presented development methodology was gradually extended based on the experience acquired from the co-modelling and co-simulation of these main case studies. The LEGO tractor case study used for field coverage testing was used to refine the co-model development process and the gradual deployment of a co-model. That case study led to the following contributions:

**Contribution 2.** A kinematic co-model of an automated LEGO tractor platform.

**Contribution 3.** Deployment of a co-model solution to a LEGO tractor to allow for two-step gradual verification and movement from simulation to an actual system.

An extended development methodology complemented by a base agricultural co-model was developed to support future model-based development. This base automated agricultural vehicle co-model was presented in Section 2.4, which described the aspects of both DE and CT modelling. This contribution will potentially support future mobile development of solutions based on axle steered ground vehicles:

**Contribution 4.** A dynamic co-model of a front- or back-axle-steered automated agricultural ground-vehicle platform.

We illustrated how the base co-model from contribution 4, can be extended for a specific purpose using the extended development methodology. This case study involved development for a mink-feeding robot vehicle, and was used for sensor-fusion-based localisation and analysis of load-distribution dynamics. The details of this study are described in Section 2.5. The contribution of this case study is summarised as:

**Contribution 5.** A specialised co-modelling solution for automated and robotic agricultural ground-vehicle solutions related to mink feeding.

#### 4.1.3 Methods to perform Design Space Exploration

DSE was applied in two agricultural cases, resulting in four contributions to this research domain. The first two contributions relate to general development using the extended development methodology and the potential results this can produce, as presented in Sections 3.2 and 3.3:

**Contribution 6.** Manual analysis of alternative design solutions using DSE for a robot where different candidates exist.

**Contribution 7.** A method for online estimation of wheel and vehicle parameters for a load-carrying ground vehicle using two or more identification tag readers.

To explore candidate solutions in a design space in a more automated manner using co-modelling and co-simulation, the ACA functionality in Crescendo was used and extended, yielding the two contributions described in Sections 3.4 and 3.5:

**Contribution 8.** Automated design space exploration to determine adaptive settings for a steering controller solution.

**Contribution 9.** A multi-domain design space exploration analysis has been illustrated, involving evaluation of solutions from different engineering disciplines for the same design problem.

Three of the contributions [C6, C7, C9] are related to different aspects of the system used in the mink-feeding agricultural case study. Throughout this PhD thesis, the extended development methodology has been used to develop these co-models for the performance of DSE. The robotic mink-feeding case study is a case that is currently being implemented in the industry for commercial use. The remaining contribution [C8] focuses on making changes to already implemented solutions in the agricultural industry and is of a more general nature. This contribution illustrates how DSE and ACA can be used to address development problems where the existing system contain locked software components.

## 4.2 Evaluation of Contributions

In this section, the contributions described in Chapters 2 and 3 are evaluated with respect to the evaluation criteria listed in Section 1.6. Evaluation of the industrial adoption of the work performed in this thesis is outside the PhD research scope; however, contributions [C4, C5, C6, and C7], developed during this PhD project, have been adopted in one form or another by industrial partners during the course of this research.

This evaluation is performed in terms of the different dimensions introduced in Section 1.6, and visually presented in Figure 4.2. The figure illustrates an informal ranking of the contributions providing an overview of how the individual contributions fulfill each criteria. The 0–4 scale used in the figure indicates the extent to which the contributions fulfil each of the evaluation criteria considered in the subfigures. The closer the shading comes to the edge of the spider-web, the greater the fulfilment of the given criterion.

An evaluation of all contributions is given below, with respect to the evaluation criteria and the individual gradings. Subfigure 4.2f illustrates the extent to which all the contributions add to the overall fulfilment of the evaluation criteria.

### 4.2.1 Multi-disciplinary collaboration support

To assist stakeholders addressing automated or robotic agricultural ground-vehicle multi-disciplinary design and to facilitate intercommunication between the engineering disciplines, an extended development methodology and a number of development cases have been created. This methodology, along with its application in the case studies and the analysis of co-models supports a common understanding between the disciplines and provides stake-

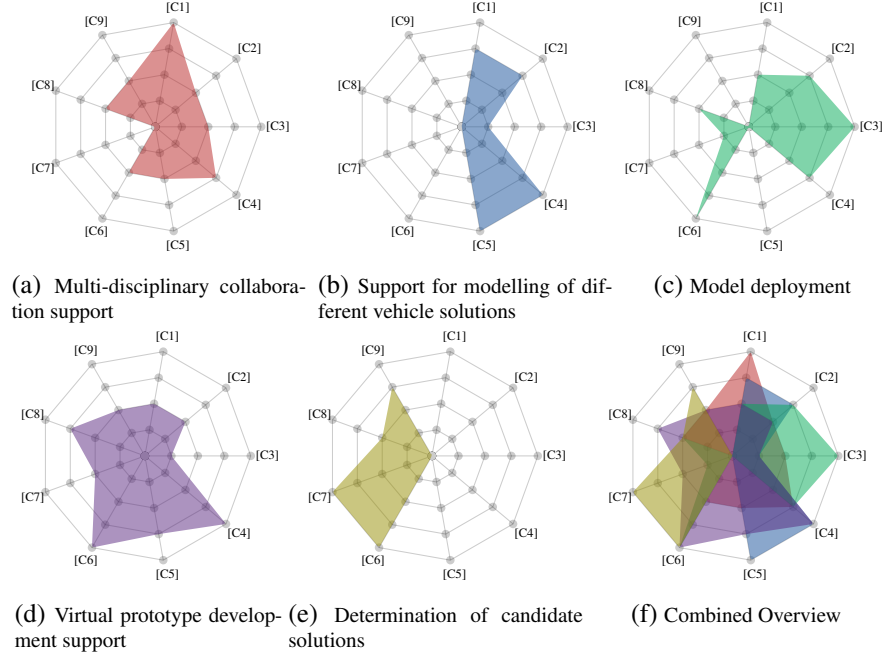


Figure 4.2: Relation between contributions and evaluation criteria.

holders with the ability to grasp concepts that are not inherent to their respective disciplines. Contribution 1, which covers the extended development methodology, is ranked as fully satisfying the multi-disciplinary collaboration support criterion, as it can be used for any vehicle type in the agricultural domain. The extended development methodology provide support for development in all phases of the project, from initiation to model deployment. Both contributions 2 and 3 support collaboration in combination with the extended development methodology, for projects on automated field coverage.

The base co-model for front- and back-axle-steered vehicles (contribution 4), in combination with the development methodology guidelines, provides general coverage support for development for projects based on such vehicle solutions. The extension made using contribution 5 is the more specialised case involving the mink-feeding system, but some aspects could be adapted to provide support for other related projects. Further, the three contributions related to the DSE part (contributions 6, 8, and 9) of this PhD thesis provide multi-disciplinary support by giving an overview of the stakeholders' current design space. Note that contribution 8 is given a low ranking here

since the determined solution requires further testing establish its the full validity.

#### 4.2.2 Model Deployment

Model deployment grades the contributions in terms of deployment of the components and results in the real-world systems. The intent is to verify that a solution developed using modelling and co-simulation applies to an actual system setting. The extended development methodology (contribution 1) has been awarded an impact level of two, as this contribution provides the guidelines for the deployment of co-model components. Both contributions 2 and 3 relate to the LEGO micro-tractor case used for testing field coverage operation. Contribution 3 has been awarded a higher ranking than Contribution 2 because full deployment to the application area was achieved here. The path-tracking methods from contribution 4 have been implemented on the AsuBot vehicle and the FixRobo mink-feeding robot from Compleks Innovation. However, contribution 4 must also be deployed for a back-axle-steered vehicle to receive the maximum grading.

Full coverage is achieved by contribution 6, where the robotic mink-feeding arm was implemented in a real-vehicle solution. Other feeding arm solutions from the DSE could also be deployed to the FixRobo vehicle solution, but the deployment procedure would be identical and would not involve new aspects of the system. The patent application of contribution 7, is awarded a ranking of one, as this solution was acquired by Compleks Innovation, but still requires implementation in a product solution.

#### 4.2.3 Determination of candidate solutions

Determining a candidate solution is related to the DSE and the use of co-models to determine solutions that can solve a design case. The intention is to determine prototype and parameter solutions for the automated or robotic agricultural ground-vehicles, on which the developers are working. Contributions 6 and 7 have the highest ranking in this area, as they provided a solution that could be ported to an actual industrial case. Contribution 8 has been awarded an average ranking for this evaluation criterion as the DE model has been deployed to the vehicle, but further testing needs to be performed to validate the solution fully. As regards contribution 9, we obtain an overview of the solutions only, and it is the task of the stakeholders to select the candidate solution they wish to implement.

#### 4.2.4 Support for modelling of different vehicle solutions

Contribution 1 can be used when developing co-models of different vehicle types that can be used to develop automated and robotic ground-vehicle solutions. Contributions 2 and 3 are related to co-models of vehicle solutions used for field coverage in the agricultural industry. Contribution 4 is a base vehicle model for front- and back-axle-steered ground-vehicle solutions, which can be adapted for new model-based development cases in combination with the extended development methodology. Contribution 5 concerns specialised co-modelling of a mink-feeding robotic ground vehicle to support system development. This mink-feeding robot co-model models the full operational aspects of the vehicle when it is operating within the mink farm.

#### 4.2.5 Virtual prototype development support

Virtual prototyping is the use of co-modelling, co-simulation, and visualisation of automated or robotic agricultural ground-vehicle solutions. To develop these virtual prototypes, we use the extended development methodology that comprises contribution 1, which must be combined with a concrete case study. The LEGO tractor co-model in contributions 2 and 3 could be used to explore alternative mechanical solutions for LEGO-based systems. However, it is concluded that directly reassembling the LEGO tractor is more appropriate and is, in itself, a form of vehicle solution prototype.

The base agricultural co-model in contribution 4 can be used to develop these prototypes conjunction with the extended development methodology. The base co-model has been used for virtual prototyping in contribution 6 and for the evaluation of the feeding arm and controller solutions respectively. Contribution 5 can primarily be used for virtual prototyping of the robotic mink-feeding systems and has been used for contributions 7 and 9.

### 4.3 PhD Project Hypothesis Validation

During the course of this PhD project, the different aspects of the hypothesis presented in Section 1.4 have been addressed using the contributions from the project. The hypothesis is comprised of two parts that have been developed into the evaluation criteria presented in Section 1.6. For completeness, the PhD project hypothesis is restated below:

- **Collaborative models can support multidisciplinary collaboration and system development.**



- **A collaborative model of a robotic or automated agricultural ground-vehicle can be utilised to explore alternative design configurations.**

The first part of the hypothesis is covered by the contributions illustrated in Figure 4.3a, using the evaluation criteria from Subfigures 4.2a, 4.2b, and 4.2c. Together, the evaluation results illustrated in Figure 4.3a are sufficient to validate the first part of the PhD project hypothesis.

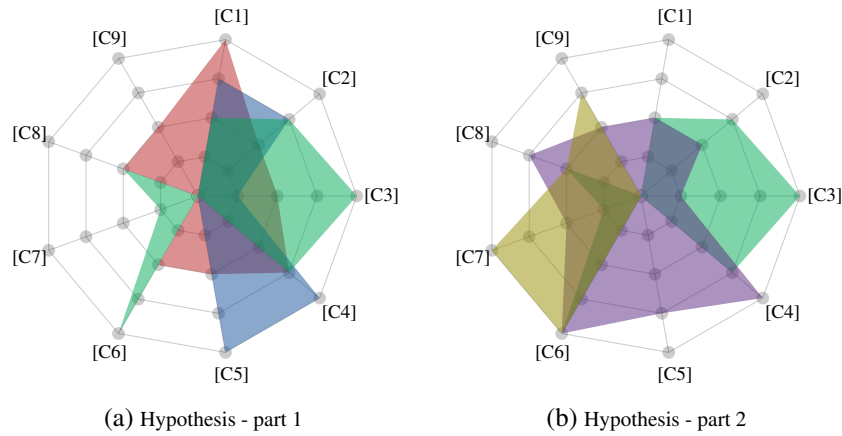


Figure 4.3: Relation between contributions, evaluation criteria, and PhD project hypothesis.

The second part of the PhD project hypothesis is covered by the contributions illustrated in Figure 4.3b, using the evaluation criteria from Subfigures 4.2c, 4.2d, and 4.2e. Coverage of the evaluation criteria based on the project contributions validates the second part of the PhD project hypothesis. The conclusion is that the project hypothesis have been fulfilled and overall progress have been made in the research area. The results achieved in this PhD thesis can be used in the future development of automated and robotic agricultural ground-vehicle solutions.

#### 4.4 Future Work

This section primarily focuses on a future industrial postdoctoral project in collaboration with the company Compleks Innovation, and is intended to extend the work conducted in this PhD thesis. We begin this section by presenting the general focus of the intended postdoctoral project, and describe how

the work conducted in this thesis can be incorporated in synergistic manner. We then describe how base co-models can be developed for additional vehicle types, and how they can be converted into an automated model generation process. The section concludes by presenting some future development cases.

#### 4.4.1 Postdoctoral project focus

The intention is to use well-known robotic development technologies, such as ROS, Gazebo, and a bullet physics engine, as part of the model-based development of robotic ground-vehicles. In existing robot simulation platforms, such as Gazebo, the developer must create a model of the robotic vehicle in terms of its physical layout, its mechanical solutions, and actuators and sensors. Even the reuse of parts of previous robotic vehicle models requires the developer to have a well-founded understanding of the inner workings of the simulation platforms.

Future work in the postdoctoral project should establish libraries specifically dedicated to the development of agricultural and other field robots, targeting a “plug-and-play” approach whenever a new robot vehicle solution is to be developed. Since the INTO-CPS project will be using the FMI interface in the research endeavours with co-modelling and co-simulation, it is expected that the FMI interface should be used to implement the development of the aforementioned robotics technologies into a co-modelling and co-simulation environment. This implementation of the FMI will not be part of the postdoctoral research, where the focus will be the development of model-based libraries for agricultural robots.

#### 4.4.2 Extending the range of base co-models

The PhD project has mainly created a basis model vehicle steered using the front or back axle. The modelling capabilities should be extended to support differential and four-wheeled steering vehicle solutions. Different pulled implement solutions, like sprayer trailers and crop tilling units, are also part of the agricultural operation, and should be part of future co-modelled solutions for providing project developmental support. These new base models would also broaden the support for the extended modelling methodology presented in Section 2.2 in this thesis. In essence, the base vehicle models should be included as components in these model-based libraries for agricultural robots.

Automating the model development process, based on these four base vehicle models, would allow production of a specialised modelling solution,

where significant parts of the model could be auto-generated, allowing the developer to manually implement only the parts that are specially developed for their specific applications. Over time, this auto-generated library could gradually be enriched by encompassing more case studies that have been developed based on the extended development methodology. Auto-generated models would also allow project developers in other disciplines with little experience in modelling and simulation to develop the ability to create full models, with little or no support from experienced developers in this area, thus achieving the intended “plug-and-play” capabilities.

#### **4.4.3 Development cases**

This subsection provides some directions on future work in the form of examples of future development cases. A number of these development cases are intended to be part of a future postdoctoral project. The development cases represent different areas of agricultural operations that would benefit from co-model-based development. These examples are also intended to allow the reader to “get new ideas” on what co-modelling can accomplish in terms of development.

##### **4.4.3.1 Mink-feeding robot ground-vehicle**

The design and co-modelling of solutions for a mink-feeding robot comprises a significant part of the contributions, which has been produced in this PhD thesis. Making the currently developed FixRobo robot solution by Kompleks Innovation into a completed commercial product that can be shipped to the market would strengthen the extended development methodology presented in this thesis. This would prove that this methodology has the potential to support development of automated and robotic agricultural ground-vehicles from the conception of the idea to a final product. Contribution 7 in this thesis that resulted in a patent application submitted last year, still needs to be deployed into a ground-vehicle realisation. The intention here is to deploy this effort in a possible future postdoctoral project.

##### **4.4.3.2 Dvorak Spider slope mower**

This machine is already in the market, but it is delivered with a manually operated remote-control system only that is supplied by another vendor. A joint co-operation with this company is currently being planned by Kompleks Innovation with the expectation for the addition of the required robot functionality. The interesting issue in relation to the suggested postdoctoral

project is that the current controller is not sufficiently fault tolerant. There-



Figure 4.4: Dvorak Spider slope mower<sup>2</sup>

fore, it is envisaged that the generic strategies for adding fault tolerance can be applied to this case study, and as a consequence, a better product can be produced. In addition, it is envisaged that DSE and adaptive control can be valuable for this case.

#### 4.4.3.3 The new Kongskilde Robotti

This robot will be modelled by the company Kongskilde (who is one of the partners in the INTO-CPS project) as a co-modelled robotic vehicle. The extended development guidelines could be used here to co-model the new robotti vehicle. The task assigned to Kompleks Innovations is to develop the controller that is going to be used for this vehicle solution. Correspondingly, this could constitute part of the postdoctoral work. Herein, DSE is



Figure 4.5: The new Kongskilde Robotti<sup>3</sup>

envisaged to be valuable in order to enable the exploration of alternative positioning technologies to determine if cheaper sensor solutions used to combine information on the current field task are able to elicit sufficient precision.

<sup>2</sup> Source: Picture of a DVORAK - machine division vehicle solution, DVORAK.

<sup>3</sup> Source: Picture of a Kongskilde Industries A/S vehicle solution, Kongskilde Industries.

#### 4.4.3.4 Analysing online adaptive path planners

Automating a mobile vehicle intended to navigate in rows of orchards is a feature relevant for plant nursing and tree cultivation. The ability to navigate reliably is depended upon the vehicle's capability to know its position and orientation relative to the trees in the orchards. Automated mobile vehicles would need a map of the orchard for navigation. Navigation and localisation in orchard-like environments has mainly been based on the a priori knowledge on relevant objects in the region.

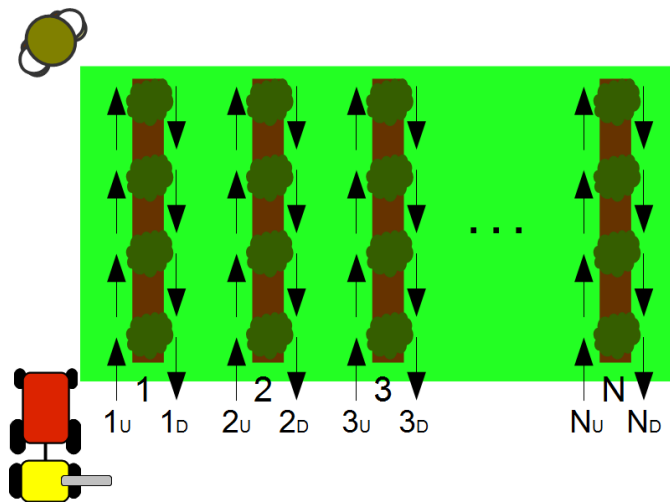


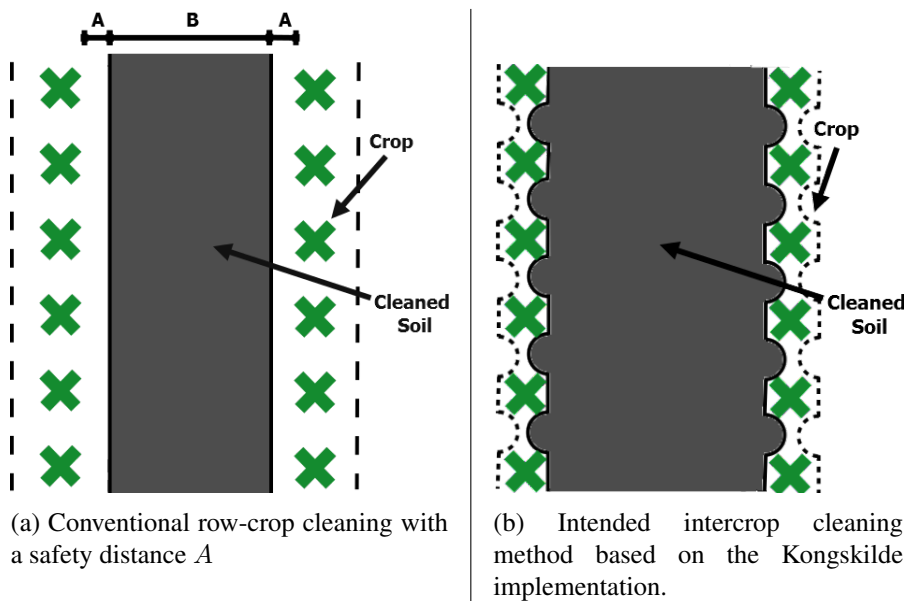
Figure 4.6: The robot vehicle intended to perform plant nursing. The schematic shows the  $N$  rows of orchard trees and intermittent lanes where the robot must move up and down. Shown also, is the pedestrian worker working in the field that the robot must avoid.

Utilising prior knowledge about the structure of an orchard does not account for changes in the existence of objects and their placement. The operations of human workers in the same environment could be in conflict with robot operations, thereby creating situations where robot operations are halted or become hazardous. Adapting online the planned route that the robotic vehicle must follow in order to account for any human worker in the field would ensure continuous and uninterrupted operation of the robot. Co-modelling and co-simulation could be used here to create these hazardous scenarios and test different strategies to handle the problems online as they arise. This type

of hazardous scenario is not only related to orchards, and a similar case can be found for mink farms where multiple farm houses are placed in rows.

#### 4.4.3.5 Tractor-implement solution for crop cleaning

Current weed control products on the commercial market focuses on weed removal between the crop rows using a solution that is entirely mechanical. This leaves a significant amount of weeds inside the rows between the crops, since a safety distance is chosen for crops to prevent the product from harming the crop (see Figure 4.7a). If the crop could be cleaned as illustrated in Figure 4.7b, or in a similar manner, a higher degree of removal can be achieved.



At this present time, this system is being implemented as a new, stand-alone, row crop cleaner system in Kongskilde Industries using camera input and vision recognition. The specific product, the tractor, and the direction of the boom side shifting, are shown in Figure 4.8. The side shifting of the boom is used to make overall corrections on the position of the boom, with respect to the position of the crops in the field and the position of the tractor. This compensation is needed since differences between GPS logged tracks and the actual crop positions exist and vary. Co-modelling, co-simulation, and DSE,

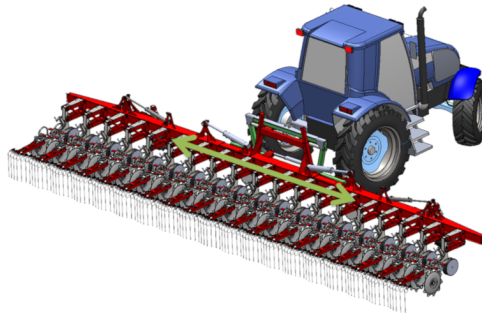


Figure 4.8: Envisioned implement solution from the KongsKilde innovation group. Intended boom side shifting operation is also shown'

could be used here to explore the different field scenarios and weed removal strategies for automated operation.





---

## Bibliography

---

- [1] ISO/TC 184/SC 2. Robots for industrial environments - safety requirements - part 1: Robot. Technical report, The International Organization for Standardization and the International Electrotechnical Commission, 2013.
- [2] J. Backman, J. Kaivosoja, T. Oksanen, and A. Visala. Simulation environment for testing guidance algorithms with realistic GPS noise model. In Nakashima Hiroshi, editor, *Third IFAC International Conference Agricontrol 2010*, pages 139–144, December 2010.
- [3] J. Backman, T. Oksanen, and A. Visala. Navigation system for agricultural machines: Nonlinear Model Predictive path tracking. *Computers and Electronics in Agriculture*, 82:32–43, March 2012.
- [4] David M. Bevly. *GNSS for Vehicle Control*. Artech House, 1 edition, 2009.
- [5] T. Blochwitz, M. Otter, J. Akesson, M. Arnold, C. Clauss, H. Elmqvist, M. Friedrich, A. Junghanns, J. Mauss, D. Neumerkel, H. Olsson, and A. Viel. The Functional Mockup Interface 2.0: The Standard for Tool independent Exchange of Simulation Models. In *Proceedings of the 9th International Modelica Conference*, Munich, Germany, September 2012.
- [6] T. Blochwitz, M. Otter, M. Arnold, C. Bausch, C. Clauß, H. Elmqvist, A. Junghanns, J. Mauss, M. Monteiro, T. Neidhold, D. Neumerkel, H. Olsson, J. Peetz, S. Wolf, Germany I T I GmbH, and D L R Oberpfaffenhofen. The Functional Mockup Interface for Tool independent Exchange of Simulation Models. In *8th International Modelica Conference*, pages 105–114, Munich, Germany, September 2011.
- [7] William Bolton. *Mechatronics: electronic control systems in mechanical and electrical engineering*. Pearson Education, 2013.
- [8] David Bradley and David W Russell. *Mechatronics in Action: Case Studies in Mechatronics-Applications and Education*. Springer Science & Business Media, 2010.
- [9] T. Brezina, Z. Hadas, and J. Vetiska. Using of Co-simulation ADAMS-SIMULINK for development of mechatronic systems. *14th International Conference Mechatronika*, pages 59–64, June 2011.
- [10] J. F. Broenink, P. G. Larsen, M. Verhoef, C. Kleijn, D. Jovanovic, K. Pierce, and F. Wouters. Design Support and Tooling for Dependable Embedded Control Software. In *Proceedings of Serene 2010 International Workshop on Software Engineering for Resilient Systems*, pages 77–82. ACM, April 2010.
- [11] J. F. Broenink and Y. Ni. Model-Driven Robot-Software Design using Integrated Models and Co-Simulation. In J. McAllister and S. Bhattacharyya, editors, *Proceedings of SAMOS XII*, pages 339 – 344, jul 2012.
- [12] Jan F. Broenink, Yunyun Ni, and Marcel A. Groothuis. On model-driven design of robot software using co-simulation. In E. Menegatti, editor, *Proceedings of SIMPAR*

- 2010 Workshops International Conference on Simulation, Modeling, and Programming for Autonomous Robots*, pages 659–668, Darmstadt, Germany, November 2010. TU Darmstadt.
- [13] Karel Capek. *RUR*. Hachette UK, 2013.
  - [14] Farzad Cheraghpour, Masoud Vaezi, Hesam Eddin Shoori Jazeh, and S. Ali A. Moosavian. Dynamic Modeling and Kinematic Simulation of Stäubli TX40 Robot Using MATLAB/ADAMS Co-simulation. In *2011 IEEE International Conference on Mechatronics*, pages 386–391, Isranbul, Turkey, 2011. IEEE.
  - [15] Byoung-suk Choi and Ju-jang Lee. Mobile Robot Localization in Indoor Environment. pages 2039–2044, 2009.
  - [16] Edwin KP Chong and Stanislaw H Zak. *An introduction to optimization*. John Wiley & Sons, 3 edition, 2008.
  - [P17] Martin Peter Christiansen, Kim Bjerger, Gareth Edwards, and Peter Gorm Larsen. Towards a Methodology for Modelling and Validation of an Agricultural Vehicle’s Dynamics and Control. In Sergio Junco, editor, *The 6th International Conference on Integrated Modeling and Analysis in Applied Control and Automation*, IMAACA, pages 112–119, September 2012.
  - [P18] Martin Peter Christiansen and Ole Green. Utilizing DESTECs co-modelling in agricultural testing. In Nils Bjurstad, Eskill Nilsson, and Gints Birzietis, editors, *NJF Seminar 452 - Testing and certification of agricultural machinery*, NJF - Nordic Association of Agricultural Scientists, pages 74–75, October 2012.
  - [P19] Martin Peter Christiansen and Rasmus Nyholm Jørgensen. Method for recording and predicting position data for a self-propelled wheeled vehicle and delivery or pick up system comprising a self-propelled, self-guided wheeled vehicle, Submitted 19-12-2014.
  - [P20] Martin Peter Christiansen, Morten Larsen, and Rasmus Nyholm Jørgensen. Collaborative Model Based Development of Adaptive Controller Settings for a Load-carrying Vehicle with Changing Loads. In Dionysis D. Bochtis and Claus Aage Grøn Sørensen, editors, *CIOSTA XXXV Conference*, July 2013.
  - [P21] Martin Peter Christiansen, Peter Gorm Larsen, and Rasmus Nyholm Jørgensen. Robotic design choice overview using co-simulation. In *NJF Seminar 477 - Agromek and NJF joint seminar. Future arable farming and agricultural engineering*, November 2014.
  - [P22] Martin Peter Christiansen, Peter Gorm Larsen, and Rasmus Nyholm Jørgensen. Robotic Design Choice Overview using Co-simulation and Design Space Exploration. *Robotics*, pages 398–421, October 2015.
  - [P23] Martin Peter Christiansen, Peter Gorm Larsen, and Rasmus Nyholm Jørgensen. Agricultural Robotic Candidate Overview using Co-model Driven Development. In *IEEE/RSJ International Conference on Intelligent Robots and Systems*, 3 Submitted 4-3-2015.
  - [P24] Martin Peter Christiansen, Morten Stiggaard Laursen, Rasmus Nyholm Jørgensen, and Ibrahim A. Hameed. Collaborative model based design of automated and robotic agricultural vehicles in the Crescendo Tool. In *NJF Seminar 477 - Agromek and NJF joint seminar. Future arable farming and agricultural engineering*, November 2014.
  - [25] John T. Cole, T.S. Stombaugh, and S.A. Shearer. Development of a Test Track for the Evaluation of GPS Receiver Dynamic Performance. In *2004 ASAE Annual Meet-*

- ing, pages 1–12, St. Joseph, Michigan., 2004. American Society of Agricultural and Biological Engineers.
- [26] Jeremy M. D’Antoni, Ashok K. Mishra, and Hyunjeong Joo. Farmers perception of precision technology: The case of autosteer adoption by cotton farmers. *Computers and Electronics in Agriculture*, 87:121–128, September 2012.
  - [27] Kalyanmoy Deb. Current trends in evolutionary multi-objective optimization. *International Journal for Simulation and Multidisciplinary Design Optimization*, 1(1):1–8, 2007.
  - [28] Tractors and machinery for agriculture and forestry - test procedures for positioning and guidance systems in agriculture - part 2: Testing of satellite-based auto-guidance systems during straight and level travel. Technical report, International Organization for Standardization, Case postale 56 - CH-1211 Geneva 20, 2011.
  - [29] R. Eaton, J. Katupitiya, K.W. Siew, and K.S. Dang. Precision guidance of agricultural tractors for autonomous farming. In *Systems Conference, 2008 2nd Annual IEEE*, pages 1–8, April 2008.
  - [P30] Gareth Edwards, Martin P. Christiansen, Dionysis D. Bochtis, and Claus G. Sørensen. A Test Platform for Planned Field Operations Using LEGO Mindstorms NXT. *Robotics*, 2(4):203–216, 2013.
  - [31] P. Eykhoff. *System Identification: Parameter and State Estimation*. Wiley-Interscience, 1974.
  - [32] Lei Feng and Yong He. Study on dynamic model of tractor system for automated navigation applications. *Journal of Zhejiang University SCIENCE*, 6A(4):270–275, April 2005.
  - [33] John Fitzgerald, Peter Gorm Larsen, and Marcel Verhoef, editors. *Collaborative Design for Embedded Systems – Co-modelling and Co-simulation*. Springer, 2014.
  - [34] John Fitzgerald, Ken Pierce, and Peter Gorm Larsen. *Industry and Research Perspectives on Embedded System Design*, chapter Collaborative Development of Dependable Cyber-Physical Systems by Co-modelling and Co-simulation. IGI Global, 2014.
  - [35] Carl Gamble and Kenneth Pierce. Design space exploration for embedded systems using co-simulation. In John Fitzgerald, Peter Gorm Larsen, and Marcel Verhoef, editors, *Collaborative Design for Embedded Systems*, pages 199–222. Springer Berlin Heidelberg, 2014.
  - [36] Hichem Geryville, Abdelaziz Bouras, Yacine Ouzrout, and Nikolaos Sapidis. Collaborative product and process model: Multiple viewpoints approach. pages 391–398, Milan, Italy, June 2006.
  - [37] L. Gheorghe. *Continuous/Discrete Co-simulation interfaces from formalization to implementation*. PhD thesis, University of Montreal, Canada, August 2009.
  - [38] Jaime Gomez-Gil, Sergio Alonso-Garcia, Francisco Javier Gómez-Gil, and Tim Stombaugh. A simple method to improve autonomous GPS positioning for tractors. *Sensors (Basel, Switzerland)*, 11(6):5630–5644, January 2011.
  - [39] Ole Green, Thomas Schmidt, Radoslaw Piotr Pietrzkowski, Kjeld Jensen, Morten Larsen, and Rasmus Nyholm Jørgensen. *Commercial autonomous agricultural platform: Kongskilde Robotti*, pages 351–356. RHEA, 2014.
  - [40] Robert Grisson, Mark Alley, and Conrad HeatWole. Precision Farming Tools: Global Positioning System (GPS). *Virginia Cooperative Extension 442-503*, 2009.

## 82 Bibliography

- [41] Marcel A. Groothuis, Arjen S. Damstra, and Jan F. Broenink. Virtual prototyping through co-simulation of a cartesian plotter. In *Emerging Technologies and Factory Automation (ETFA)*, pages 697–700. IEEE, September 2008.
- [42] D.L. Hall and J. Llinas. An introduction to multisensor data fusion. *Proceedings of the IEEE*, 85(1):6–23, 1997.
- [43] SG Hall and M. Lima. Problem-solving approaches and philosophies in biological engineering: challenges from technical, social, and ethical arenas. *Transactions of the ASAE*, 44(4):1037–1041, 2001.
- [44] Stefan Hallerstede, Finn Overgaard Hansen, Claus Ballegaard Nielsen, , and Klaus Kristensen. Guidelines for Architectural Modelling of SoS. Technical report, COMPASS Deliverable, D21.5, September 2014. Available at <http://www.compass-research.eu/>.
- [45] Søren Hansen, Enis Bayramoglu, Jens Christian Andersen, Ole Ravn, Nils Andersen, and Niels Kjolstad Poulsen. Orchard navigation using derivative free kalman filtering. In *American Control Conference (ACC), 2011*, pages 4679–4684. IEEE, 2011.
- [46] Scarlett R Herring, Chia-Chen Chang, Jesse Krantzler, and Brian P Bailey. Getting inspired!: understanding how and why examples are used in creative design practice. In *Proceedings of the SIGCHI Conference on Human Factors in Computing Systems*, pages 87–96. ACM, 2009.
- [47] Peter W. V. Jørgensen. Evaluation of Development Process for co-models. Master’s thesis, Aarhus University/Engineering College of Aarhus, December 2012.
- [48] Peter W. V. Jørgensen, Kenneth Lausdahl, and Peter Gorm Larsen. An Architectural Evolution of the Overture Tool. In *The Overture 2013 workshop*, August 2013.
- [49] Wang Jun, Zhou Zhou, and Du Xiaodong. Design and co-simulation for tomato harvesting robots. In *Control Conference (CCC), 2012 31st Chinese*, pages 5105–5108. IEEE, 2012.
- [50] Rudolph Emil Kalman. A new approach to linear filtering and prediction problems. *Transactions of the ASME—Journal of Basic Engineering*, pages 35–45, 1960.
- [51] Lawrence J Kamm. *Understanding electro-mechanical engineering: an introduction to mechatronics*, volume 3. John Wiley & Sons, 1996.
- [52] Manoj Karkee and Brian L. Steward. Study of the open and closed loop characteristics of a tractor and a single axle towed implement system. *Journal of Terramechanics*, 47(6):379–393, December 2010.
- [53] Manoj Karkee and Brian L. Steward. Parameter estimation and validation of a tractor and single axle towed implement dynamic system model. *Computers and Electronics in Agriculture*, 77(2):135–146, July 2011.
- [54] Wajahat Kazmi, Morten Bisgaard, Francisco Garcia-Ruiz, Karl Damkjær Hansen, and Anders la Cour-Harbo. Adaptive Surveying and Early Treatment of Crops with a Team of Autonomous Vehicles. In *European Conference on Mobile Robots ECMR 2011*, pages 253–258, 2011.
- [55] C. Kleijn. *20-sim 4C 2.1 Reference Manual*. Controllab Products B.V., Enschede, First edition, 2013. ISBN 978-90-79499-05-2.
- [56] Christian Kleijn. Modelling and Simulation of Fluid Power Systems with 20-sim. *Intl. Journal of Fluid Power*, 7(3), November 2006.

- [57] Tamás Kovács, Attila Pásztor, and Zoltán Istenes. A multi-robot exploration algorithm based on a static bluetooth communication chain. *Robotics and Autonomous Systems*, 59(7):530–542, 2011.
- [58] Michael LaLande. An Integrated Methodology for Defining, Modeling, and Validating Complex Automotive Systems. Technical report, April 2014.
- [59] Peter Gorm Larsen, Joao M. Fernandes, Jacek Habel, Hanne Lehrslov, Richard J.C. Vos, Oliver Wallington, and Jan Zidek. A Multidisciplinary Engineering Summer School in an Industrial Setting. *European Journal of Engineering Education*, August 2009.
- [60] Ming Li, Kenji Imou, Katsuhiko Wakabayashi, and Shinya Yokoyama. Review of research on agricultural vehicle autonomous guidance. *International Journal of Agriculture and Biological Engineering*, 2(3):1–26, 2009.
- [61] Hung-hsing Lin, Ching-chih Tsai, and Hsu-yang Chang. Global Posture Estimation of a Tour-guide Robot using REID and Laser Scanning Measurements. pages 483–488, 2007.
- [62] Leonardo Marín, Marina Vallés, Ángel Soriano, Ángel Valera, and Pedro Albertos. Multi sensor fusion framework for indoor-outdoor localization of limited resource mobile robots. *Sensors (Basel, Switzerland)*, 13(10):14133–60, January 2013.
- [63] R. Merzouki, B. Ould-Bouamama, M.a. Djeziri, and M. Bouteldja. Modelling and estimation of tire-road longitudinal impact efforts using bond graph approach. *Mechatronics*, 17(2-3):93–108, March 2007.
- [64] G. Molari, L. Bellentani, A. Guarnieri, M. Walker, and E. Sedoni. Performance of an agricultural tractor fitted with rubber tracks. *Biosystems Engineering*, 111(1):57–63, January 2012.
- [65] Yunyun Ni, Jan F. Broenink, Kenneth G. Lausdahl Augusto Ribeiro, Frank Groen, Ken Pierce Marcel Groothuis, Carl Gamble, and Peter Gorm Larsen. Design space exploration tool support. Technical report, The DESTecs Project (INFSO-ICT-248134), December 2012.
- [66] G. Nicolescu, H. Boucheneb, L. Gheorghe, and F. Bouchhima. Methodology for Efficient Design of Continuous / Discrete-Events Co-Simulation Tools. In J. Anderson and R. Huntsinger, editors, *Proceedings of the 2007 Western Multiconference on Computer Simulation WMC 2007, San Diego*, San Diego, January 2007. SCS, SCS, San Diego.
- [67] Michael O'Connor, Thomas Bell, Gabriel Elkaim, and Bradford Parkinson. Automatic steering of farm vehicles using GPS. In *Proc. of the 3rd Intern. Conf. on Precision Agriculture*, volume 3, pages 767–778. Minneapolis, MN, 1996.
- [68] Dhanesh Padmanabhan. *Reliability-based optimization for multidisciplinary system design*. PhD thesis, Notre Dame, Indiana, 7 2003.
- [69] Richard Paul, Robert Niewoehner, and Linda Elder. *The thinker's guide to engineering reasoning*. Foundation Critical Thinking, 2006.
- [70] Andrzej Pawlowski, Jose Luis Guzman, Francisco Rodríguez, Manuel Berenguel, José Sánchez, and Sebastián Dormido. Simulation of greenhouse climate monitoring and control with wireless sensor network and event-based control. *Sensors*, 9(1):232–252, 2009.
- [71] M. Pérez-Ruiz, D.C. Slaughter, C.J. Gliever, and S.K. Upadhyaya. Automatic GPS-based intra-row weed knife control system for transplanted row crops. *Computers and Electronics in Agriculture*, 80:41–49, jan 2012.

- [72] K. G. Pierce, C. J. Gamble, Y. Ni, and J. F. Broenink. Collaborative Modelling and Co-Simulation with DESTeCS: A Pilot Study. In *3rd IEEE track on Collaborative Modelling and Simulation, in WETICE 2012*. IEEE-CS, June 2012.
- [73] Ken Pierce, John Fitzgerald, Carl Gamble, Yunyun Ni, and Jan F. Broenink. Collaborative Modelling and Simulation — Guidelines for Engineering Using the DESTeCS Tools and Methods. Technical report, The DESTeCS Project (INFSO-ICT-248134), September 2012.
- [74] Zexiang Li Richard M. Murray and S. Shankar Sastry. *A Mathematical Introduction to Robotic Manipulation*. CRC Press, March 1994.
- [75] Francisco Rovira Más, S. Han, and J.F. Reid. Evaluation of automatically steered agricultural vehicles. In *Position, Location and Navigation Symposium, 2008 IEEE/ION*, pages 473–478. IEEE, 2008.
- [76] Francisco Rovira Más, Qin Zhang, and Alan C. Hansen. *Mechatronics and Intelligent Systems for Off-road Vehicles*. Springer London, London, 2011.
- [77] Arno Ruckelshausen. Autonomous robots in agricultural field trials. In *Proceedings of the International Symposium “Agricultural Field Experiments—Today and Tomorrow*, pages 190–197, 2007.
- [78] Per Schjønning, Mathieu Lamandé, Frede a. Tøgersen, Johan Arvidsson, and Thomas Keller. Modelling effects of tyre inflation pressure on the stress distribution near the soil-tyre interface. *Biosystems Engineering*, 99(1):119–133, January 2008.
- [79] Fabian Sellmann, Waldemar Bangert, Slawomir Grzonka, Martin Hänsel, Sebastian Haug, Arnd Kielhorn, Andreas Michaels, Kim Möller, Florian Rahe, Wolfram Strothmann, et al. Remotefarming.1: Human-machine interaction for a field-robot-based weed control application in organic farming. In *4th International Conference on Machine Control & Guidance*. Springer-Verlag, March 2014.
- [80] Olivier Simonin and Olivier Grunder. A cooperative multi-robot architecture for moving a paralyzed robot. *Mechatronics*, 19(4):463–470, 2009.
- [81] Aaron Staranowicz and Gian Luca Mariottini. A survey and comparison of commercial and open-source robotic simulator software. *Proceedings of the 4th International Conference on Pervasive Technologies Related to Assistive Environments - PETRA '11*, pages 121–128, 2011.
- [82] Sebastian Thrun. Is robotics going statistics? The field of probabilistic robotics. *Communications of the ACM*, pages 1–8, 2001.
- [83] Sebastian Thrun, Wolfram Burgard, and Dieter Fox. *Probabilistic robotics*. MIT press, 2005.
- [84] Feng-lei TIAN and Rong-lei SUN. The Flexible Robot Arm Simulation System Based on ADAMS and Simulink. *Machinery & Electronics*, 10:020, 2006.
- [85] Marcel Verhoef and Peter Gorm Larsen. Enhancing VDM++ for Modeling Distributed Embedded Real-time Systems. Technical Report (to appear), Radboud University Nijmegen, March 2006. A preliminary version of this report is available on-line at <http://www.cs.ru.nl/~marcelv/vdm/>.
- [86] Hong Jun Wang, Guo Gang Huang, Xiang Jun Zou, and Yan Chen. Modeling and performance simulation for a picking manipulator based on modelica. *Key Engineering Materials*, 579:467–475, 2014.
- [87] Greg Welch, Gary Bishop, and Chapel Hill. An Introduction to the Kalman Filter. Technical report, 2006.

- [88] Kyle Wiens. New high-tech farm equipment is a nightmare for farmers, February 2015. [Online; posted 5-February-2015].
- [89] Sune Wolff. *Methodological Guidelines for Modelling and Design of Embedded Systems*. PhD thesis, Aarhus University, Department of Engineering, 2013.
- [90] Jo Yung Wong. *Theory of ground vehicles*. John Wiley & Sons, 2008.
- [91] S.C. Young, C. E. Johnson, and R. L. Schafer. A vehicle guidance controller. *Transactions of the American Society of Agricultural Engineers*, 26(5):1340–1345, 1983.
- [92] Qin Zhang and Francis J. Pierce. *Agricultural automation: fundamentals and practices*. CRC Press, 2013.
- [93] Junyi Zhou and Jing Shi. A comprehensive multi-factor analysis on RFID localization capability. *Advanced Engineering Informatics*, 25(1):32–40, January 2011.





# **Part II**

# **Publications**



# 1

---

## **TOWARDS A METHODOLOGY FOR MODELLING AND VALIDATION OF AN AGRICULTURAL VEHICLES DYNAMICS AND CONTROL**

---

The paper presented in this chapter is a peer-reviewed conference paper and has been presented at IMAACA 2012.

[P17] Martin Peter Christiansen, Kim Bjerger, Gareth Edwards, and Peter Gorm Larsen. Towards a Methodology for Modelling and Validation of an Agricultural Vehicle's Dynamics and Control. In Sergio Junco, editor, *The 6th International Conference on Integrated Modeling and Analysis in Applied Control and Automation*, IMAACA, pages 112–119, September 2012

## TOWARDS A METHODOLOGY FOR MODELLING AND VALIDATION OF AN AGRICULTURAL VEHICLE'S DYNAMICS AND CONTROL

Martin Peter Christiansen<sup>(a)</sup>, Kim Bjerger<sup>(b)</sup>, Gareth Edwards<sup>(c)</sup>, Peter Gorm Larsen<sup>(c)</sup>

Department of Engineering, Aarhus University  
Finlandsgade 22, 8200 Aarhus, Denmark

<sup>(a)</sup>[mapc@djf.au.dk](mailto:mapc@djf.au.dk), <sup>(b)</sup>[kbe@iha.dk](mailto:kbe@iha.dk), <sup>(c)</sup>[Gareth.Edwards@agrsci.dk](mailto:Gareth.Edwards@agrsci.dk), <sup>(d)</sup>[pgl@iha.dk](mailto:pgl@iha.dk)

### ABSTRACT

A model-oriented approach aimed at cost-effective development of autonomous agricultural vehicles is presented. Here a combination of discrete-event modelling of a digital controller and continuous-time modelling of the vehicle is used for co-simulation. In order to have confidence in the simulation results it is paramount to be able to relate the simulation results to the behaviour of the real system. The cost of physical tests is high and we argue that using such collaborative models is a cost-effective way to experiment with the most significant design parameters influencing the optimal system solution. The suggested methodology is exemplified on a Lego®Mindstorms®NXT micro-tractor. Testing is performed based on measurements from a localisation system and internal sensors on the tractor. Our tests show that we are able to predict the performance with a high accuracy indicating that this is worthwhile for a full-scale model.

Keywords: Auto-steering, Bond graph, Lego Mindstorms NXT, Vienna Development Method

### 1. INTRODUCTION

Modern agricultural machinery is gradually moving towards a higher degree of autonomous operation (Grisson et al. 2009). Global Navigation Satellite Systems (GNSS) in combination with other sensors are used to estimate the position of the vehicle. Operational tasks like ploughing, spraying and harvesting are commenced by the autonomous vehicle. A pre-planned route for the agricultural vehicle to follow for a specific broad-acre field is supplied in advance. The onboard auto-steering system then aims to adjust the current position so it gets as close as possible to the pre-planned route. The ability to automatically correct the position helps deal with physical conditions, such as the terrain (Fang et al. 2005), which may affect the vehicle's movements in unpredictable ways.

Methods to determine the precision of the vehicle's control equipment have been proposed in a ISO test standard (DS-F/ISO/DIS 12188-2). Testing is performed over a period of more than 24 hours, repeating the testing scenarios multiple times. Full-scale testing of performance and operation is both time-consuming and very costly. Utilising a simulated model

of an agricultural machine and auto-steering system, could lower some of these costs. Relevant testing scenarios can be determined based on flaws found through evaluation of the simulations. These scenarios could then be tested to determine if they would produce similar results as in the real physical system.

The aim of this work is to develop collaborative models of agricultural vehicles and their auto-steering systems, combining discrete-event models of control elements with continuous-time modelling of the physical elements and the surrounding environment. The Vienna Development Method (VDM) is utilised for discrete-event modelling of the vehicles control equipment and 20-sim is used as the continuous-time framework for modelling the tractor. In this paper collaborative modelling (co-modelling) is used to model a concrete physical system and its controller.

The aim of this work is to develop collaborative models of agricultural vehicles and their auto-steering systems, combining discrete-event models of control elements with continuous-time modelling of the physical elements and the surrounding environment. The Vienna Development Method (VDM) is utilised for discrete-event modelling of the vehicles control equipment and 20-sim is used as the continuous-time framework for modelling the tractor. In this paper collaborative modelling (co-modelling) is used to model a concrete physical system and its controller.

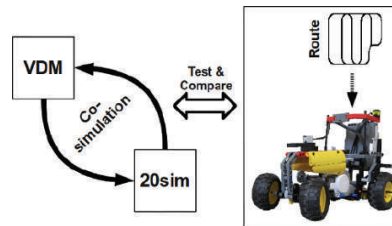


Figure 1: Overview of the micro-tractor and the co-modelling method. 20-sim models the vehicle and VDM the control part

An agricultural tractor system is a complex system to model, simulate and test. Many of the parameters in

such a complex system are unknown, making it difficult to verify the complete model based on testing and analysis. To simplify the process, a model and co-simulation based on a Lego®Mindstorms®NXT tractor (micro-tractor) has been developed. The micro-tractor is a representative scaled model of agricultural machinery used to test and demonstrate autonomous operations.

This prototype model of the autonomous vehicle is intended to provide an abstraction with key components in autonomous vehicle steering and explore alternative requirements and design decisions.

The model of the system will provide the functionality to control the motors for the front and back wheels, using the inputs from motor encoders and Inertial Measurement Unit (IMU) in VDM. Subparts of the 20-sim model were modelled separately and combined after verification of each subpart (component). The output from the co-simulation model is the dynamic movements of the vehicle while commencing a pre-planned route.

The article is structured as follows: a short presentation of the underlying method and technologies used for co-modelling and co-simulation is given in section 2. The case study with the scaled-down tractor and a short description of the proposed development process is provided in section 3. The verification and validation of the model in relation to the real physical system is found in section 4. Finally section 5 provides concluding remarks together with directions for future work.

## 2. TECHNOLOGIES APPLIED

Models of control systems can be complex when they account for many different scenarios. Testing the final model to determine the sources of a specific problem is complicated and time consuming. The work presented in this paper uses a methodology that integrates tests as an essential part of the development process.

The idea is to discover errors and faulty assumptions at an early stage in the development process. It is expected that combined analysis and testing throughout the development will provide a good methodology for developing the multi-domain models.

In the initial part of the development phase a subcomponent of the system is selected. This subcomponent is analysed and an initial sub-model is created. A test scenario will then be created to determine the sub-model's accuracy compared to the actual setup. If flaws are found in the sub-model, extensions and improvements are made until the model represents the actual sub-component.

After the subcomponents have been modelled independently they are put together as a first version of the system intended to be modelled. This model will then be tested using the same process as the sub-models. The process is an iterative incremental development process that improves and extends the model.

### 2.1. DESTECs and Co-simulation

This paper is based on the DESTECs ("Design Support and Tooling for Embedded Control Software" (see [www.destecs.org](http://www.destecs.org))) co-simulation technology (Broenink et al. 2010) that supports a model-based approach to the engineering of embedded control systems. Models are built in order to support various forms of analysis including static analysis and simulation — the latter is our focus here.

The technology supports models where the controller and plant or environment is modelled using different specialized environments and tools. In particular, it supports co-simulation by allowing the collaboration of two simulation engines in order to produce a coherent combined simulation of a co-model of a digital controller expressed in a Discrete-Event (DE) formalism and a model of the plant/environment expressed in a Continuous Time (CT) notation.

In order to link the DE and CT models together, a contract is established between them. The contract includes information about the shared design parameters as well as monitored and controlled variables exchanged between the two simulators. Once co-models have been constructed, they can be evaluated by co-simulation. Evaluation is done using criteria's chosen by the developer, intended to select the best candidate co-model termed Design Space Exploration (DSE).

VDM is used for modelling DE controllers, and 20-sim as the CT framework for modelling the environment. VDM Real Time (VDM-RT) is the dialect used in DESTECs (Verhoef et al. 2006; Verhoef 2009). Both VDM and 20-sim are well-established formalisms with stable tool support and a record of industry use.

### 2.2. 20-sim and Bond graph modelling

20-sim is a modelling and simulation tool, developed by Controllab Products in the Netherlands. The tool is able to model complex multi-domain dynamic system, such as combined mechanical, electrical and hydraulic systems. 20-sim models (Kleijn 2006) may use iconic diagrams, Bond graphs and equation models. Iconic diagrams generally contain a sub-model based on equations or Bond graph models. In this context a sub-model means a part on the overall model describing a dynamic system.

Bond graphs are a type of directed graph representing the idealized power flows in a dynamic system (van Amerongen 2010). Every element in a Bond graph is represented by a multiport, describing a subpart (sub-model) of the system. The connections between sub-models, called bonds, represent the exchange of energy. Each port element describes the energy flow, using the product of the variables effort ( $e$ ) and flow ( $f$ ). The meaning of different ports elements changes based on the current system domain. In an electrical domain ( $e$ ) and ( $f$ ) could represent voltage and current and in a mechanical domain torque and angular velocity. This abstraction of ports provides a huge advantage, in terms of reuse and movement between different physical domains.

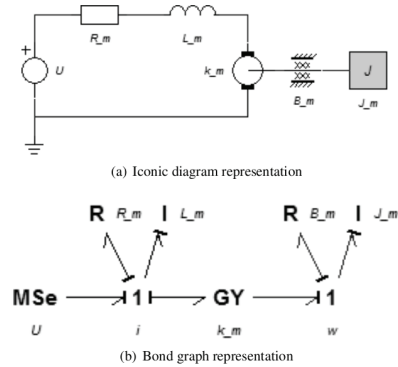


Figure 2: Motor representations using iconic diagrams.

An iconic diagram representation of a DC-motor can be seen in Figure 2(a). In a Bond-graph terminology voltage source would mean an effort source for the motor system. In Figure 2(b) the bond-graph represents the Direct Current (DC)-motors mechanical and electrical domains. In the electrical domain the I-element represents the inductance  $L_m$  and R the resistance  $R_m$  connected to the electrical 1-junction. The gyrator GY relates the effort and flow between the electrical and mechanical domain. In the mechanical domain the R-element represents the internal friction  $B_m$  and the I-element the moment of inertia  $J_m$ . In the bond-graph model  $i$  represent the current and  $w$  the rotational speed of the DC-motor.

### 2.3. The Vienna Development Method

The 20-sim tool environment also provides techniques to allow for mixed modelling and simulation of digital controlled physical systems. Using the equation models different discrete-event scenarios can be simulated and tested. This provides the ability to simulate both continuous and discrete time events of a dynamic system. Most modern digital control systems are complex and hard to model in a single model block. The 20-sim tool provides the ability for external software to connect and communicate with a specific model. An external environment could therefore be used to model the discrete time event parts of a dynamic model (Fitzgerald et al. 2011).

VDM is a formal method for specification, analysis, modelling and identification of significant features in a computer system. VDM originate from work done at IBM's Vienna Laboratory in the 1970's on semantics of programming languages (Björner and Jones 1978). VDM provides the ability to model at a level higher of abstraction, than is realizable in a normal programming language. Validated models can then be turned into a concrete implementation in a programming language. The current tools focus are to

provide modelling and analysis techniques used for simulation rather than proof checking. VDM tool support is provided by the open-source Overture tool (Larsen et al. 2010).

The demands and assumptions about the system intended for modelling is a significant part, when describing the functionality of the system. Functionality is performed on different data types, ranging from basic type like Booleans, tokens, integers and real numbers and collections such as sets, mappings and sequences. Functions can be either implicit or explicit specified in VDM, for a modelled system in terms of describing the relations. The VDM functionality has been extended to include the Object-oriented structuring (Fitzgerald et al. 2005) using the VDM++ extension. For VDM to be used in a real-time embedded system context, it requires explicit modelling of computation time. The capabilities to describe real-time, asynchronous, object-oriented features are provided in the VDM-RT extension. Using the VDM formalism for both control and modelling of the environment is not an ideal solution, since the CT environment would be expressed in DE formalism based on simplifying assumptions. A co-simulation with a CT event tool would be a significant improvement, in terms of simulating the VDM controller.

### 3. THE MICRO-TRACTOR CASE STUDY

The micro-tractor was developed to represent an average 150 bhp tractor. A scale ratio of 1:14 was used. The micro-tractor is described in (Edwards et al. 2012).

The micro-tractor's steering range was between  $\pm 30$  (degrees) and controlled by an NXT servo motor and gearbox.

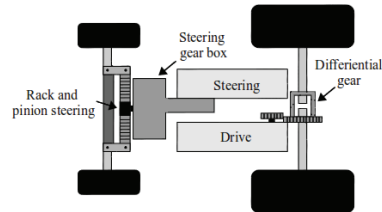


Figure 3: Sketch of the micro-tractors steering and drive components.

The rear wheels were powered by another NXT servo motor. A differential gear was used on the drive axle to allow the wheels to turn at different speeds and reduce slip (see Figure 3).

The navigation sensor is the CruizCore R XG1300L IMU. The IMU measures heading of the micro-tractor based on relative initial heading. The IMU contains a single axis MEMS gyroscope and a three axis accelerometer. The signals from these sensors are processed onboard the IMU.

### 3.1. Co-simulation

A co-simulation engine is responsible for exchange of shared parameters and variables between the CT and DE models. The co-simulation engine coordinates the 20-sim and VDM simulation by implementing a protocol for time-step synchronisation between the two simulation tools. A contract defines the parameters and variables to be exchanged during simulation as illustrated in Figure 4. Here the start and stop times of the co-simulation are shared, to ensure common reference. The micro-tractor (CT Model) updates the shared angle parameters of the motor encoders and IMU and the controller (DE model) drives the shared input parameters the motors.

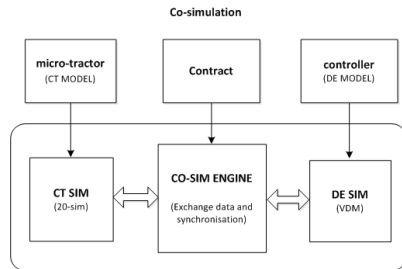


Figure 4: Co-simulation engine and synchronisation of the CT and DE simulation.

### 3.2. Bond graph model

The motor is modelled as the first component of the vehicle model, since it is used for control of both drive and steering.

To exemplify the development method, the motor subpart will be described in detail. The NXT controls the average voltage output to the motors using Pulse Width Modulation (PWM). This makes it possible to compare input/output between model and actual Lego DC-motor: A representation of a bond graph DC-motor model can be seen in Figure 2(b).

To test if the model works as intended, the bond graph is supplied with motor parameters for the Lego DC-motor. An impulse-function (0V-7.4V-0V) is used to apply a voltage to both Bond graph and real DC-motor.

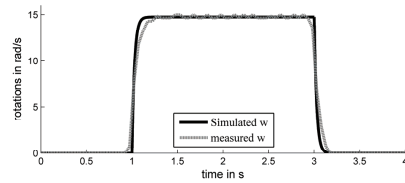


Figure 5: Impulse test of DC-motor model and real system.

From the plot in Figure 5 it can be seen, the plots correlate to a high degree. Based on these findings, the DC-motor bond-graph is accepted and development on other subparts is initiated.

A similar methodology is applied when modelling the remaining components in 20-sim.

The controller is connected to the DC-motor implementation, providing the interface for communication with VDM. Gearing for steering and drive components are modelled using Transformer TF elements. Each TF element corresponds to a gearing ratio effort with effort out causality. A Bond-graph equivalent of a spring damper ( $C_g, R_g$ ) system is used to model the effects of rotating gears using a 0-Junction.

Change in angle of the front wheels are represented using a friction and moment of inertia ( $B_{f\_wheel}, J_{f\_wheel}$ ). Interactions between wheels and ground plane are only considered for a smooth surface to keep the complexity of the model down.

Only the longitudinal effects on the wheel are considered, since tire-road normal effort (Merzouki et al. 2007) is expected to be minimal. Effects of the wheels moment of inertia is represented with a 1-junction and an I-element  $J_{b\_wheel}$ . A TF-element converts between rotational and linear speed. A spring-damper system ( $C_{b\_wheel}, R_{b\_wheel}$ ) is used to represent the longitudinal surface interaction with the wheel contact-point.

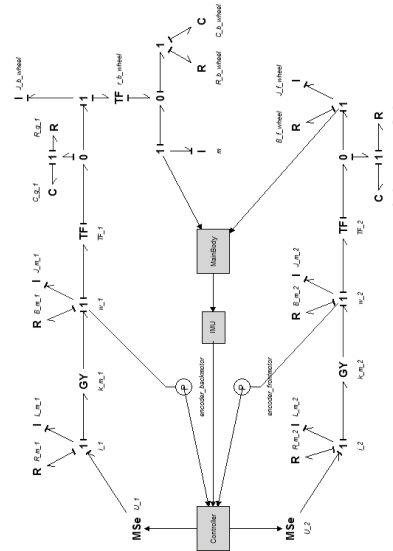


Figure 6: The micro-tractor model in 20-sim. A combination of bond graphs and iconic diagram blocks are used for modelling the micro-tractor.

To combine the dynamic effects of the back and front wheels a first order bicycle model (Figure 7) has been chosen. The first order bicycle model is a pure kinematic model (Rovira M Rovira Más et al. 2011) of the chassis movements, without regards for the forces acting on the body.

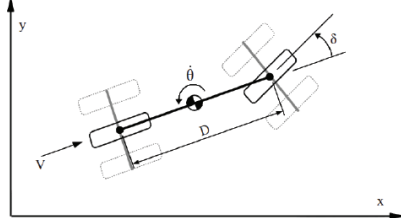


Figure 7: Bicycle vehicle model used to model the body of the micro-tractor.

Translational speed ( $V$ ) from the back wheel in combination with the rotational speed ( $\dot{\theta}$ ) of the front steering system is used as input for the model.

Equation (1), (2) and (3) are used to calculate the vehicle rotation and speed in  $x, y$  direction in a global reference frame.

$$\dot{x} = \cos(\theta) \cdot V \quad (1)$$

$$\dot{y} = \sin(\theta) \cdot V \quad (2)$$

$$\dot{\theta} = (\tan(\delta)/D) \cdot V \quad (3)$$

$D$  represents the distance between front and back wheels,  $\delta$  the orientation of the front wheels. To represent backlash in the steering system Gaussian noise is added to the rotational change.

A Bond graph model of backlash in the front wheel orientation is not incorporated, since modelling of the external forces on both front wheels would be needed. Position and orientation of the vehicle over time is calculated using numerical integration of equation (1), (2) and (3). The positioning and orientation of the vehicle is the intended output from the model.

### 3.3. VDM model

The discrete event control system modelling the NXT's steering of the micro-tractor is modelled in VDM-RT. A pre-planned route is given to the autonomous system. This route is used when the micro-tractor commences its task in an area.

The route is based on a collection of continuous curve elements. Each continuous path element is either a line segment or circular arc with constant radius, containing a start and stop waypoint (Bevly 2009).

The micro-tractor is aware of its current position and is able to use this information when following the

route. A route-manager ensures that each route segment is performed in the order described in the route. The VDM model uses invariants and pre and post-conditions to ensure only a viable route and route segments are commenced. The description is given to provide the reader with a perspective of what the VDM capabilities could be used for. Details of the route-manager will not be given in this paper but similar systems can be found in (Fitzgerald et al. 2005).

When a route element is commenced a control loop is needed to keep the micro-tractor on track. In this model the inputs from the back-motor encoder and the IMU is used to determine the current position and orientation. The model for executing a line function segment can be seen in Listing 1.

```
class controlStraight

instance variables
public rotations: real; -- 20-sim variable
public ImuOrient: real; -- 20-sim variable
P: real; --proportional control factor
MotorOutput: real; -- output value in %
distance: real; -- distance to travel
wOrient: real; -- Wanted orientation

operations
public ControlStep: () ==> ()
ControlStep() ==
( if abs rotations >=
distance/(2*MATH*pi*R_BACK_WHEEL)
then drivingMotor := 0.0;
else driveMotor := MAX_OUTPUT*MotorOutput;
steerMotor := MAX_OUTPUT*P*(ImuOrient-
wOrient)
);

thread
periodic(10E5,0,0,0)(controlStraight); -- 100Hz
end controlStraight
```

Listing 1: VDM++ model of control loop for driving a straight path.

A line segment is followed until the distance between start and stop point is reached. The control loop allows the micro-tractor to steer off track, since any positioning error is accumulated. A more advanced control system could compensate for this and is intended for the future.

## 4. MODEL VERIFICATION AND VALIDATION

Measurement data from the testing of the micro-tractor is compared against the vehicle co-model to determine the accuracy of the co-model. To accomplish this task measurement data from an external source is compared against data from the co-simulation. The testing, measurement method and results thereof are presented in this section.



#### 4.1. Test scenario

The testing will determine the difference between the actual system and the co-simulation, in terms of position and orientation. Running the same route-scenario in will make them comparable and provide a means of comparing different parts of the route. Testing is performed on a route with 3 straight segments of 2-3 meters and 2 circle arcs in opposite direction. A more complex route with more route-segments could introduce larger accumulative errors in terms of position.

Since this is not taken into account in the current co-model, comparison would clearly fail. The selected route ensures the testing is done for movements with different rotational speeds  $\theta$  of the micro-tractor body, which is a major part of the micro-tractor dynamics. The model parameters used in the co-simulation of the bicycle vehicle model are given in Table 1.

Table 1: Testing and co-simulation parameters

Sub-system	Parameter Values	
Motor:	$R_m = 5.2637(\Omega)$ $k_m = 0.4952$ $J_m = 0.0013(\text{kgm}^2)$	$L_m = 0.0047(\text{H})$ $B_m = 6^{-4} \text{ Nm/(rad/s)}$
Gearing:	$TF_{g1} = 20/28$ $C_g = 10^{-5}$	$TF_{g2} = 3/70$ $R_g = 10^{-5}$
Back-Wheels :	$J_{\text{wheel}} = 3.67^{-6}$ $C_{b \text{ wheel}} = 1.1\mu$	$r_{b \text{ wheel}} = 0.0408(\text{m})$ $R_{b \text{ wheel}} = 0.3$
Body:	$m = 2.2374(\text{kg})$	$D = 0.175(\text{m})$

Parameters with the equal value in Figure 8 like  $k_{m\_1}$  /  $k_{m\_2}$  is represented with same symbol (ex  $k_m$ ).

#### 4.2. Testing equipment

To determine the position of the micro-tractor over time the iGPS system from Nikon is used. iGPS measurement technology is a laser-based indoor system with optical sensors and transmitters to determine the 3D position of static or moving objects. The iGPS technology is based on internal time measurements related to spatial rays that intersect at sensor positions in the measuring area. The iGPS measurement system has been evaluated in experimental studies (Depenthal, 2010) of the capabilities for tracking applications.

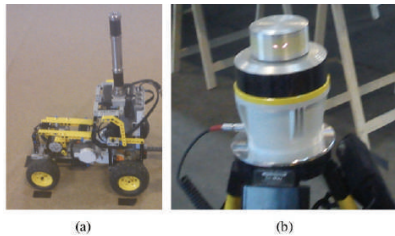


Figure 8: Nikon iGPS receiver mounted at the micro-tractors CoR (a) and transmitter used in the testing (b).

The intention is to use the iGPS technology to evaluate full-scale autonomous agricultural vehicles based on the ISO. The system is able to measure the micro-tractor position over time to provide capabilities for direct analysis of auto-steering system.

The iGPS sensor is mounted on top of the micro-tractor close to the Centre of Rotation (CoR) (see in Figure 8(a)). Using the CoR as measurement point ensures measurement data is comparable directly with co-simulations. The vehicle was driven at 20% of full motor power output when running the pre-planned route. The low motor-output was chosen to ensure safe driving, when using the iGPS sensor system.

The testing was repeated 10 times to account for any variation in performance.

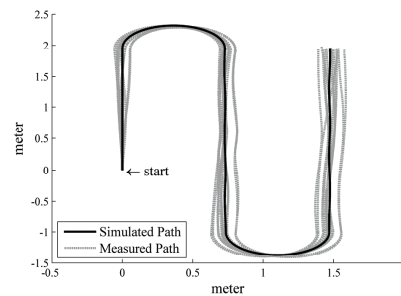


Figure 9: Measured and simulated path of the micro-tractor. Measured path shows the variation in 10 runs.

Figure shows the micro-tractor drifts in position but keep it's heading throughout the path. The small variations in angle can mostly be described to variation in initial placement, since the IMU is a relative sensor any misalignment is kept throughout the path. These initial misalignments are not part of the simulation, resulting in a path moving in the middle of the actual measure paths.

Position measurements are determined to have a precision of 0.4-0.5 mm, based on estimates provided by the iGPS system.

#### 5. CONCLUDING REMARKS AND FUTURE WORK

Based on testing of the current co-model it can be concluded, that the model can emulate the basic performance intended for the micro-tractor. Visual presentation of results and comparisons show a high consistency between actual system and co-model. The current model can be seen as a first step towards a full scale co-model of an autonomous agricultural vehicle. Different routes can be tested in the co-model, to determine their efficiency on the actual system. The co-model will allow for detailed analysis, without the need to start the process of the testing each time.

The need for testing can be diminished significantly and thereby saving development costs. The development process has shown exemplary initial results, to produce dynamic models. Splitting design of the model into smaller steps helps ensure sub-part errors could be determined easily throughout testing. Experience from this project has indicated an iterative modelling method with testing to be a beneficial development and modelling approach.

Continuing to use the current approach to model development is therefore seen as a promising way of continuing the development.

The current version of the co-model is used to test and develop more advanced control algorithms for the micro-tractor driving and steering system. Only selected versions of the control system need to be tested on the actual system, to confirm any improvements. Obtained measurements could be used to improve the model, should a different result be produced in the testing from simulation using the co-model. Many errors and shortcomings in the control loop can also be tested using the co-model to determine their source and provide the mean to test solutions to the problems.

The co-model currently has a number of shortcomings in terms of describing the dynamics between the front and back wheels. At the current state, a kinematic description is used to describe the overall changes to the vehicles placement and orientation. Forces acting on front and back wheels need to be described in more detail in the co-model to account for their interaction. The forces introduced by the back wheels when rotating and thereby driving the vehicle forward influences the front wheels and the backlash introduced in the orientation. Occurrences of backlash are seen when the micro-tractor is moving in a straight line in figure 9 as small changes in orientation over time. Body rotation of the vehicle introduced by the front wheels will introduce forces on the back wheel and the differential gearing drive. Accounting for these factors is expected to provide a model able to run more complex route scenarios and provide a reliable estimate of the real system.

These improvements to the model are planned to be part of the next stage of the co-model development. Later versions should also account for the external factors like uneven terrain and 3-dimensional movement.

#### ACKNOWLEDGMENTS

The authors want to thank Ole Green for supervision and support of the work. We would like also to acknowledge Joey W. Coleman and Sune Wolff for provided invaluable input regarding the content and structure of this work. Thanks are due to Jens Kristian Kristensen at Research Centre Foulum for providing assistance in connection with the experiments. We acknowledge partial support from the EU FP7 DESTECs project on co-simulation. Financial support given by the Danish Ministry of Food, Agriculture and Fisheries is gratefully acknowledged.

#### REFERENCES

- Bevly, D.M., Cobb, S., 2009. *GNSS for Vehicle Control*. 1st ed. Norwood: Artech House.
- Björner, D., Jones, C.B., 1978, The Vienna Development Method: The Meta-Language, *Lecture Notes in Computer Science*, 61, 24-217.
- Broenink, J. F., Larsen, P.G., Verhoef, M., Kleijn, C., Jovanovic, D., Pierce, K., Wouters, F., 2010, Design Support and Tooling for Dependable Embedded Control Software, *Proceedings of Serene 2010 International Workshop on Software Engineering for Resilient Systems*, 77-82, April, New York (USA).
- Claudia, D., 2010, Path tracking with iGPS, *Proceedings of International Conference on Indoor Positioning and Indoor Navigation*, 1-6, September. Zurich (Switzerland).
- DSF/ISO/DIS 12188-2, 2011, Tractors and machinery for agriculture and forestry - test procedures for positioning and guidance systems in agriculture - part 2: Testing of satellite-based auto-guidance systems during straight and level travel, *International Organization for Standardization*, Denmark
- Edwards, G., Bochtis, D., Sørensen, C.G., 2012, Developing a field robotic test platform using Lego®Mindstorm®NXT. *Proceedings of CIGR International Conference on Agricultural Engineering*, July 8-12, Valencia (Spain).
- Fang, H., Lenain, R., Thuilot, B., Martinet P., 2005, Robust Adaptive Control of Automatic Guidance of Farm Vehicles in the Presence of Sliding, *Proceedings of the 2005 IEEE International Conference on Robotics and Automation*, 3102-3107, April 18-22, Barcelona (Spain).
- Fitzgerald, J., Larsen, P.G., Mukherjee, P., Plat, N., Verhoef, M., 2005, *Validated Designs for Object-oriented Systems*, 2nd ed. New York: Springer.
- Fitzgerald, J., Larsen, P.G., Pierce, K., Verhoef, M., 2011, *A Formal Approach to Collaborative Modelling and Co-simulation for Embedded Systems*, Technical Report, Newcastle University.
- Grisson, R., Alley, M., HeatWole, C., 2009, Precision Farming Tools: Global Positioning System (GPS). *Virginia Cooperative Extension*, 442-503.
- Kleijn, C., 2006, Modelling and Simulation of Fluid Power Systems with 20-sim. *Intl. Journal of Fluid Power*, 7(3), November, West Lafayette (USA).
- Larsen, P.G., Battle, N., Ferreira, M., Fitzgerald, J., Lausdahl, K., Verhoef, M., 2010, The Overture Initiative – Integrating Tools for VDM. *ACM Software Engineering Notes*, 35(1), January.
- Merzouki, R., Ould-Bouamama, B., Djeziri, M.A., Bouteldja M., 2007, Modelling and estimation of tire-road longitudinal impact efforts using bond graph approach, *Mechatronics*, 17(2-3), 93-108, March-April.

- Rovira Más, F., Zhang, Q., Hansen, A.C., 2011, *Mechatronics and Intelligent Systems for Off-road Vehicles*, 1st ed. London: Springer-Verlag
- van Amerongen, J., 2010, *Dynamical Systems for Creative Technology*, 1st ed. Ensched (Netherlands): Controllab Products.
- Verhoef, M., 2009, *Modeling and Validating Distributed Embedded Real-Time Control Systems*, PhD thesis, Radboud University Nijmegen.
- Verhoef, M., Larsen, P.G., Hooman, J., 2006, Modeling and Validating Distributed Embedded Real-Time Systems with VDM++, *FM 2006: Formal Methods, Lecture Notes in Computer Science* 4083, 147–162, Springer-Verlag.



## 2

---

### **Collaborative Model Based Development of Adaptive Controller Settings for a Load-carrying Vehicle with Changing Loads**

---

The paper presented in this chapter has been presented at CIOSTA (Commission Internationale de l'Organisation Scientifique du Travail en Agriculture).

[P20] Martin Peter Christiansen, Morten Larsen, and Rasmus Nyholm Jørgensen. Collaborative Model Based Development of Adaptive Controller Settings for a Load-carrying Vehicle with Changing Loads. In Dionysis D. Bochtis and Claus Aage Grøn Sørensen, editors, *CIOSTA XXXV Conference*, July 2013

## Collaborative Model Based Development of Adaptive Controller Settings for a Load-carrying Vehicle with Changing Loads

Martin Peter Christiansen<sup>1</sup>, Morten Larsen<sup>1,2</sup>, Rasmus Nyholm Jørgensen<sup>1</sup>

<sup>1</sup>Department of Engineering, Aarhus University, Finlandsgade 22, 8200 Aarhus N, Denmark

<sup>2</sup>Compleks Innovation Aps, Fælledvej 17, 7600 Struer, Denmark

Corresponding author: [mpc@iha.dk](mailto:mpc@iha.dk)

### ABSTRACT

Load-carrying agricultural vehicles can experience load changes during operation. The change in load is present in operational tasks where animal food is dispensed, sprayer tanks are emptied or operational implements change position over time. The change in load is influencing the weight distribution of the vehicle and consequently the steering and driving performance. The surface conditions the vehicle traverses also changes dependent on the environment. As a consequence automated guidance controllers for such agricultural vehicles should be able to adapt to changes in load and surface conditions.

Implementing the controller directly on the vehicle to accommodate load change will require the vehicle to be tested under expected conditions. The developers design space may be rather larger, and direct implementation on the vehicle can be seen as both time-consuming and costly. This paper describes a collaborative model of a load-carrying vehicle using the DESTECs framework. Collaborative modelling is utilized to design and develop a continuous-time (CT) model of a vehicle with onboard sensors and a discrete-event (DE) model of automated guidance controller. Collaborative models are known as co-models, and their execution are co-simulations intended for automated testing and evaluation.

Automatic co-model analysis (ACA) is used to simulate and explore the vehicles operational speed range in relation the vehicle's center of gravity (CG) and surface conditions. Based on ACA results and the design criteria of a maximum error of 0.3m, viable candidate controller settings are determined. The ACA also provide the developer with a set of 16 control settings of the total design space of 2040, to test and evaluate in terms of fidelity on the actual vehicle.

**Keywords:** Co-simulation, discrete event, continuous time, precision agriculture, vehicle dynamics, DESTECs

### 1. INTRODUCTION

The introduction of automated precision agriculture machinery is a means to improve field efficiency and productivity. Research and development to improve automated machine efficiency and production output has been on-going for several decades (Bell, Elkaim, and Parkinson 1996; Pérez-Ruiz et al. 2012).

---

M. P. Christiansen, M. Larsen, R. N. Jørgensen. "Collaborative Model Based development of an Adaptive Steering controller for a Load-carrying Vehicle with Changing Loads". International Commission of Agricultural and Biological Engineers, Section V. CIOSTA XXXV Conference "From Effective to Intelligent Agriculture and Forestry", Billund, Denmark, 3-5 July 2013. The authors are solely responsible for the content of this technical presentation. The technical presentation does not necessarily reflect the official position of the International Commission of Agricultural and Biosystems Engineering (CIGR), and its printing and distribution does not constitute an endorsement of views which may be expressed. Technical presentations are not subject to the formal peer review process by CIGR editorial committees; therefore, they are not to be presented as refereed publications.

One of the main obstacles the developer needs to overcome is the comparison of different control setups. Repeating scenarios is difficult because of the semi-controlled outdoor environment, compared to the controlled soundings of the manufacturing industry. Geographical conditions are influencing operation and varies based on weather and terrain conditions (Hall and Lima 2001; Eaton et al. 2008).

Utilizing a computer simulation can be a means for the controller developer to reproduce, compare and evaluate results. The literature contains references to robotics and agricultural machinery simulation software. In (Staranowicz and Mariottini 2011) the authors provides a comparison between commercial and open-source robotic simulation software. (Karkee and Steward 2011) developed a model implementing back and front wheel cornering stiffness. A 2D kinematic model of the tractor and implement is used in (Backman, Oksanen, and Visala 2012) to test Nonlinear Model Predictive Control.

The aim in this paper is to evaluate that modelling and simulation of the vehicle and controller can be used as a means to select likely viable control setting candidates. Vehicle and controller modelling and simulation are performed in the DESTTECS ("Design Support and Tooling for Embedded Control Software") framework<sup>1</sup> (Fitzgerald et al. 2012). The DESTTECS framework allows for multi-disciplinary modelling (collaborative models) that combines continuous-time (CT) system models with discrete-event (DE) digital controller modelling.

The modelled vehicle in this paper is ASuBot<sup>2</sup> (Aarhus and Southern Denmark University Robot) testing platform used in the research and development of intelligent agricultural applications. The goal of introducing simulation and modelling to this vehicle is to evaluate the potential speedup in the implementation of new applications for agricultural autonomous vehicles.

The remainder of this paper is structured as follows. Section 2 describes the materials used in project in terms of the ASuBot vehicle and the DESTTECS technology. Section 3 describes the modelling of the vehicle and guidance controller and methods used to determine viable control setups. Section 4 presents and discusses the results of the simulations and the expected control setups that are able to ensure route-following performance at different load distributions. Finally, we provide a few concluding remarks in Section 6.

## 2. MATERIALS

### 2.1 The ASuBot platform

The ASuBot vehicle used in the modelling is a Massey Ferguson MF 38-15SD garden tractor. The garden tractor has been retrofitted with electrically controllable steering wheel (Topcon AES-25) and an electrical linear actuator for controlling the continuously variable transmission. Furthermore, a 6:1 reduction gear has been fitted on the steering column in order to reduce the load on the steering wheel. The garden tractor has also been equipped with a mechanical load displacement mechanism, which enables experiments with center of gravity (CG) placement.

<sup>1</sup> <http://destecs.org/>

<sup>2</sup> <http://fieldrobot.dk/pages/asubot.php>

---

M. P. Christiansen, M. Larsen, R. N. Jørgensen. "Collaborative Model Based Development of an Adaptive Steering Controller for a Load-carrying Vehicle with Changing Loads". International Commission of Agricultural and Biological Engineers, Section V. CIOSTA XXXV Conference "From Effective to Intelligent Agriculture and Forestry", Billund, Denmark, 3-5 July 2013.

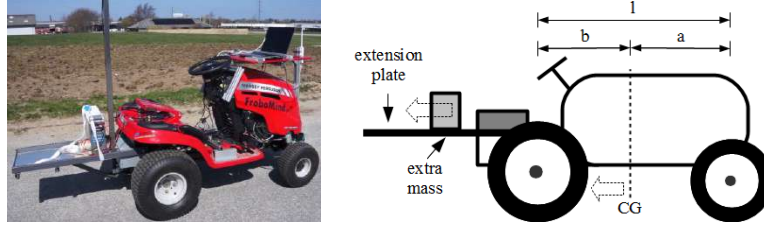


Figure 1. ASuBot equipped with load displacement mechanism controlling load distribution between the front and rear wheels.

A Global Navigation Satellite System (GNSS) based sensor systems is mounted on top of the garden tractor together with an IMU (VectorNav VN-100 Rugged). Encoders (Leine & Linde RSA/RHA 607) are mounted on each back wheel and the right front wheel for measuring the vehicle speed and steering angle. All sensors and actuators is interfaced to a PC via CAN (controller area network) bus or serial interfaces. The software for performing the practical tests is based upon ROS and FroboMind. FroboMind is a software platform for field robots (Jensen, Larsen, and Green 2012).

## 2.2 The DESTECs tool

DESTECs co-simulation technology (Broenink et al. 2010) provides a model-based approach to the engineering of embedded control systems. The technology supports models where the controller and plant or environment is modelled using different specialised tools. The overture tool and VDM formalism models the DE controller, and 20-sim tool models CT components. 20-sim is a modelling and simulation tool, able to model complex multi-domain dynamic systems, such as combined mechanical, electrical and hydraulic systems. VDM Real Time (VDM-RT) (Verhoef, Larsen, and Hooman 2006) is the dialect used in DESTECs with the capabilities to describe real-time, asynchronous, object-oriented features. Both VDM and 20-sim are well-established formalisms with stable tool support and a record of industry use.

DESTECs contains a feature known as automated co-model analysis (ACA) that provides the means to do Design Space Exploration (DSE) of a co-model (Pierce et al. 2012). ACA provides the ability to test different parameter and system configurations, by running all combinations chosen by the user. This paper utilizes the output from the ACA for evaluation of controller performance based on a predetermined cost function of the simulated route following.

## 3. METHODS

The full details of the modelling of the CT and DE system and estimation of system parameters is not presented in this paper, and only a brief description is given. Details on the parameters estimation and DESTECs modelling are instead present in a technical report (Christiansen et al. 2013) in relation to this article.

---

M. P. Christiansen, M. Larsen, R. N. Jørgensen. "Collaborative Model Based Development of an Adaptive Steering Controller for a Load-carrying Vehicle with Changing Loads". International Commission of Agricultural and Biological Engineers, Section V. CIOSTA XXXV Conference "From Effective to Intelligent Agriculture and Forestry", Billund, Denmark, 3-5 July 2013.



### 3.1 DESTECS modelling

The modelling of the ASuBot system is split up in the parts intended to be modelled by the DE and CT tools. The CT models the ASuBot vehicle, the GNSS and IMU sensors, and the actuators used in the automatic guidance system. The onboard wheel encoders are not parts of this model since they are mainly used to measure system parameters. The DE side models the path tracking method used to select the next waypoint in a route-plan and a path tracking controller. The path tracking method is based on the classical controller principle of pure-pursuit. The route-plan consists of a sequence of waypoints with relative UTM (Universal Transverse Mercator) coordinates, describing the path the vehicle must follow.

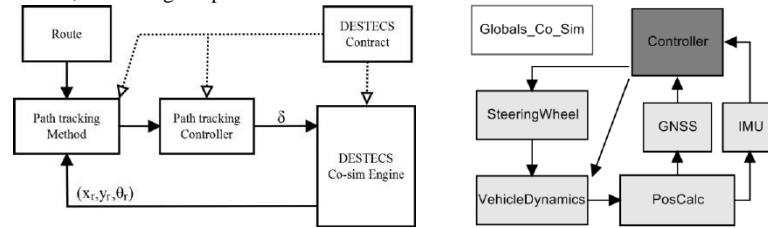


Figure 2. The structures of the CT and DE models used in the DESTECS modelling of ASuBot

The DESTECS tool binds the DE and CT models together using the DESTECS contract and is responsible for exchange of shared variables and parameters. The co-simulation engine coordinates the 20-sim and VDM simulation by implementing a protocol for time-step synchronisation between the two tools.

A contract defines the parameters and variables to be exchanged during simulation. In the contract the parameter  $\mu$  describes the surface the vehicles wheels are moving in the CT model in terms of wheel slip. The parameter  $u$  is the speed of ASuBot in a simulation. The shift of CG using  $\Delta cg$  is intended to model a load changing operation of the garden tractor. The CT model shares the output GNSS position from the GNSS block and IMU derived orientation variable. The DE model controls the set point steering wheel angle that is an input to the CT SteeringWheel block.

### 3.2 System Parameters

In the DESTECS simulation of ASuBot, the parameters in Tabel 1 are used on the CT side.

Tabel 1. CT model parameters used in the co-modelling and co-simulation

Sub-system	Parameter values
Vehicle	$m = 323\text{kg}$ $a = 0.5\text{m}$ $b = 0.68\text{m}$ $l = 1.18\text{m}$
dynamic	$C_{af} = 34377\text{N/rad}$ $C_{ar} = 42972\text{N/rad}$
Steering	$\delta_{sw} = \pm 40^\circ$ $\tau_w = 0.265\text{s}$
wheel	$\delta_{ss} = \pm 41^\circ$ $\tau_s = 0.2\text{s}$
GNSS	$x_{gnss} = 0.5\text{m}$ $y_{gnss} = 0.0\text{m}$

The parameters  $m$  describes the vehicle total mass,  $a$  and  $b$  the vehicles normal CG position.

M. P. Christiansen, M. Larsen, R. N. Jørgensen. "Collaborative Model Based Development of an Adaptive Steering Controller for a Load-carrying Vehicle with Changing Loads". International Commission of Agricultural and Biological Engineers, Section V. CIOSTA XXXV Conference "From Effective to Intelligent Agriculture and Forestry", Billund, Denmark, 3-5 July 2013.

$C_{af}$  and  $C_{ar}$  describes the wheel cornering stiffness.  $\delta_{sw}$  and  $\delta_{ss}$  represents the steering wheel and front steering limits.  $\tau_w$  and  $\tau_s$  defines the control response time delay and steering backlash.  $x_{gnss}$  and  $y_{gnss}$  describes the coordinates of the GNSS receiver relative to normal CG.

### 3.3 Automatic Co-model Analysis

The ACA implementation utilized in this project intend to select the best control setup candidates based on DSE. The ACA is set to perform a DSE for a backwards shift in CG between 0 and 0.4. The ACA explores the speed  $u$  in the range 1-2 m/s representing the controllable area. The ACA also explores wheel-surface  $\mu$  friction coefficients between 0.55 and 0.7, representing the conditions of asphalt/concrete, soil, gravel and sand (Wong 2008).

To evaluate the results from the ACA run, a cost function was used to compare vehicle movement against the evaluation route. Starting from the first waypoint in the route sequence the direct distance between GNSS-receiver and route is determined also known as relative cross-track error (XTE) (Danish Standard 2011). The viable control candidates setting are determined based on a maximum 0.3m XTE criterion for each simulation.

## 4. RESULTS AND DISCUSSION

The ACA is run for the chosen DSE and produces the output path for each simulation. Each simulation is run until the vehicle has traversed the route or the controller is unable to steer towards any remainder route-waypoints. The results from the simulation are coloured based on the evaluation criteria. The plot in both Figure 3 and 4 is plotted in relation to  $\mu=0.55$  representing the wheel-surface contact of wet soil.

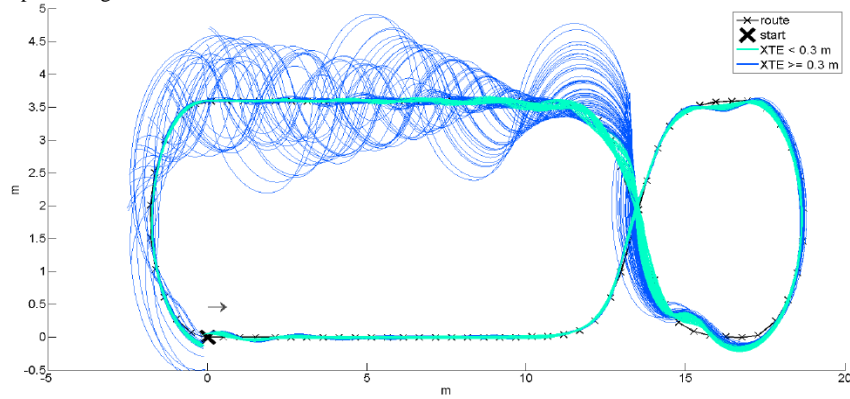


Figure 3. The simulated paths from ACA are plotted in relation to the route for  $\mu=0.55$ . Simulation maximum XTE is used to colour the path based on 0.3 m criteria.

Wet soil is some of the worst case wheel sliding conditions for the vehicle in terms of expected operational area. The viable candidates are chosen based on the criteria of wet soil since the

vehicle could be unaware of the current wheel surface conditions. The results from the ACA provide the developer the ability to design an adaptive controller regulating the speed in relation to the vehicles current CG. The ACA produces a smaller subset of the total explored design space that determines the margin between viable and unviable control setting candidates.

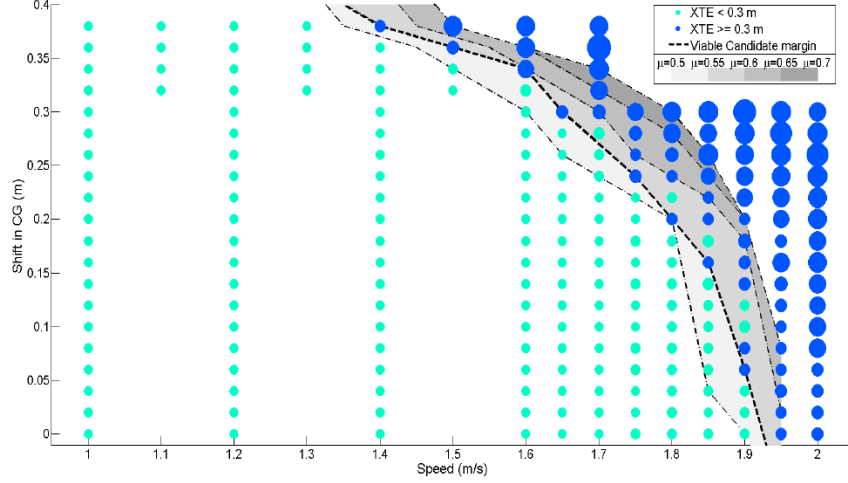


Figure 4. The results from the full ACA, blue represents the unviable speed setting candidates for  $\mu=0.55$ . The safety margins are plotted for the range  $\mu=0.5-0.7$ . The scenario  $\mu=0.5$  is plotted to illustrate the conditions outside the worst case range.

Testing these candidates could be used to determine the fidelity of future ACA results produced by the co-model. The 16 testing candidates derived from the ACA can be found in table 2.

Table 2. Control setting candidates to be tested on the actual ASuBot

Factors	Viable candidates	Unviable candidates
$u$ (m/s)	1.40;1.50;1.60;1.65;1.75;1.80;1.85;1.90;	1.40;1.50;1.60;1.65;1.75;1.80;1.85;1.90;
$\Delta cg$ (m)	0.36;0.34;0.32;0.28;0.22;0.18;0.14;0.04;	0.38;0.36;0.34;0.30;0.24;0.20;0.16;0.06;

The fidelity of the DECTECS co-model of the ASuBot vehicles is still in question and need to be validated with actual testing. Factors not accounted for in the co-model are types of imprecision from the GNSS receiver, IMU and steering wheel. The current GNSS model are missing the influences of are dropouts, multipath and precision mode. Repeated testing could be used to account for these factors, when evaluating the fidelity of the co-model. Future versions of the model should also be able to account for changes in mass and instantaneous change in wheel-surface conditions to model a more realistic environment. The result indicates that simulation and DSE method could be used to improve performance, for classical guidance controller systems on load-changing vehicles.

M. P. Christiansen, M. Larsen, R. N. Jørgensen. "Collaborative Model Based Development of an Adaptive Steering Controller for a Load-carrying Vehicle with Changing Loads". International Commission of Agricultural and Biological Engineers, Section V. CIOSTA XXXV Conference "From Effective to Intelligent Agriculture and Forestry", Billund, Denmark, 3-5 July 2013.

## 5. CONCLUSION

This paper proposes an approach to the design of adaptive automated guidance controllers settings using modelling, simulation and DSE. The model accounts for vehicle dynamics phenomena's in terms of wheel sliding effects, actuator delays and steering wheel response. The case of a classical guidance controller in combination with speed adaption to the vehicles current CG is analysed to determine safe operational parameter settings. The described DSE method could be used to improve the performance of classical guidance controller on load-changing vehicles.

DSE in terms of vehicle speed and shift in CG is performed using the ACA tool in DESTECs. An XTE algorithm evaluated the simulated ASuBot movements compared to a pre-planned route. The ACA carried out the total design space of 2040 combinations, provides the developer with a set of 16 control settings to test and evaluate in terms of fidelity on the actual vehicle. An adaptive guidance controllers could be develop and tested on the ASuBot based on the ACA results. We are currently working on testing and evaluating the co-model of the ASuBot to optimize system parameters and determine the models level of fidelity.

Finally, the co-model can be improved to account for changes in mass on a load-carrying vehicle and movement between different surface conditions. The improved model could be used extend the robustness evaluation of different automated guidance controllers.

## ACKNOWLEDGEMENT

Financial support given by the Danish Ministry of Food, Agriculture and Fisheries is gratefully acknowledged. We acknowledge partial support from the EU FP7 DESTECs project on co-simulation. Thanks are due to Jens Kristian Kristensen at Research Centre Foulum and Conpleks Innovation for providing assistance in connection with the experiments. We would like to acknowledge our colleagues Kjeld Jensen and Søren Hundevadt Nielsen at University of Southern Denmark for providing key components in the Frobomind software platform. We would also like to acknowledge our colleague Michael Nørremark who provided input and expertise that assisted the research.

## REFERENCES

- Backman, J., T. Oksanen, and A. Visala. 2012. "Navigation System for Agricultural Machines: Nonlinear Model Predictive Path Tracking." *Computers and Electronics in Agriculture* 82 (March): 32–43.
- Bell, Thomas, Gabriel Elkaim, and Dr. Bradford Parkinson. 1996. "Automatic Steering of Farm Vehicles Using GPS." In *Proc. of the 3rd Intern. Conf. on Precision Agriculture*.
- Broenink, J F, P G Larsen, M Verhoef, C Kleijn, D Jovanovic, K Pierce, and Wouters F. 2010. "Design Support and Tooling for Dependable Embedded Control Software." In *Proceedings of Serene 2010 International Workshop on Software Engineering for Resilient Systems*, 77–82. ACM.
- 
- M. P. Christiansen, M. Larsen, R. N. Jørgensen. "Collaborative Model Based Development of an Adaptive Steering Controller for a Load-carrying Vehicle with Changing Loads". International Commission of Agricultural and Biological Engineers, Section V. CIOSTA XXXV Conference "From Effective to Intelligent Agriculture and Forestry", Billund, Denmark, 3-5 July 2013.

- Christiansen, Martin P., Morten Larsen and Rasmus N. Jørgensen. 2013. "System parameters estimation and modeling of the ASuBot vehicle platform." To appear in Technical Reports. Electrical and Computer Engineering. Department of Engineering, Aarhus University.
- Danish Standard. 2011. "Dsf/iso/dis 12188: Tractors and Machinery for Agriculture and Forestry - Test Procedures for Positioning and Guidance Systems in Agriculture" *International Standard Organization*.
- Eaton, R, J Katupitiya, K W Siew, and K S Dang. 2008. "Precision Guidance of Agricultural Tractors for Autonomous Farming." In *2008 2nd Annual IEEE Systems Conference*, 1–8. IEEE.
- Fitzgerald, John S, Peter Gorm Larsen, Ken G Pierce, and Marcel H G Verhoef. 2012. "A Formal Approach to Collaborative Modelling and Co-simulation for Embedded Systems." *Mathematical Structures in Computer Science*: 1–27.
- Hall, S G, and M Lima. 2001. "Problem-solving Approaches and Philosophies in Biological Engineering: Challenges from Technical, Social, and Ethical Arenas." *Transactions of the ASAE* 44 (4): 1037–1041.
- Jensen, Kjeld, Morten Larsen, and Ole Green. 2012. "FroboMind, Proposing a Conceptual Architecture for Field Robots." *CIGR-Agend2012*.
- Karkee, Manoj, and Brian L. Steward. 2011. "Parameter Estimation and Validation of a Tractor and Single Axle Towed Implement Dynamic System Model." *Computers and Electronics in Agriculture* 77 (2) (July): 135–146.
- Pérez-Ruiz, M., D.C. Slaughter, C.J. Gliever, and S.K. Upadhyaya. 2012. "Automatic GPS-based Intra-row Weed Knife Control System for Transplanted Row Crops." *Computers and Electronics in Agriculture* 80 (January): 41–49.
- Pierce, Ken, Carl Gamble, Yunyun Ni, and Jan F. Broenink. 2012. "Collaborative Modelling and Co-simulation with DESTECs: A Pilot Study." In *2012 IEEE 21st International Workshop on Enabling Technologies: Infrastructure for Collaborative Enterprises*, 280–285. IEEE.
- Staranowicz, Aaron, and Gian Luca Mariottini. 2011. "A Survey and Comparison of Commercial and Open-source Robotic Simulator Software." *Proceedings of the 4th International Conference on Pervasive Technologies Related to Assistive Environments - PETRA '11*: 1.
- Verhoef, Marcel, Peter Gorm Larsen, and Jozef Hooman. 2006. "Modeling and Validating Distributed Embedded Real-Time Control Systems with VDM++." In *FM 2006: Formal Methods*, 147–162. Springer-Verlag.
- Wong, Par J. Y. 2008. *Theory of Ground Vehicles*.
- 
- M. P. Christiansen, M. Larsen, R. N. Jørgensen. "Collaborative Model Based Development of an Adaptive Steering Controller for a Load-carrying Vehicle with Changing Loads". International Commission of Agricultural and Biological Engineers, Section V. CIOSTA XXXV Conference "From Effective to Intelligent Agriculture and Forestry", Billund, Denmark, 3-5 July 2013.



# 3

---

## **A Test Platform for Planned Field Operations Using LEGO Mindstorms NXT**

---

The paper presented in this chapter has been published in MDPI Robotics).

[P30] Gareth Edwards, Martin P. Christiansen, Dionysis D. Bochtis, and Claus G. Sørensen. A Test Platform for Planned Field Operations Using LEGO Mindstorms NXT. *Robotics*, 2(4):203–216, 2013

## A Test Platform for Planned Field Operations Using LEGO Mindstorms NXT

Gareth Edwards \*, Martin P. Christiansen, Dionysis D. Bochtis and Claus G. Sørensen

Department of Engineering, University of Aarhus, Blichers Allé 20, Tjele 8830, Denmark;  
E-Mails: martinp.christiansen@agrsci.dk (M.P.C.); dionysis.bochtis@agrsci.dk (D.D.B.);  
claus.soerensen@agrsci.dk (C.G.S.)

\* Author to whom correspondence should be addressed; E-Mail: gareth.edwards@agrsci.dk;  
Tel.: +45-8715-7631.

*Received: 25 September 2013; in revised form: 15 November 2013 / Accepted: 19 November 2013 /  
Published: 27 November 2013*

---

**Abstract:** Testing agricultural operations and management practices associated with different machinery, systems and planning approaches can be both costly and time-consuming. Computer simulations of such systems are used for development and testing; however, to gain the experience of real-world performance, an intermediate step between simulation and full-scale testing should be included. In this paper, a potential common framework using the LEGO Mindstorms NXT micro-tractor platform is described in terms of its hardware and software components. The performance of the platform is demonstrated and tested in terms of its capability of supporting decision making on infield operation planning. The proposed system represents the basic measures for developing a complete test platform for field operations, where route plans, mission plans, multiple-machinery cooperation strategies and machinery coordination can be executed and tested in the laboratory.

**Keywords:** field robots; indoor simulation; micro-tractor; operations management; area coverage

---

### 1. Introduction

Full-scale testing of agricultural operations management can often prove both costly and time consuming, while computer simulations often make assumptions and estimates about the environment,



sensors and actuators in the system. In particular, when considering agricultural operations, full-scale testing can only be carried out at certain times of the year, possible only a few months, and tests on the same area cannot be easily repeated, *i.e.*, a crop can only be harvested once.

Computer models intended to simulate sensors and actuators are only a representation of reality with a certain level of accuracy. The models are designed to simulate scenarios the developers have deemed relevant to test design parameters. In [1], GPS signals are simulated to realize the external noise sources affecting the operations of an agricultural vehicle's auto-steering system. The GNSS and vehicle model are tested with a nonlinear model predictive controller. The current system models are still only designed to test the scenarios the developers want to research based on current domain knowledge.

Software tools for modeling and simulation of robot vehicles exist in the form of tools, such as player-stage-gazebo and Microsoft robotics studio. Game engines for physical simulation or model-based differential equations allow a robotics simulation tool to simulate the system physics [2]. Robotics simulation frameworks have been used to move directly from simulation to full deployment on a vehicle. Robotics simulation frameworks provide a number of generalized building blocks (vehicle, sensors and actuators) that can be modified to describe different setups. To select viable solutions, extensive domain knowledge of the system type and tool building blocks is needed. The authors of [3] first use computer simulation and then real life testing to gather results on the effectiveness of a system to control small robots during an environment discovery procedure. Simply procedural algorithms were tested in the computer simulation, and once their robustness was proven, real life testing was carried out on a small scale.

An intermediate step between simulation and deployment has been developed in recent years, by utilizing a Hardware-In-the-Loop [4] test setup to evaluate an algorithm's control response and robustness. A Hardware-In-the-Loop test setup is still dependent on the correct modeling of sensors and actuators, for evaluation of the control loop.

In the case of field machinery operations, whilst there are a number of examples for the implementation of test platforms and small-scale machines, these are limited. The authors of [5] used two iRobot Magellan Pro robots in an indoor environment in order to demonstrate a methodology for real-time docking of combined harvesters and transport carts. The authors of [6] used the iRobot platform to test a swarm intelligence algorithmic approach for multi-robot setup for controlling weed patches distributed within a field area, and [7] developed a robotic platform equipped with cameras for row guidance and weed detection for the mapping of weed populations in fields, which was used to demonstrate intelligent concepts for autonomous vehicles.

Nevertheless, the above-mentioned examples are customized tools developed specifically for each application under study and do not build in a common standard framework.

LEGO Mindstorms is an example of a common framework that has been used in other scientific disciplines related to robotics, *e.g.*, robotic exploitation [8] and team intelligence [9]. LEGO Mindstorms provides a proven, versatile framework for prototyping mechanical robotic systems that are programmed with a high degree of complexity. It also provides a system that has the ability to add and remove functionalities, as well as to reconfigure its architecture. This allows it to adapt to the needs of the different requirements of various applications, giving it an advantage over other

frameworks. This critical notion is in accordance with the requirements of future innovative agricultural fleet management systems, as have been outlined [10].

In order to quickly test operational management techniques, a test platform was developed, utilizing a LEGO Mindstorms micro-tractor, allowing for easily replicable results that can be evaluated while interpreting collected data. The test platform also consists of control and display modules that enable it to execute and monitor management techniques. Compared to a Hardware-In-the-Loop, solution the micro-tractor allows for the evaluation of software components using actual sensory input. This test platform is seen as an intermediate between simulation and full-scale testing, rather than a replacement of either.

In this paper, the test platform is described in terms of its hardware and software components. The performance of the platform is demonstrated and tested in terms of its capability of supporting decision making on field operation planning by indoor environment simulations. Following this introduction, the LEGO Mindstorms suite is described in Section 2. In Section 3, the hardware and the software components are described. Section 4 outlines the tests, which were conducted to prove the test platforms' fitness for the purpose, and finally, conclusions are made in Section 5.

## 2. The LEGO Mindstorms NXT

LEGO Mindstorms is a suite developed by LEGO containing the "NXT Intelligent Brick" as the main controlling unit. It is programmed either using LEGO's own Mindstorms IDE (integrated development environment) or various third-party development tools. The NXT Brick is capable of controlling three LEGO NXT servo motors in terms of rotation speed and direction, via voltage regulation. The NXT servo motors also have built-in rotary encoders that can deliver 720 steps, equivalent to an accuracy of  $0.5^\circ$ , which are used to monitor the angular position respective to their starting position, which is deemed to be zero degrees. The NXT Brick can have up to four sensors as inputs through either analogue or I2C connections. These sensors include standard LEGO sensors, such as light sensors, touch sensors and ultra-sonic sensors, and sensors developed from other companies (e.g., ViTech, Microinfinity, Dexter Industries), such as temperature sensors, color sensors, chemical sensors, *etc.*, coping with the measuring requirements of scientific experimentations.

## 3. Methods

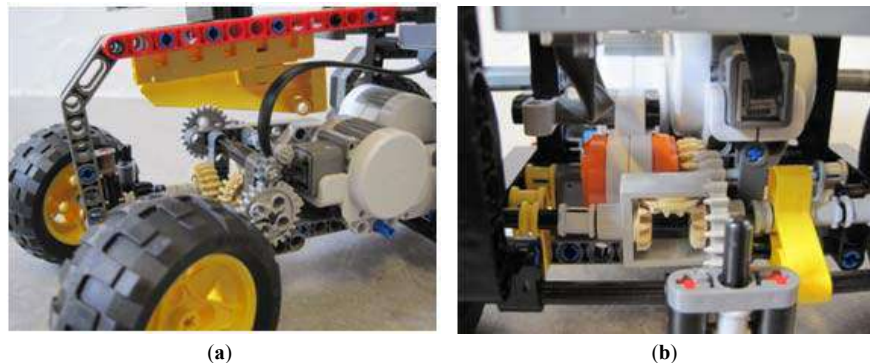
### 3.1. Hardware

The steering of the tractor is actuated with a rack and pinion system, which allows the front wheels to turn through  $\pm 30^\circ$ . A standard NXT motor was used to control the steering (Figure 1a) with a gearing at a ratio of 7:1 to increase the range of the control. The rear wheels are controlled by another NXT motor (Figure 1b), which transmits the power to the back axles via a differential gear. This allows the vehicle to turn corners without the back wheels slipping. The specific relation of the gearing ratio and the size of the rear wheels tires results in a 0.51 mm movement of the tractor for each degree that the drive motor turns.

The micro-tractor was designed to be a representation of a generic tractor, rather than a specific tractor, so as to allow more flexibility in the transferability of the results. The micro-tractor has a

wheelbase of 175 mm and a turning radius of 370 mm. Considering that an average medium-sized tractor (150 hp) has a wheelbase and turn radius of approximately 2.5 m and 5.2 m, this would correspond to a scaling of 1:14. If there is a need for the test result to demonstrate a specific tractor, the use of LEGO would allow for fast modification.

**Figure 1.** Photos of the steering and drive components.

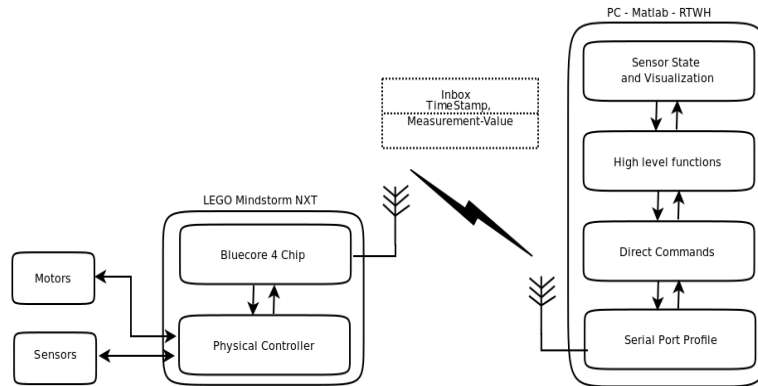


The main navigation sensor is the CruizCore<sup>®</sup> XG1300L IMU, which is mounted on the front of the micro-tractor and is able to measure the relative heading of the micro-tractor compared to the starting position with a relative accuracy stated as  $<0.1^\circ$ . The device contains a single axis MEMS gyroscope and a three-axis accelerometer. The signals from these sensors are processed onboard the device, applying factory set compensation factors, which helps to reduce the most significant errors. The measured heading is susceptible to a maximum error of  $10^\circ$ , according to the product specifications, during one hour of continuous operation.

As part of developing a platform to demonstrate various agricultural operations, implements can be constructed using additional NXT units. However, the micro-tractor has one motor port and three sensor ports available for implements that are not equipped with an NXT unit. The micro-tractor is equipped with a drawbar suitable for connecting implements.

### 3.2. Software

The BrickCC (Brick Command Center), an open source Windows program that uses the NXC programming language [11], is used to compile the programs contained on the NXT Brick. Matlab (MathWorks<sup>®</sup>) and the RWTH-Mindstorms NXT toolbox [12] were used for remote communication with the NXT Brick via Bluetooth (Figure 2).

**Figure 2.** The communication architecture.

### 3.2.1. Communication

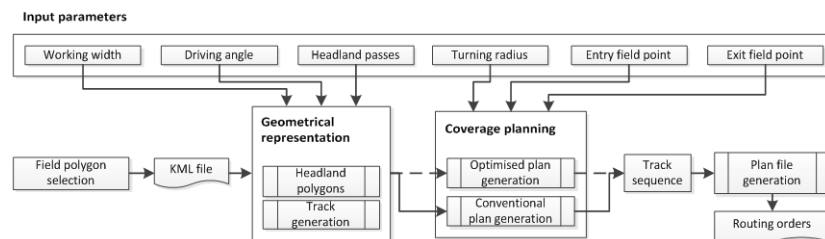
The Bluetooth protocol utilized by LEGO is placed on top of the Serial Port Profile (SPP) protocol. Direct control commands provide the ability to remote control the NXT from a computer. Each NXT command over a Bluetooth connection takes approximately 100 ms to successfully process, making it too slow for precision control of the tractor. As a consequence, the micro-tractor was chosen to be programmed in the NXC programming language, and the compiled code was loaded directly onto the NXT for execution. Programming the NXT directly provides the ability to control the position and angle with a much higher accuracy, compared to the Bluetooth solution. If communication between the computer and brick is lost at any point during the testing, the NXT makes a sound, so that testing can be aborted and restarted.

### 3.2.2. Route Planning

The route planning for the micro-tractor was implemented offline using the Matlab programming language. The input for planning includes the boundaries of the working area, which can be selected in a digital map, and a number of operational parameters (Figure 3). Based on the input, as the first step, the geometrical representation of the field is generated. The geometrical representation regards the definition, in terms of their coordinates, of the geometrical entities inherent in a field area representation. These entities include the parallel field-work tracks and the peripheral boundary passes (headland area). The next step includes a coverage path generation, which could be either a conventional plan (e.g., sequential ordering of the tracks) or optimized according to the principle of *B-patterns*, that algorithmically results in an optimal field-work track traversal sequence according to an optimization criterion [13,14]. In the latter case, the coverage plan does not follow the repetition of standard motifs, but the plan is a unique result of the optimization approach on the specific combination of the mobile unit kinematics, the operating width and the optimization criterion, such as, total or non-working travelled distance, total or non-productive operational time, a soil compaction measure [15], *etc.* In the presented case, the non-working travelled distance has been considered as the

minimization criterion. The optimization problem is that of finding the optimal track sequence:  $\sigma^* = \arg \min_{\sigma} \sum_{i=1}^{|T|-1} c_{p^{-1}(i+1), p^{-1}(i)}$ , where  $T = \{1, 2, 3, \dots\}$  is the arbitrarily ordered set of the field tracks that cover the entire field area,  $\sigma = \langle p^{-1}(1), p^{-1}(2), \dots, p^{-1}(|T|) \rangle$  is a permutation,  $p(\cdot) : T \rightarrow T$  is the bijective function, which for any field track  $i \in T$  returns the position of the  $i$ th field track in the track traversal sequence, and  $c_{p^{-1}(i+1), p^{-1}(i)}$  is the cost for moving between tracks,  $p^{-1}(i+1)$  and  $p^{-1}(i)$ , which, in the particular case, corresponds to the nonworking travelled distance.

**Figure 3.** The architecture of the route planning.



The final function is the generation of the routing orders, which include a sequence of straight lines and turnings executions. Straight line segments are described by the heading, the distance to be travelled, the driving speed and the starting X and Y coordinates. Turning segments are described by the initial heading, the final heading, the direction of the turn (clockwise or anti-clockwise) and the driving speed.

### 3.2.3. Position Determination

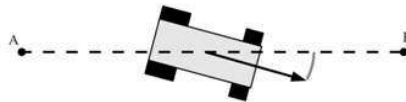
The micro-tractor determines its position onboard the NXT using the heading value from the IMU and the encoder value from the drive motor. Using these values, the position and heading are calculated relative to the micro-tractor's starting position and heading. While communicating with the visualization computer, the micro-tractor samples the IMU and drive motor encoder and calculates its position, at a rate of approximately 12 Hz. Using these techniques for position determination requires the micro-tractor to be operated on a face surface with minimal slip between the wheels and surface occurring.

### 3.2.4. Vehicle Navigation Control

The route maintains its structure of a straight line and turning segments. The segment commands are passed to the NXT one at a time from the Matlab control system; this allows for the execution of management techniques that require real-time adaption of the route. During straight segments, the NXT calculates the number of revolutions of the drive motor it needs to make to drive the prescribed distance. While this is executing, the NXT monitors the micro-tractors distance from the line normal to the direction of travel and the angular error in the heading to that direction of travel (Figure 4). These two calculated errors are entered into a transfer function, and the NXT makes an adjustment to the

steering wheels in order for the micro-tractor to reduce these errors and follow the line as described. A similar control system is described in [16] for use with a full-scale four-wheeled machine, where the errors are referred to as the lateral and angular error. The LEGO test platform also assumes that it is operating on a hard, flat surface with minimal slip. The parameters for the transfer function used were determined empirically.

**Figure 4.** Heading error and distance from the line to travel.



To execute a turn segment, a second control function is used. The micro-tractor sets its wheel in a full lock position in the direction of the turn and then starts the drive motor. During the turn, the heading is monitored until the micro-tractor reaches its desired angle, at which point the drive motor is stopped and the steering wheels are turned back to the zero position. The reason the steering wheels are moved while the vehicle is stationary is to ensure that the micro-tractor traces perfect circles.

### 3.2.5. Visualization

The estimated current heading and position of the micro-tractor are written to a text string and passed into separate mailboxes with 100 ms division, overwriting the old message in the mailbox, along with a timestamp. The task of the Matlab system is to read the content of the mailbox and store and display the results. The current state of the tractor is then calculated and plotted on the map, the travelled path and the desired path are also plotted for comparison reasons.

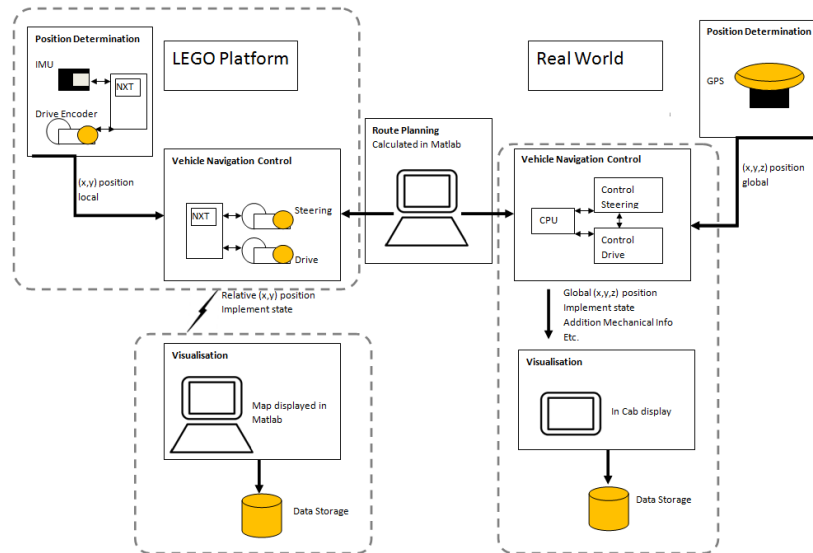
### 3.3. Test Platform Architecture

The architecture of the LEGO test platform aims at mimicking the real-world system in a meaningful way (Figure 5). The main three modules of the system are the Position Determination, Vehicle Control and Visualization. Each of these modules is replicated within the test platform. Within the LEGO platform, although the Route Planning and Visualization are separate systems, they are run on the same computer. The dashed lines on Figure 4 indicate the components of the system that contain the modules. There are some differences between the component setups in the systems; however, this does affect the functionality. For example, the connection between the Vehicle Control and Visualization modules is implemented via a wired connection in the real-world system and a wireless, Bluetooth connection in the LEGO platform. The functionality of these connections is simply to pass information from the Vehicle Control module to be displayed by the Visualization module. The rate at which this information is sent, approximately 10 Hz, is well within the tolerance of the Bluetooth connection; plus, as mentioned in Section 3.2.1, if the connection is interrupted, the test is aborted. Therefore, the Bluetooth connection has the same functionality as the wired connection.

A similar full-scale testing system is described in [17]. Route plans are first generated on a computer and transferred to the test tractor via USB. The tractor then executes the plan, while performing vehicle navigation, and displays the results on a small onboard computer. By using a

similar architecture on the test platform as in the real world, the solutions that are found, such as route plans and management techniques, are able to be transferred to the real-world system more effectively.

**Figure 5.** Depiction of LEGO platform and real-world architectures.



The methods used in the Position Determination modules of the LEGO platform and the real world are vastly different; however, their outputs are the same. A limitation of the current Position Determination module in the LEGO platform is that the operation surface must be flat and provide minimal tire slip, which is not the case in the real world. A limitation of the real-world GPS system is the need for contact with many satellites, which can be susceptible to overhead obstructions, such as trees or cloud cover. Since the LEGO platform operates indoors, the use of a GPS system would be extremely difficult. In the real world, a combination of sensors, such as computer vision techniques or multiple GPS antennae, would be required to obtain an accurate estimate of the vehicle's heading; however, in the LEGO platform, the IMU sensor is sufficient. In both systems, the Position Determination modules provide the Navigation Control module with an estimation of the current position and the current heading, so that steering corrections can be made, and in this way, they can be considered to be comparable.

The system architecture of the platform is built in a modular manner, so that components, such as the Navigation Control or Visualization, could be easily exchanged with another module, as long as the new module takes the same inputs and gives the same outputs. To increase the functionality of the system to allow for real-time operations management, the link between the Route Planning and Navigation Control modules should be modified to a two-way connection, so that data can flow between them. This connection would allow the Route Planning module to update the current plan due

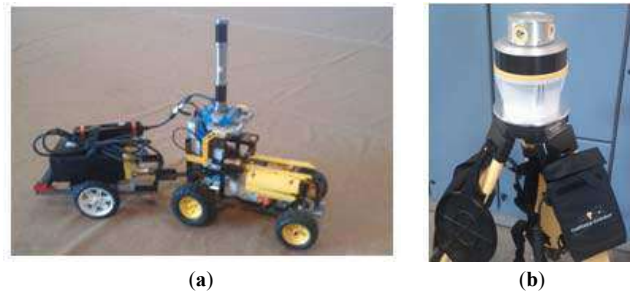
to any changes that may be observed. The micro-tractor can receive commands to execute each segment of the path separately; therefore, the remaining segments of the path, after the current segment, are still open to being altered. This modification of the architecture will be investigated in future work.

#### 4. Implementation of the Test Platform

##### 4.1. Position Accuracy

An indoor GPS (iGPS) was used to test the accuracy of the micro-tractor position determination. The iGPS system (Nikon Metrology, NV Europe) combines a transmitter sensor placed at the center of the rear axle of the micro-tractor (Figure 6a) and six beacon posts (Figure 6b) located around the working area. The author of [18] documented the iGPS system capabilities to track movement up to 3 m/s with an accuracy of 0.3 mm. Opposite planar and angular motions were tested to ensure an unbiased dataset for evaluation. This confirms that iGPS is usable for both static and kinematic spatial positioning and tracking. The kinematic measurement mode of the iGPS was used to track the movements of the micro-tractor with a frequency of 40 Hz.

**Figure 6.** (a) The micro-tractor with mounted iGPS sensor and power source trailer; (b) the iGPS beacon.



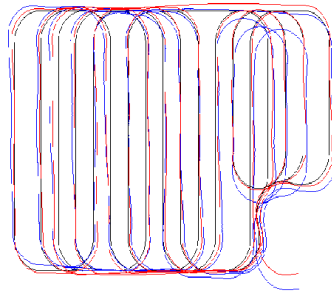
A series of navigation accuracy tests were performed in “virtual” fields for different combinations of operating width and driving directions. For example, Figure 7 presents the three paths (off-line planned, on-line estimated and actual measured) on a “virtual” field for the case of a 250-mm working width and 0° driving direction. Based on the tests, for a basis driving distance of 71.43 m (corresponding to 1 km full-scale distance), including straight line driving (operating on a field-work track) and 180° maneuvering (headland turnings), the average cross-track error between the estimated path and the iGPS path executed by the micro-tractor was 0.028 m, corresponding to 0.39 m full-scale cross-track error. This error is comparable with a typical error in field machinery navigation based on a standard GPS system, thereby showing that the Position Determination is satisfactory for use.

In order to simulate the capabilities of RTK- and DGPS-based navigation systems, the accuracy of the proposed system would need to be increased. However, the improved system should be low-cost and flexible, which excludes the use of precise, but expensive systems, such as iGPS; therefore, further examples were executed using only the tractor’s position determination. The inclusion of a more



accurate position determination, once developed or sourced, would be relatively simple, due to the modular setup of the architecture described in Figure 5.

**Figure 7.** The planned path (the black line), the estimated path by the micro-tractor internal sensors (red line) and the actual path recorded by the iGPS (blue line).



#### 4.2. Demonstration Examples

To demonstrate the capabilities of executing and evaluating routing plans, the test platform was used to test area coverage plans with different setup parameters, such as working widths, driving angles, number of headland passes, *etc.* Figure 8 presents the executed plans from different operational scenarios on the same field. The accuracy of the micro-tractor's ability to maintain the predefined paths are detailed in Table 1, each test scenario was executed three times by the micro-tractor, and the results were then averaged.

**Figure 8.** Four different scenarios show prescribed route (black line) and driven route (red line) for working width and driving angle (a) 0.650 m—90°, (b) 0.8 m—90°, (c) 0.5 m—0° and (d) 0.25 m—120°. The axes are in the micro-tractors-scale and are in mm.

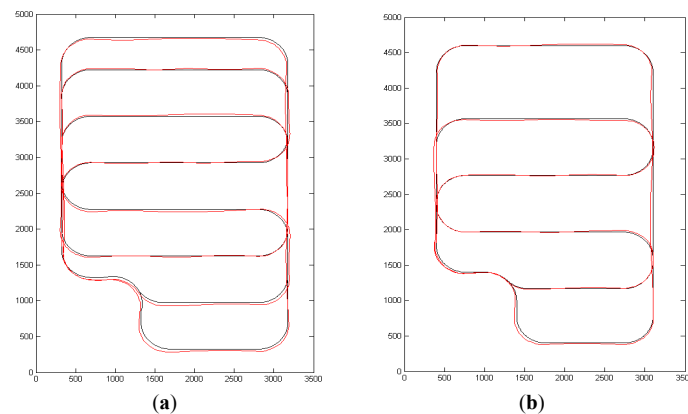


Figure 8. Cont.

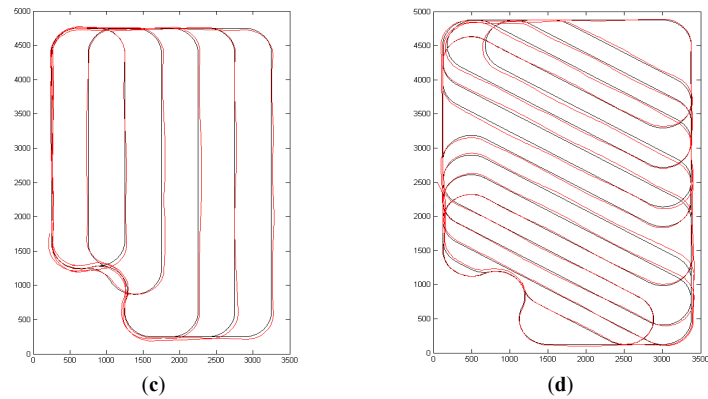


Table 1. Results from test scenarios.

Working Width (mm)	Driving Angle	Expected Path Length (m)	Actual Path Length (m)	Path Length Error	Average CPD * (mm)	Shown in
250	120	82.95	83.10	0.18%	26.76	Figure 8d
250	90	73.76	74.68	1.24%	24.15	
500	0	56.57	57.98	2.49%	20.25	Figure 8c
650	90	38.84	39.16	0.81%	20.27	Figure 8a
800	90	26.98	27.37	1.44%	15.92	Figure 8b
760	0	115.35	116.40	0.91%	52.03	Figure 9

\* Cross Path Divergence.

To demonstrate the system's ability to test real-world scenarios, a real field was used in the final test scenario (Figure 9).

Figure 9. (a) The demonstration field; (b) predefined route (black line) and driven route (red line).



The field used is located at 52.42° N, 2.58° W, and the dimensions were sampled from Google Earth and scaled down by 1:14 to be relative to the test platform. The route was planned using a working width of 0.714 m (approximately, in full scale, 10 m) and driving parallel to the longest edge of the field.

## 5. Conclusions

The proposed system represents the basic measures for developing a complete test platform for field operations, where route plans, mission plans, multiple-machinery cooperation strategies and machinery coordination can be simulated and tested in the laboratory. The laboratory tests are easy to demonstrate and replicate at any time of the year; full-scale testing is often limited by weather and field conditions. Furthermore, using a small-scale test platform eliminated a lot of the safety concerns associated with operating large driverless machinery. The test platform should be seen as an extension to simulations-based evaluation rather than a replacement. Even the most stringently programmed simulations are susceptible to errors or to things being overlooked. The test platform provides another stage of quality assurance, with systems interacting with real collected data, before full-scale testing is attempted. The results from the test platform also add credence when planning full-scale testing and eliminate costly, superfluous tests.

The proposed system also provides many opportunities as an educational tool. Students can quickly and easily test management techniques in a classroom environment and see their ideas implemented in a physical way. Moreover, the modular setup of the system architecture allows students to develop and test new modules, gaining many insights into system engineering and controller design. While the use of the IMU and encoder values adequately estimates the micro-tractors position, it limits the system, as the surface it is run on must be smooth, flat and solid. For the purposes of testing operational management techniques, this is of no consequence, as fields are often simplified using flat 2D representation. However, if another method for efficiently determining the micro-tractor position were deemed necessary, this module could be replaced without affecting the rest of the system.

The execution of coverage plans was chosen to show the capabilities of the test platform to implement agricultural operations management techniques. The demonstration examples also show that it is possible to evaluate coverage plan scenarios, involving different operational features (e.g., working widths, driving angles and number of headland passes), in terms of different operational efficiency measures, e.g., the measured non-working travelled distance, overlapped or missed area and operational time. The example using the real field (Figure 9) could be used as the first step in developing a Control Traffic System for the real-world field. Since the route planning has been shown to be effective, the full-scale testing could proceed more quickly.

The next steps are envisioned to be, for example, the inclusion of additional sensors (e.g., for mapping spatial variations within an area, crop row following, collision detection and enhanced navigation accuracy) and the implementation of multiple micro-tractor systems.

### Acknowledgments

The authors would like to thank the Danish Ministry of Food, Agriculture and Fisheries for their funding of this research. The authors also want to thank Ole Green for initial supervision and support of the work. Thanks are due to Jens Kristian Kristensen at Research Centre Foulum for providing assistance in connection with the experiments. We would also like to acknowledge our colleague, Michael Nørremark, who provided input and expertise that assisted the research. We acknowledge Aachen University's Institute of Imaging and Computer Vision for providing the RWTH Toolbox.

### Conflicts of Interest

The authors declare no conflict of interest.

### References

1. Backman, J.; Kaivosoja, J.; Oksanen, T.; Visala, A. *Simulation Environment for Testing Guidance Algorithms with Realistic GPS Noise Model*; International Federation of Automatic Control: Winterthur, Switzerland, 2010; pp. 139–144.
2. Harris, A.; Conrad, J.M. Survey of popular robotics simulators, frameworks, and toolkits. *Southeast. Proc. IEEE* **2011**, doi:10.1109/SECON.2011.5752942.
3. Cepeda, J.S.; Chaimowicz, L.; Soto, R.; Gordillo, J.L.; Alanis-Reyes, E.A.; Carrillo-Arce, L.C. A behavior-based strategy for single and multi-robot autonomous exploration. *Sensors* **2012**, *12*, 12772–12797.
4. Rossmann, J.; Schluse, M.; Sondermann, B.; Emde, M.; Rast, M.; Advanced Mobile Robot Engineering with Virtual Testbeds. In Proceedings of the 7th German Conference, Munich, Germany, 21–22 May 2012; pp. 1–6.
5. Hao, Y.; Laxton, B.; Benson, E.R.; Agrawal, S.K. Differential flatness-based formation following of a simulated autonomous small grain harvesting system. *CiteSeer* **2004**, *47*, 933–941.
6. Kumar, E.V. *A Swarm Intelligence Algorithm for Multi-Robot Weed Control an Emotion Based Approach*; Anna University Chennai: Tamil Nadu, India, 2008.
7. Bak, T.; Jakobsen, H. Agricultural robotic platform with four wheel steering for weed detection. *Biosyst. Eng.* **2004**, *87*, 125–136.
8. Kovacs, T.; Pasztor, A.; Istenes, Z. A multi-robot exploration algorithm based on a static bluetooth communication chain. *Robot Auton. Syst.* **2011**, *59*, 530–542.
9. Simonin, O.; Grunder, O. A cooperative multi-robot architecture for moving a paralyzed robot. *Mechatronics* **2009**, *19*, 463–470.
10. Sorensen, C.G.; Bochtis, D.D. Conceptual model of fleet management in agriculture. *Biosyst. Eng.* **2010**, *105*, 41–50.
11. Bricx Command Center. Available online: <http://bricxcc.sourceforge.net/> (accessed on 30 August 2013).
12. RWTH—Mindstorms NXT Toolbox for MATLAB. Available online: <http://www.mindstorms.rwth-aachen.de/> (accessed on 30 August 2013).

13. Bochtis, D.D.; Sorensen, C.G. The vehicle routing problem in field logistics part I. *Biosyst. Eng.* **2009**, *104*, 447–457.
14. Bochtis, D.D.; Vougioukas, S.G.; Griepentrog, H.W. A mission planner for an autonomous tractor. *Trans. Asabe* **2009**, *52*, 1429–1440.
15. Bochtis, D.D.; Sorensen, C.G.; Green, O. A DSS for planning of soil-sensitive field operations. *Decis. Support Syst.* **2012**, *53*, 66–75.
16. Oksanen, T. Path Following Algorithm for Four Wheel Independent Steered Tractor. Available online: <http://cigr.ageng2012.org/comunicaciones-online/htdocs/principal.php?seccion=posters&idcomunicacion=12878&tipo=3> (accessed on 5 November 2013)
17. Blackmore, B.S.; Griepentrog, H.W.; Nielsen, H.; Nørremark, M.; Resting-Jeppesen, J. Development of a Deterministic Autonomous Tractor. In Proceedings of *CIGR* International Conference, Beijing, China, November 2004.
18. Depenthal, C. Path Tracking with IGPS. In Proceedings of Indoor Positioning and Indoor Navigation (IPIN), Zurich, Switzerland, 15–17 September 2010; pp. 1–6.

© 2013 by the authors; licensee MDPI, Basel, Switzerland. This article is an open access article distributed under the terms and conditions of the Creative Commons Attribution license (<http://creativecommons.org/licenses/by/3.0/>).



## 4

---

### **Method for recording and predicting position data for a self-propelled wheeled vehicle, and delivery or pick up system comprising a selfpropelled, self-guided wheeled vehicle**

---

This patent application was submitted to the Danish Patent and Trademark Office 19 of December 2014).

[P19] Martin Peter Christiansen and Rasmus Nyholm Jørgensen. Method for recording and predicting position data for a self-propelled wheeled vehicle and delivery or pick up system comprising a self-propelled, self-guided wheeled vehicle, Submitted 19-12-2014

Method for recording and predicting position data for a self-propelled wheeled vehicle, and delivery or pick up system comprising a self-propelled, self-guided wheeled vehicle.

- 5 The present invention relates to a method to online estimate vehicle and environment parameters, where the vehicle changes transporting load throughout the operational task. The invention relates particularly, but not exclusively, to automated load changing vehicle applications, that need vehicle and environment parameter estimates for operational purposes.

10

The invention may be used in areas such as:

- . Automated animal fodder distribution,
- . Vehicle mounted robots with position changing implements
- 15 . Plant spraying/watering,
- . Robotic package and parcel transportation and delivery and/or garbage pickup at private households,
- . Robot assisted building such as brick or tile laying and painting,
- Robot assisted manufacture of large items such as wind turbine blades.

20

Vehicles are utilized in a number of applications of the above sort to transport a load that is changing over time. Animal fodder distribution along lines of feeding places or at animal cages is an example of a load changing vehicle where on-board load is diminished until the fodder tank is empty.

- 25 When the tank is refilled, a new load change takes place. The change in on-board load affects the amount of load on each wheel, effecting vehicle/tire parameters (and vehicle driving performance).

- Automatically guided vehicles require some method of determining their
- 30 location and system parameters so that they, over time, can achieve the desired positions and velocities. In a load changing setting the vehicle



location can be used automatically to place part of the on-board load in the surrounding environment at the desired cartesian x,y,z coordinates. The vehicle guidance system and load placement system can be combined into a single system dependent on the same localization source.

5

Existing vehicle localization methods include the use of Global Navigation Satellite System (GNSS)/Global Position System (GPS); wheel rotary encoders; Inertial Measurement Unit (IMU)/Inertial Navigation Systems (INS); Ultra sound; Doppler radar; Differential radio triangulation, Laser triangulation; Laser range scanner; Camera vision; Tag/Landmark; and others. These methods (Sensors) all have individual shortcomings in terms of increased cost or demands to the conditions and environments the localization methods can be used.

10

15 The GPS/GNSS solutions demand a direct, clear signal path between receiver and satellite, making it mostly usable in open outdoor scenarios. Position location systems depending on line-of-sight can be effected by emitting light sources, heat, electromagnetic fields and field-of-view blocking structures. Systems based on IMU; wheels encoders and Doppler radar provides only relative localization coordinates, which needs to be referenced by a known location. Tag/landmark based solutions can be costly in the number of units needed to cover the desired area and is dependent on an accurate map of each tag/landmarks position.

20

25 Wheel rotary encoder (wheel odometry) provides a means to estimate vehicle change in position over time. Rotary encoders come in 2 main versions:

30

- Incremental encoder, measures the changes in angle (rotation speed) by A/B pulse that need to be counted by a device (ex. micro-controller),
- .Absolute encoder measures the angle of the encoder and in some

cases the number of rotations.

Both incremental and absolute encoders are used to measure the rotational speed of the vehicle wheels. To calculate the speed of the vehicle, a rough estimate can be based on  $V = R \cdot \omega$  Where  $V$  is vehicle speed,  $R$  is the wheel radius  $\omega$  is the measured wheel rotational speed. Encoders on vehicle wheels can be used to estimate both speed  $V$  of the vehicle and rotational speed  $\omega$  of the wheel.

Numerical integration of obtained rotational data from encoders at wheel shafts may be used to estimate the change in position. The vehicle speed estimates are dependent on a precise wheel radius  $R$ , slip free surface movement of the wheel, and an even surface. Any error in the wheel rotation measurement or deviation from the above dependency provides accumulative errors in the positioning estimate. The change in load can affect the tire parameter and result in over or under-estimation of current speed and position. Methods have been developed to compensate for these load changes but tends dependent on offline calibration based measurements of effect from current on-board load. The surface condition could also deviate from the expected flat even surface, and this may result in less reliable speed and position estimates.

Identification tags like Radio Frequency Identification (RFID) have been used for the last decade to provide local and global positioning information about a vehicle. The vehicle is equipped with an RFID reader with a known position in the vehicles own coordinate frame. RFID tags with known positions are placed along the vehicles path to provide fixed position corrections (landmarks). Using an a priori map of the RFID tags location, the vehicle is able to get absolute positioning estimates in relation to the surroundings. Positioning estimates from the RFID tags are provided to the vehicle, when the RFID reader is within the detection zone of each tag. Combining the RFID tag information with other on board positioning

sensors like wheel encoders, IMU, laser scanner and/or Vision cameras the vehicle can continually update the position estimate. The distance between RFID tags is dependent on the demanded position accuracy and available data from other sensor sources.

5

Document CN102004893 discloses a vehicle positioning method based on radio frequency identification (RFID) self-calibration using a rotary encoder installed on a spindle of a vehicle driving motor to obtain the vehicle displacement information; using an RFID electronic tag installed on the vehicle track to calibrate the displacement information measured by the rotary encoder; selecting the weighting distribution coefficient according to the deviation range of the measurement coordinate value of the rotary encoder and the coordinate value of the RFID electronic tag and calibrating the dynamic deviation of the rotary encoder and the RFID electronic tag by the self-learning weighed least square method to reduce the measurement error of the rotary encoder caused by impact of the mechanical factors of the vehicle.

10

15

Other prior art documents in the field are:

20

US6750769 Method and apparatus for using RFID tags to determine the position of an object

WO2010068716A1 Method and system for determining a position of a vehicle

25

WO2010083977A2 Localization system for determining a position of a device that can be moved on the floor

US7648329 Automatic transport loading system and method

EP2376869A1 Method and system for determining a position of a vehicle

US6377888 System for controlling movement of a vehicle

30

US1885023 System for locating moving bodies

US5483455 Method and apparatus for determining the location of a vehicle

- US4658373 Position detecting apparatus
- DK177425B1 Method, feed cart and system for feeding of fur animals
- WO2009010421A1 Device and method for determining a position and orientation
- 5 DE102006004938A1 Positioniersystem
- US8400270B2 Systems and methods for determining an operating state using RFID
- US8587455 Localisation of vehicle or mobile objects based on embedded RFID tags
- 10 US8319955 Device and method for determining a position and orientation
- US7916022B2 Agricultural information gathering system
- US20090267741A1 RFID Floor Tags for Machine Localization and Delivery of Visual Information
- DE102006004400A1 Navigation system, navigation device and method
- 15 US20050099302 System for detecting radio-frequency identification tags
- US7648329B2 Automatic transport loading system and method
- WO1998035276A1 Navigation system for automatic guided vehicle

20 A simple and effective way of determining current vehicle position which is robust with respect to possible shifts in the load position and load size, and also with respect to changes in tire pressure and wear as well as changes in surface structure and quality is desired.

25 A method according to claim 1 is thus provided. Hereby it is assured, that any shift in load between consecutive absolute position readings of the vehicle is reflected in the predictions of vehicle position based on measured shift in angular position or speed, when the vehicle moves forward.

30 As stated in claim 2, the method further allows the position of the vehicle with respect to the surface to be determined several times due to vehicle positions being determined with respect to one surface position and at least

two different spaced apart locations on the vehicle. Especially the locations on the vehicle are spaced apart in the direction of movement of the vehicle so that the vehicle may be moved a well-defined distance between two consecutive absolute position readings.

5

In a further embodiment as claimed in claim 3, the method prescribes one vehicle reader and a number of predetermined fixed surface points for recording vehicle positions.

- 10 In a preferred embodiment as claimed in claim 4, the predetermined surface locations are initially mapped out and provided with RFID transmitter/receiver devices. And further the vehicle is provided with first and second RFID reader devices. These RFID systems combined with rotary encoders, which provide information on angular shift of the wheels,
- 15 allows a safe and precise determination of the vehicle position during combined operations such as load changes and motion.

Further embodiments of the method are listed in claims 5 – 9.

- 20 The invention also concerns a delivery or pick up system as claimed in claim 10.

- 25 With this system, the spaced apart tag readers may ensure that each readable tag is read with the vehicle in two different positions, whereby the travelled distance between the two positions will be the exact distance between the tag reader devices. It is suggested in an embodiment that the tags are RFID tags, and the tag reader devices are RFID readers.

- 30 Such a system may include that the computing device is adapted to calculate absolute distances between two consecutive absolute positions of the vehicle  $P_n$  and  $P_{n+1}$  as the location  $L_1$  and  $L_2$  passes a readable tag and

that the on board computing device is adapted to calculate a conversion factor  $\beta$  which determines the displacement of the vehicle obtained by a predetermined fixed angular shift of the at least one wheel, and adapted to further calculate the current position based on the latest obtained absolute position  $P_{n+1}$  and corresponding conversion factor  $\beta$  and angular rotation data.

The delivery and pick up system may further be defined in that the load comprises animal fodder, and the straight line trajectory passes along an array of animal feeding stations  $F_1$  through  $F_n$ , and that the delivery system is adapted to deliver a predetermined portion of fodder at each feeding station. The mapped out locations  $S_m$  are provided with corresponding RFID tags with respect to a number of preselected feeding stations, and the onboard computing means is adapted to calculate the change in conversion factor  $\beta$  between a mapped out location  $S_{m+1}$  and a previous passed mapped out location  $S_m$  this change in conversion factor designating a calculated load change  $\Delta L_0$ , such that the on-board computing device is adapted to calculate the load change based on the total mass of animal fodder intended to be delivered at feeding stations between  $S_m$  and  $S_{m+1}$  and corresponding load change  $\Delta L$  whereby the onboard computing device is adapted to report a state of error whenever the numeric value of the difference between  $\Delta L_0$  and  $\Delta L$  is above a predefined value.

A program for on-board computing device to a delivery or pick up system according to the above is also provided.

Further, an on-board computing device for a delivery and pick up system as described with such a program is provided.

The invention shall be explained in the following with reference to the figures in which:

Fig. 1 shows a schematic view of a wheeled vehicle with means for obtaining positioning data, and

Fig. 2 shows, in schematic form, the changes of the wheels of a wheeled vehicle with pneumatic wheels with and without load,

Fig. 3 shows in schematic form the sensors inside an IMU,

Fig. 4 shows a schematic view of a vehicle with only one RFID reader and a track with a range of RFID tags,

Fig. 5 shows in the right hand side a vehicle with the RFID tag reader leaving a detection zone, and in the left hand side the tag reader is entering a detection zone,

Fig. 6 a diagram over the main functional parts of the software used in determining the position of the vehicle 1,

Fig. 7 shows a more comprehensive diagram of functional software parts within the onboard computer,

Fig. 8 shows vehicle inside a building housing animal cages,

Fig. 9 is a different angle of view of essentially the same situation as shown in Fig. 8 and

Fig. 10 shows a comprehensive view of animal sheds such as for mink.

In fig. 1 a schematic view of a selfpropelled vehicle 1 is shown. A Load 14 on such a vehicle 1 is shown in fig. 2. By usual means such as an electromotor and an on-board battery (not shown) the vehicle 1 is caused to move along a ground surface 5 shown in Fig. 2. It moves substantially along a straight line trajectory 17, and in order to do this, on board steering means are also provided (not shown in the figures). The steering means are not described in any further detail.

Sensor data relating to position from all on-board sensors are forwarded to a central computer 20 to be fused together to provide a better estimate of the current position P of the vehicle 1. The following inputs are described:

RFID readers 10, 11; wheel rotary encoders 12; IMU 13.

5 An IMU 13 is used to measure acceleration and rotational speed of the object to which it is attached, here the vehicle 1. As the starting position and orientations are known, the measurements from the IMU 13s feeds into the on board computer 20 and are used to estimate the pose, by use of numeric integration. The measurements are provide along all the 3-axis in 3D space, providing for all 6 degrees of freedom (DOF) as seen below in Fig. 3, with accelerometers and gyro's indicated.

10

An IMU 13 normally provides data at high update rate, which is an advantage over other sensors used for orientation. Compared to wheel encoders which has a slip from ground problem, the IMU 13 provides correct data continuously since all its measurements are global. The disadvantage of using IMU's for localization it that they suffer from accumulated errors. Since the measured values are integrated onto its previously-calculated positions, any measurements errors are accumulated from measurement to measurement. The accumulated errors can lead to drift or even produce a totally inaccurate estimate of the actual location.

20

The vehicle 1 is disclosed with four pneumatic wheels, and has a pair of smaller wheels 2 and a set of larger wheels 3. The smaller wheel pair may be used for steering, whereas the larger pair are used to propel the vehicle forward, in that this wheel pair 3 is driven by an engine, such as an electro motor or combustion motor (not shown in the drawing). Connected to the drive of the larger pair of wheels 3 is also a tachometer or the like 12, which may register wheel angular position and/or change of angular position or angular speed of the wheel. In any case a signal 12s from this meter 12 is fed into the computer 20 and corresponding time and angular data from the wheels 3 are stored.

25

30



The number of wheels may differ from the four wheels shown in the example, and may comprise 3, 5, 6 or even more wheels.

5 A wheel rotary encoder (wheel odometry) 12 provides a means to estimate vehicle change in position over time. Encoders on the driving vehicle wheels 3 are used to estimate both speed  $V$  of the vehicle and rotational speed of the wheel 3.

10 The system according to the embodiment of fig. 1 is envisioned to have two or more tag readers of the same or different types. Both readers must be able to read the same tag. A tag could for example both contain a bar-code string and RFID information, making it possible to utilize a combination of different tag readers.

15 As seen in fig. 2 the wheels may change shape such that they are not exactly round, when the load bay 19 of the vehicle comprises a load 14. Thus the connection between travelled distance and angular displacement of a load carrying wheel 3 changes with respect to the weight and position of the load 14. The vehicle transports a varying load that impacts the steering and operational performance. When a wheel rotary encoder is  
20 used to estimate travelled distance, one normally assumes a priori known effective radius of the wheel. By measuring the number of wheel-rotations using the rotary encoder the vehicle computer can provide an estimate of the travelled distance. When operating with a load transporting vehicle the  
25 effective rotational radius will change dependent on the current load transported. This make is relevant to provide a means to estimate wheel parameters. It should also be mentioned, that the driven wheels 3 rely on friction for propelling the vehicle 1 forward, and thus slippage may take place. This cannot be readily observed by the meter 12, and thus slippage  
30 between wheel 3 and surface 5 may further mis-align travelled distance with measured angular shift of the driven wheel 3. According to the

disclosed example, the standard system utilizes pneumatic tires for wheels, but other tire solution could be used. A pneumatic tire is pumped with air (or similar gas) to a chosen pressure making it somewhat flexible in shape. The tire-shape and surface -grip will change when different forces are applied to a pneumatic tire. The transported load has an effect on the normal force pressing the vehicle down towards the ground. According to the disclosed example the vehicle is transporting a max load in the range of 50 kg. to 10000 kg. Higher loads could be transported, but it is not expected to be part of the standard usage. Another way to define the transport load limits, in the envisioned invention, is as a percentage of vehicle weight, and here it is expected to dimension load capability from 10% of vehicle weight and up.

Two tag readers, e.g. RFID tag readers 10, 11 with known mounting location on the vehicle are shown in fig. 1. Each is to read the respective tags 15 that the vehicle 1 passes by in movement. The tag readers 10, 11 must be mounted on a rigid vehicle body part such as a frame part 16. Usually tags are embedded in surface 5, but they may as well be embedded in or attached to other structures such as ceilings, animal cages or the like.

A multitude of RFID tags 15 may be positioned along a straight path or straight line trajectory 17.

Two DOF or higher IMU 13, which are able to measure vehicle acceleration and rotation speed, and estimate orientation in relation to center of earth may be provided.

A computer 20 mounted on the vehicle 1, receives the RFID tag information, the tachometer readings through feed line 12s, plus possibly IMU data through feed line 13s and encodes this sensory and possibly

further sensory data, to compute the absolute vehicle position on the surface 5 on which the vehicle 1 travels. Here it is assumed that an absolute tag map is available, and that each tag 15 is unique, such that when the vehicle on board computer 20 receives the information from the foremost RFID reader 10, it may retrieve the absolute position  $P_n$  of tag reader 10, and when at a later point in time it receives the information from rearmost RFID tag reader 11 it may then retrieve the absolute position  $P_{n+1}$  of tag reader 11. As the two tag readers 10,11 are placed with a fixed and known distance apart from each other in the direction of travel, the computer may calculate a precise distance travelled from  $P_n$  to  $P_{n+1}$  and an average speed of the vehicle 1 during passage of RFID tag 15 by readers 10 and 11. The locations with respect to the vehicle 1 of RFID reader 10 may be termed  $L_1$  and the location of RFID reader 11 may be termed  $L_2$ . More tag readers could be provided on frame 16.

During this passage, also the computer 20 receives data from the tracking of the angular position shift of the wheel pair 3. As the distance travelled is now known, it is possible to relate this distance to the angular shifts of the wheel pair 3 by computing a conversion factor  $\beta$  which directly links angular shift of the wheel pair with travelled distance. Further, at the passage of the RFID reader 11 past the RFID tag 15, precise information of the position of the vehicle is gained, and based on this information, the current angular shift of the wheel, and the conversion factor  $\beta$ , the position of the vehicle 1 may be calculated while it moves forward.

The load may however change during movement, and it is thus necessary to have RFID tags at regular intervals, in case a precise prediction of the whereabouts of the vehicle 1 is needed.

In a number of instances the data from the IMU 13 could be left out of the solution. IMU data could be left out where the surface is flat and even and

the main intend is to calibrate data from the wheel rotary encoder as just explained. In cases where the IMU is left out, the system ground unevenness and load effects are not directly measurable.

- 5 The system can be extended with other localisation capabilities like ultra sound; doubler radar; laser range scanner; camera vision; and other line-of-sight sensors. Such sensor inputs could be used to determine the position of the vehicle 1 at regular intervals either as substitute for the RFID tag system or as a supplement thereto. These line-of-sight sensors could
- 10 measure the distance to the tags and improve the position estimate each tag provides. This is especially important for the RFID tag positioning system, as the RFID reader receives a positive response from an RFID tag once the two are within reading distance of each other. This distance determines a window of positive indication, however the tag reader cannot
- 15 determine how far away and in what direction the tag is actually placed, once the reader is within the window. The supplementary positioning system may help in gaining this information.

- During motion from one RFID tag to the next, the vehicle 1 may shift its
- 20 load 14 receive more load or load off and become lighter, and in each case, a new conversion factor  $\beta$  is to be calculated. Thus it is preferred that at each passage of an RFID tag, the vehicle on board computer 20 performs a new calculation of the conversion factor  $\beta$  based on the latest measured absolute distance and angular shift of a wheel 3.

- 25 As seen in fig. 4 the vehicle 1 may use only one of RFID tag readers 10,11 but in this case passage past two fixed locations  $S_n$  and  $S_{n+1}$  with tags is required in order to update the on board computer 20 with respect to conversion factor  $\beta$ . Thus more locations with tags are required in order to
- 30 obtain the same update rate for  $\beta$ , or for a fixed distance between locations  $L$  the number of tag readings may be increased by having more readers on

the vehicle 1.

The vehicle parameters can be used to improve both automatic vehicles guidance and load placement in surroundings. A load placement could be  
 5 open loop, meaning that the on-board computer 20 will not get any feedback on load placement. Over timer the on-board load should be changing, but blocking of the load output could occur as well as other disturbances in on-loading actions. The sensor combination could be used to detect problems in the load output and utilize the information to either  
 10 warn an operator or stop the current operation automatically, thus providing a closed loop load placement, whereby positive feedback on deliveries is obtained. This may be set up to work in the following way:

The  $\beta$  value change from one RFID passage to the next, is actually an  
 15 estimate of load change  $\Delta L_0$  occurred between the two RFID positions. The on board computer 20 may also gain information on load changes from other sources, such as by counting delivered items or portions of material, or possible by measuring out the weight of delivered material. This load change may be termed  $L_0$ . The on board computer 20 may now compare  
 20 these two values, and in case their difference is too high, a state of malfunction or error may be reported. This condition may be indicative of on-loading or off-loading not taking place as expected.

It would be a simple matter to calculate vehicle average speed between  
 25 consecutive RFID measurements and this information may contribute to the on board computer data sets acquired during passage and can be useful in guiding the vehicle and prevent such problems as speeding. This is especially important in areas where humans are present in the vicinity of the vehicle, as in such areas there are speed limit to be observed by self-  
 30 guided vehicles for safety reasons.

Preferably the information gained on vehicle movement is used to calculate the next RFID tag passage, and when the vehicle tag reader 10 is supposedly at the predicted tag, and no RFID signal is received, it may report and store a state of malfunction. Depending on the actual lay out of the system such a malfunction may or may not cause the vehicle to stop working. Possible it is caused by a non –functioning RFID tag, or reader, and in case more readers are available on the vehicle 1, forward motion to the next RFID tag may be safe to perform.

10 However, in a situation where many consecutive runs along the same lane are performed, the data on non-functioning items such as RFID tag or reader may be stored in the system and reported to service-workers, in order that the non-functioning items be replaced.

15 In some environments such as in animal stables for husbandry or zoo gardens, dirt and other spills may soil the surface, and at some point this may become a problem to the vehicle. However, by means of detection of vehicle and RFID parameters such as described above, this may be detected and reported timely to service workers.

20

In short this means that:

- Online vehicle parameter estimates can be used to improve the localisation data received from the relative sensors encoder and IMU.

25

- Better sensor data from the relative sensor, can be used to increase the distance between tags like RFIDs. By increasing the distance between the tags, the number of tags needed to cover the same area can be diminished, resulting in less costly tag setup.

30

- Each tag has the possibility to be read by more tag readers on each vehicle, this in itself increases the number of position updates using

the same number of tags.

As mentioned, the time between the RFID reader's passages of the same tag, can be used as a speed estimate source. Compared with IMU and encoders, RFID reader speed measurement is not based on a derived measurement in terms of wheel rotational speed or measured acceleration by the IMU. The precision of the speed estimate may have a direct influence on the precision of on-loading and off-loading actions, since many systems have a reaction time; that is a time delay from a load action signal is produced to the actual load action takes place. This time delay must be taken into account, as the vehicle will move during this time, and dependent on the actual speed the displacement will vary. Possibly this displacement is calculated from an actual measured speed of the vehicle and the load action signal is produced earlier in time, to assure that the load action is performed at the right vehicle position.

Fig. 5 is an example of the tag detection using RFID. The RFID readers 10, 11 have a zone 18 within which it is able to receive identification information from a tag 15 such as the ID number. This zone 18 is also displayed in Fig 1. The vehicle computer 20 receives the RFID reader information at specific time periodic interval such as by reading rates of 10Hz or 100Hz. When no tag is inside the readers receiving range, or the zone 18 the reader either transmits no data; tag misreading or no tag in range. When the reader 10,11 get within the zone 18 where it is able to detect a tag, a reader event is logged by the computer and time stamped. This corresponds to the situation displayed in the left hand side of the figure.

The next event occurs when the tag-reader moves outside the tags detection zone 18, which is shown at the right hand side of the figure, where the vehicle has moved forward in the direction of the arrow.

Both events can be defined as specific events in time and used as time interval references when both readers 10,11 have passed the tag 15. The edges of the tag-readers receiving zone 18 can be seen or perceived as points on the vehicle in the lateral direction. RFID tag readers will provide updates in specific time intervals, such as at a 10Hz or 100Hz rate. When a bar-code, QR or visual tag-reader is utilized the principle remains the same in terms of detection edges, even though the readers have different types of receiving zones, such as cone shaped for the bar-code reader and oval/circular for the RFID tag reader.

10

Calculation example:

Encoder:

4096 count pr. revolution (tick pr. rev)

15 (meaning 1 count equals  $360(\text{degree})/4096 = 0.0878 \text{ degree}$ )

Distance between reader events: 2 m

Time between events 8.1 seconds

Sample rate 20 Hz

20 Counted ticks: 4200

(calculated by summing all the sample difference in position together)

Average Ticks pr. second: 520

Estimated effective radius calculations:

$R_{ee\_1} = 2 \cdot \pi \cdot (O / L) = (2 \cdot \pi \cdot (4200 \text{ ticks} / 4096 \text{ ticks})) / (2\text{m}) = 0.310\text{m}$

25  $R_{ee\_2} = V_{\text{average}} / w_{\text{average}} = \text{speed} / \text{rotational speed} =$   
 $((2\text{m}) / (7.8\text{s})) / ((520 \text{ tick/s}) \cdot (2 \cdot \pi / 4096 \text{ ticks})) = 0.309\text{m}$ 

One can choose to use one or the other version or take the average of the values.

30 The above case is for a single encoder on a flat surface. If two encoders are available as depicted above one calculates average the value for each



sample. Based on the estimated effective radius, Hooks law can be used to determine current transport load on the tires with encoders.

5  $F_{n\_load} = k \cdot x$ , where  $x$  represents difference current between effective radius and effective radius without any load.

Based on tire characteristic one can also estimate current grip surface area. In the cases where rotational speed of the tire is increasing or decreasing over time, one can use the two measurements (time and ticks) in a least  
10 square method to estimate current wheel slip on the surface.

Either least squares estimation method or direct calculation should be used when vehicle only will pass a single tag.

15 When multiple tags are passed when the vehicle is moving along a straight path kalman filtering or least squares should be used. Both least square and kalman utilizes the weight of multi measurement to provide a more accurate parameter estimate.

20 When the vehicle has passed a single tag it will in total produce four measurable distance estimates and time intervals. In the most basic form the method can be illustrated using word flow diagram in figure 6.

In terms of the vehicles movement direction we denote the two readers,  
25 front tag reader unit 10 and rear tag-reader unit 11. The movement direction determines when to start the parameter estimation procedure. The procedure commences by checking "Front tag-reader event?" and in case the front RFID tag reader is active, a "Start Timer" activates. Until the expected event has been triggered on the rear tag reader, the computer  
30 continues to log data from encoders and IMU according to the "Acquire encoder and IMU data" process. Once the rear tag reader 11 has acquired

data from a tag passage according to the "Rear tag-reader event?" check, the "Acquire time interval between tag-reader events" sequence is activated. Once this sequence is finalized, the "perform vehicle system parameter calibration using known distance" may be performed. Here the  
 5 connection between travelled distance and wheel rotation measurements is established and will be used until the next distance measurement based on reader and tag locations is performed.

Multiple methods can be used to estimate the relevant parameters related  
 10 to the vehicle. Below is mentioned a number of these methods (but not limited to):

- Direct calculation for single sample
- Least squares estimation
- Kalman filtering methods
- 15 - Standard Kalman filter
- Extended Kalman filtering
- Unscented Kalman filtering
- Adaptive learning methods
- Neural networks
- 20 - B-spline networks

To give an example for direct calculation:

Encoder: 4096 count pr. revolution (tick pr. rev) (meaning 1 count equals  
 $360(\text{degree})/4096 = 0.0878 \text{ degree}$ )

Distance between reader events: 2 m

25 Either least squares estimation method or direct calculation should be used when vehicle only will pass a single tag. When multiple tags are passed when the vehicle is moving along a straight path Kalman filtering or least squares should be used. Both least square and Kalman utilizes the weight  
 30 of multi measurement to provide a more accurate parameter estimate.

Adaptive learning methods can be used to include a priori information training information.

In fig. 7 the procedure for detecting tag error or tag reader error is included in the diagram. The logic of this diagram is embedded in the on board computer, and it ensures that the vehicle is stopped if tag reader modes are not acceptable and that as long as this is not the case, the latest known travelled distance measured by the tag and tag-reader devices is used in determining the present position of the vehicle.

If the "Front tag-reader event?" question is negated, the polling is not just performed again, but a sequence of error finding is initiated by the "new tag detected by rear reader?" question. If the rear RFID tag reader 11 is activated un-expectedly by a new tag this could be down to an error on the front RFID tag reader 10 and thus this case needs to be examined, and the YES line out of this decision box leads to a series of actions adapted to establish if an error is at hand. A counter "Log front tag-reader error" firstly counts up such errors. If "Front errors > Threshold?" is negated, it is taken as an indication, that no reader error is at hand, however if affirmed, it is determined, that the front RFID reader is possibly out of order, and both front and rear tag readers are checked in the "Tag reader mode acceptable?" check. If the reader mode is acceptable, it can be concluded that one or both tag readers are not really working and the "Stop vehicle operation" action is performed. If the tag reader modes are somehow not acceptable, a reset or other corrective action may be performed, and the vehicle may continue operation.

The "Log rear tag-reader error" is operated when a front tag reader event is not followed within an expected threshold of wheel rotation by a "Rear tag-reader event". This is examined by the "Wheel rotations>Threshold?" check. If the wheel has rotated too far, a "Log rear tag-reader error" event is

initiated, and in case "Rear errors>Threshold" is affirmed the "Send alarm about reader failure" is initiated as explained above. In case the threshold of rear errors is not met, the "New tag detected by rear reader?" is checked as explained above.

5

Fig. 8 shows a vehicle 1 in the process of doling out portions of animal fodder 6 on top of animal cages 7, by way of an automatic fodder arm 8, which may shift position by way of pivotal or telescopic movement. This motion of the fodder arm 8 as well as the placement of fodder causes weight shifts and this again changes the pressure distribution on the tires, which again changes the motion of the vehicle with regards to angular shift of driven wheels. The animal cages 7 are provided in rows and usually there is roofing over the cages to keep the animals comfortable. When driving under the roofing, the vehicle 1 must rely on IMU and readings of pre-arranged tangs for orientation. In the figure the roofing is left out to improve the view of other elements. Thus on the sides of the animal cages 7 RFID tags (or other readable tags) are provided. And on the vehicle frame corresponding readers 10, 11 are provided. As previously explained, this arrangement allows the vehicle to keep track of its position, and thus the animal fodder 6 may be correctly placed on top of each cage 7. It is also possible to dole out metered portions to each animal, as now the vehicle onboard computer may actually calculate which animal cage each portion will arrive at. This would only require the fodder arm to be able to dole out individually metered portions. Also medications or vitamins may be added to the fodder on an individual animal cage basis for treatment of various conditions. The presented graphics of figs. 8, 9 and 10 relates to mink husbandry where mink fodder is placed directly on top of the animal cages. The cages are made from wire mesh and the animals may easily take the fodder through the top mesh of the cage as the fodder is mixed and processed into a pasty like substance. However, other kinds of animal husbandry may use similar systems.

Fig. 9 shows a computer-generated view along the aisle of animal cages 7 arranged above ground 5 and with RFID or similar tags 15 arranged on the vertical front thereof at regular intervals. The tag readers 10, 11 on the vehicle 1, mounted to the frame 16 are schematically indicated on the figure, and they are naturally provided at the same level above ground as the tags 15 on the cages. The tags may in real life be quite flat and when mounted sit flush with the surface of the animal cages in order that they are not inadvertently knocked off the cage front by the vehicle or persons passing along the animal cages. A tag will always be provided at the foremost cage in a row, so that the vehicle when starting its passage along the cages may calibrate its position from the start to ensure that it knows where to start doling out fodder.

In fig. 10 an overview of a mink farm is disclosed. Here 18 double rows of cages are disclosed. The vehicle 1 is about to enter along the aisle between two rows in order to deliver the animal fodder, presently loaded onto the load bay 19. An area 20 in front of and to the side of the vehicle is scanned by a well-known laser scanner, in order that the vehicle may deviate from a planned course in case un-foreseen obstacle should show up in its path. Such laser scanners are also known under the names of Lidar-scanner or Laser measurement system. The entire arrangement allows automatic feeding of the animals with a minimum of labor force being occupied.

A vehicle for feeding mink is provided with a system that could utilize this invention. Both fully automated versions and version driven by a human driver with automatic feeding could benefit from this invention. Each mink cage would get a portion of fodder in the range of 80-300 grams, based on mink gender; age; number and race. The farmer chooses the amount of fodder each cage gets based above criteria and personal experience. With

fodder tank load-range in the order of 500 – 2500 kilo gram, a machine would be able to feed a range of cage units from 1500 to 30000 units. Each feeding position is normally in the range 0.27-0.4m (0.33m standard in Denmark for standard unit). Therefor the feeding must be placed within a

5 narrow position range of plus/minus 0.10-15 m. Placing the fodder at these specific requires a localization system on-board the vehicle able to determine current position in relation to the surroundings.

Used Names and corresponding reference signs:

- 10
- 1 vehicle,
  - 2 smaller set of wheels or steering wheels,
  - 3 larger set of wheels or driven wheels,
  - 5 surface
- 15
- 6 Portions of animal fodder,
  - 7 Animal cages
  - 8 Automatic fodder arm,
  - 10 RFID tag reader
  - 10s RFID tag reader signal
- 20
- 11 RFID tag reader
  - 11s RFID tag reader signal,
  - 12 tachometer or angular change sensor
  - 12s angular data feed line,
  - 13 IMU
- 25
- 13s IMU signal feed line,
  - 14 Load
  - 15 RFID tag
  - 16 fixed frame
  - 17 straight line trajectory
- 30
- 18 detection zone
  - 19 Load bay

20 scanned area

**Claims**

1. Method for recording and predicting position data for a self-propelled wheeled vehicle (1) carrying a load (14) whereby the vehicle (1) is caused to move along a ground surface (5) along a predominantly straight line trajectory (17) by rotating at least one load carrying wheel (3) in frictional engagement with the surface (5), angular rotation data of at least one wheel (3) is obtained, absolute position data are obtained at different predetermined fixed positions  $P_n$  of the vehicle (1) with respect to the surface (5) along the straight line trajectory (17), whereby the following steps are performed:
  - a. at two different predetermined positions  $P_n$  and  $P_{n+1}$  of the vehicle (1) with respect to the surface (5), corresponding passage of the vehicle and angular rotation data of the vehicle wheel (3) are recorded and
  - b. a conversion factor  $\beta$  is calculated which determines the displacement of the vehicle (1) obtained by a predetermined fixed angular shift or rotation of the at least one wheel (3) between positions  $P_n$  and  $P_{n+1}$  and
  - c. during further movement of the vehicle (1) the current position of the vehicle (1) is predicted based on the value of the conversion factor  $\beta$ , measured angular shift of the at least one wheel (3) and recorded absolute location coordinates at position  $P_{n+1}$ ,
  - d. the load is increased, decreased, or shifts position with respect to the gravitational center of the vehicle (1) and
  - e. points a, b and c are repeated at the passage of each further predetermined position  $P$ .



2. Method for recording and predicting position data for a self-propelled wheeled vehicle (1) as claimed in claim 1, whereby absolute positions  $P_n$  and  $P_{n+1}$  of the vehicle (1) are recorded with respect to one and the same surface location  $S_m$  and with respect to one first location  $L_1$  and one further location  $L_2$  on a fixed frame (16) of the vehicle (1) whereby  $L_1$  and  $L_2$  are spaced apart in a direction of movement of the vehicle (1) when it is caused to move along the straight line trajectory (17).
3. Method for recording and predicting position data for a self-propelled vehicle (1) as claimed in claim 1, whereby the absolute positions of the vehicle  $P_n$  and  $P_{n+1}$  are determined between the first fixed location  $L_1$  on the vehicle and a first surface location  $S_m$  and a second surface location  $S_{m+1}$ .
4. Method as claimed in claim 2 or claim 3 whereby each surface location is initially mapped out and provided with a RFID transceiver device (15), and whereby the locations  $L_1$  and  $L_2$  on the vehicle (1) are fitted with RFID reader devices (10,11).
5. Method as claimed in claim 1 whereby further devices (13) for detecting and recording position and rotational changes are provided on board the vehicle (1) and that at each time absolute position data are recorded using RFID or other tags, the position change data recording means are reset.
6. Method as claimed in claim 1, whereby a load change value  $\Delta L$  is predicted based on preprogrammed delivery or reception of load, and a load change value  $\Delta L_0$  is determined by the change of the conversion value which is calculated each time the points a, b and c are carried out and whereby further  $\Delta L$  and  $\Delta L_0$  are compared each

time  $\Delta L_0$  is determined, and that a state of malfunction is determined in case the numeric value of the difference between  $\Delta L$  and  $\Delta L_0$  is above a predetermined threshold value.

- 5        7. Method as claimed in claim 4, whereby the current position of the vehicle (1) as predicted and used to calculate the distance to the closest surface location comprising a RFID transceiver device, and in case the predicted distance is smaller than a predefined minimum distance and no RFID signal is obtained, a state of malfunction is reported and stored.
- 10
8. Method as claimed in claim 7, whereby stored states of malfunction relating to RFID device locations are processed in order to diagnose non function of RFID tags as well as non function of RFID reader.
- 15
9. Method as claimed in any of the above claims, whereby a batch of animal fodder, such as mink fodder is initially loaded onto a load bay (19) of the vehicle (1), and that the straight line trajectory (17) passes along a range of animal feeding stations such as mink cages, and that at each feeding station a predetermined portion of mink fodder is of-loaded from the vehicle (1).
- 20
10. Delivery or pick up system comprising a self-propelled, self-guided wheeled vehicle (1) adapted to drive along a surface (5) and having a load bay (19), a movable on- and/or of-loading arm, at least one load carrying driven wheel (13) in frictional engagement with the surface (5) for propelling the vehicle (1), whereby the vehicle (1) comprise a sensor (12) adapted to collect angular rotation data with respect to at least one load carrying wheel (3), the system further comprising a predetermined track with at least one straight line trajectory (17) having one or more mapped out locations  $S_m$  along
- 25
- 30

the length of the straight line trajectory (17) provided with readable tags (15) and whereby the vehicle comprises two fixed frame locations  $L_1$  and  $L_2$  spaced apart in the direction of movement, the fixed frame locations  $L_1$  and  $L_2$  comprises tag reader devices (10,11), whereby an on board computing device (20) comprise means for receiving and storing tag information identifying two absolute positions  $P_n$  and  $P_{n+1}$  of the vehicle with respect to the surface (5).

10

15

**Summary**

A method for recording and predicting position data for a self-propelled  
5 wheeled vehicle (1) carrying a load (14) is provided whereby the vehicle (1)  
is caused to move along a ground surface (5) along a predominantly  
straight line trajectory (17) by rotating at least one load carrying wheel (3) in  
frictional engagement with the surface (5), angular rotation data of at least  
one wheel (3) is obtained, absolute position data are obtained at different  
10 predetermined fixed positions  $P_n$  of the vehicle (1) with respect to the  
surface (5) along the straight line trajectory (17), whereby the distance  
travels is measured independently and used to calibrate motion sensors on  
board the vehicle. The invention also comprises a delivery or pick up  
system, a program for an on-board computing device and an on-board  
15 computing device.

Fig. 1 is to be published.

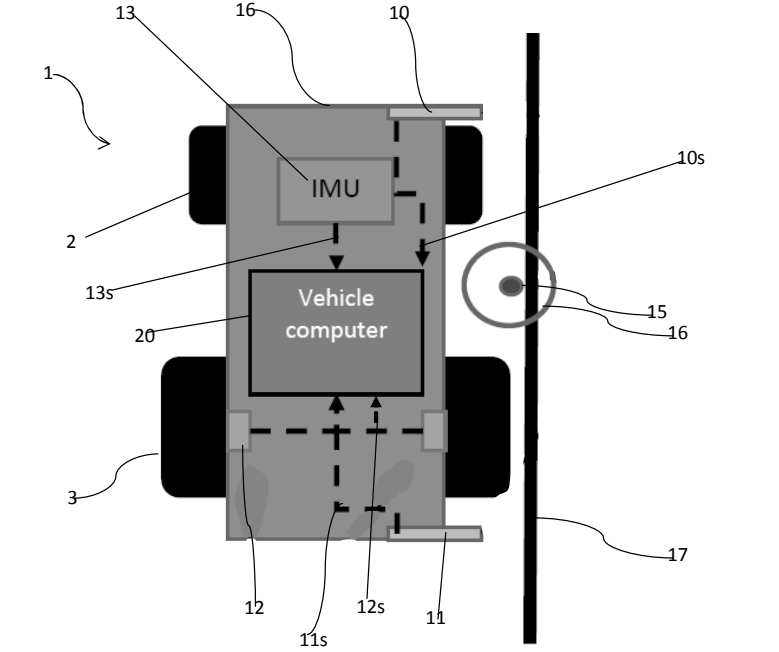


Fig. 1

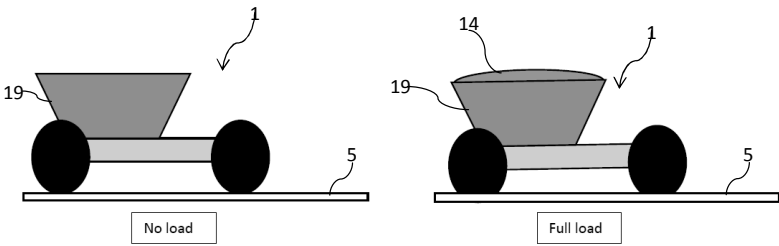


Fig. 2

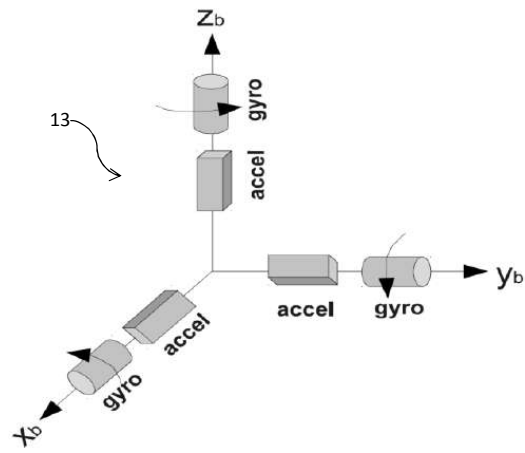


Fig. 3

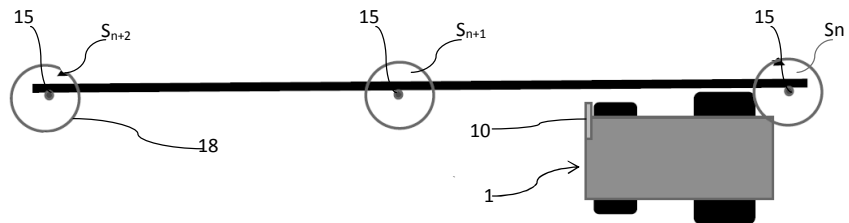


Fig. 4

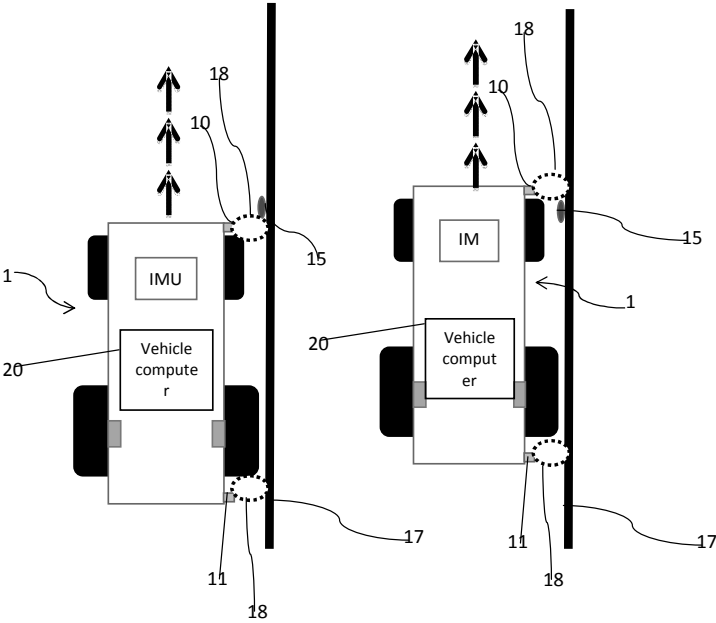


Fig. 5

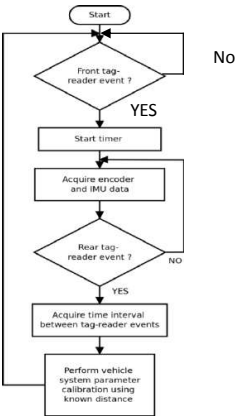


Fig. 6

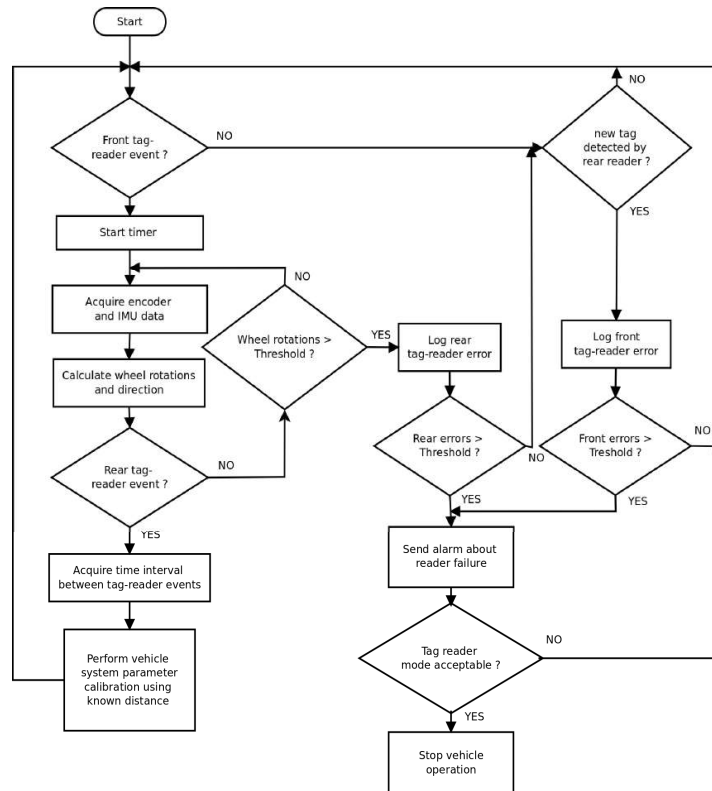


Fig. 7



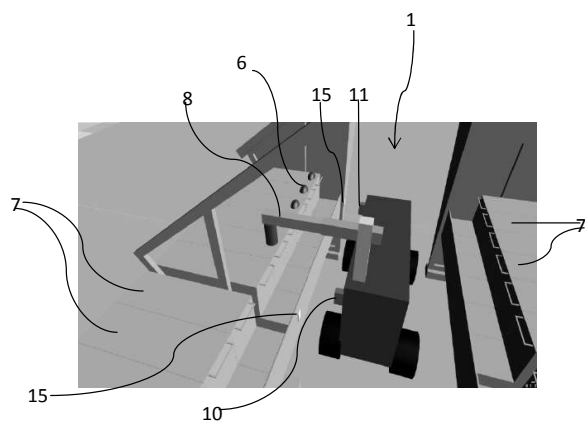


Fig. 8

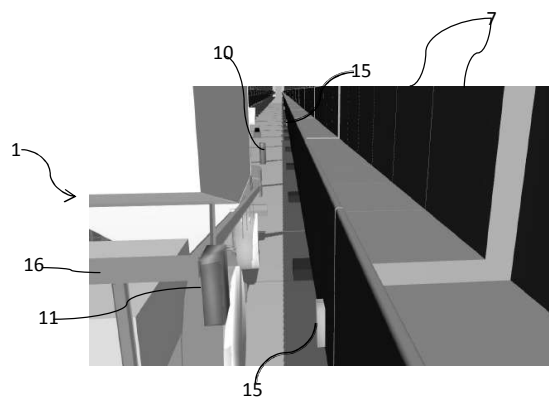


Fig. 9

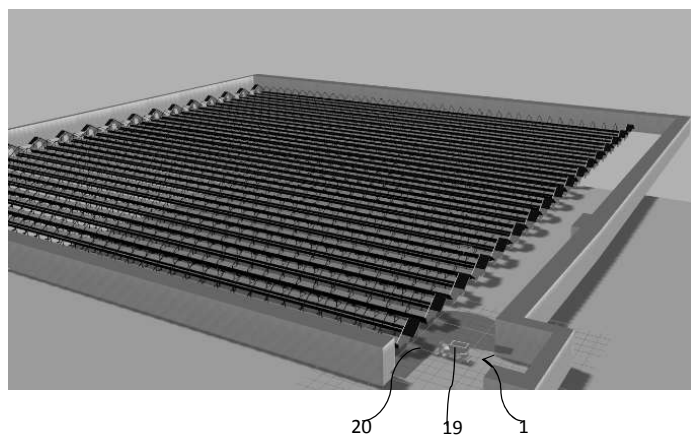


Fig. 10

# 5

---

## Agricultural Robotic Candidate Overview using Co-model Driven Development

---

The paper presented in this chapter has been submitted to IROS (International Conference on Intelligent Robots and Systems)

[P23] Martin Peter Christiansen, Peter Gorm Larsen, and Rasmus Nyholm Jørgensen. Agricultural Robotic Candidate Overview using Co-model Driven Development. In *IEEE/RSJ International Conference on Intelligent Robots and Systems*, 3 Submitted 4-3-2015

## Agricultural Robotic Candidate Overview using Co-model Driven Development

Martin Peter Christiansen<sup>1</sup>, Peter Gorm Larsen<sup>1</sup> and Rasmus Nyholm Jørgensen<sup>1</sup>

**Abstract**—Multi-disciplinary technologies can be used to explore and compare design candidates in order to enhance the time-to-market development for robotic systems. The Crescendo technology lets software designers and engineers collaborate in the development for models containing discrete-event (DE) parts of the controller and continuous-time (CT) parts for the robot-environment interaction. Such models are defined as collaborative (co-models) and their joint execution is called a co-simulation. In this paper, we illustrate the development of a robot mink feeding system using the model-based Crescendo technology. The results of the co-simulations provided an overview of the candidate solutions in the chosen design space entirely in a virtual setting. The candidate overviews provided valuable input for selecting a candidate to develop into an actual robot. The selected candidate solution was subsequently deployed directly on a robot operating system (ROS) based platform and tested on a mink farm.

### I. INTRODUCTION

Modelling and simulation are gradually being adopted as integral parts of the development process for robotic systems [10], [17]. Modelling provides developers with the capability to explore the interaction between hardware and software solutions before developing the actual component. The modelling and simulation approach allows for the automatic evaluation of a much larger potential design space compared to a manual trial and error approach. The alternative approach to robotic systems involves significant time spent on ad-hoc trial-and-error testing to reach a usable system configuration of the physical system. The prime challenge here is that many complementary disciplines are necessary to determine viable solutions i.e. electrical, mechanical, software, embedded systems and signal processing [18], [21]. Each discipline has different cultures, tools and methodologies, which can restrict the development of a cross-disciplinary project. Collaborative simulations (co-simulations) allow developers to examine different aspects of the system to explore design alternatives. Co-simulations are based on models that the developers utilise to describe the different aspects of the robotic system. Co-modelling and co-simulation are performed using the Crescendo technology [9]<sup>2</sup>. Design space exploration (DSE) is the analysis of different candidate solutions using co-simulation. The idea behind DSE is to explore the various candidates being considered by the developers to determine a viable candidate solution. The design challenge presented

in this paper is based on a robotic feeding system for agricultural farming applications.

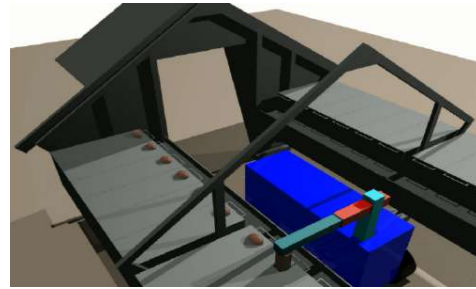


Fig. 1. 3D visualisation of final version of co-simulated fodder dispensing robot operating inside mink farm house.

### II. RELATED WORK

In industrial robotic designs for indoor applications, research has indicated that a model-driven design approach incorporating co-simulation improves the cross-disciplinary design dialogue [3], [4]. Co-simulation has been used in the development of robot manipulators, where the tools Matlab Simulink and ADAMS were used to model the controller and robot body/environment, respectively [2], [26]. The ADAMS/Simulink combination has also been used to design a tomato harvesting robot manipulator [14].

The Crescendo technology has been used to select viable candidate sensor positions on an R2-G2P line-following robot with a fixed controller setup [23]. The robot's performance was evaluated against a predefined set of marked curve segments to determine the most viable candidate solution. An adaptive controller solution was designed for an agricultural vehicle with a commercial GNSS based auto-steering solution. The solution was focused on finding the maximum safe speed for different load distributions on a tractor; these results were used to design the controller solution [5].

Feeding robots for animal husbandry have previously been developed and documented in the literature. In [25], a static feeding system was utilised in combination with an RFID reader to dispense food to cows with an attached RFID tag. The company Lely has developed a commercial mobile cow feeding robot which combines of ground metal wires for line following and ultrasound sensor for in-row movement.

<sup>2</sup>Financial support given by the Danish Ministry of Food, Agriculture and Fisheries is gratefully acknowledged.

<sup>1</sup>All authors are with the Department of Engineering, Aarhus University, Finlandsgade 22, 8200 Aarhus N, Denmark mpc@eng.au.dk

<sup>2</sup>See [www.crescendotool.org](http://www.crescendotool.org).

To date, the Lely Vector feed robot has not been documented in the academic literature, but it is a well-known commercial product.<sup>3</sup> In [13], outdoor piglet feeding was realised using a mobile feeding platform. The pig-feeding robot was utilised to influence the behavioural pattern and manure output of the piglets by daily changes of the feeding position in the field.

Feeding minks is a high precision task compared to cows and pigs because the normal feeding area has been empirically to be  $0.2\text{--}0.35\text{m}$  for each cage. Each mink cage must be dosed with a predetermined amount of fodder placed on top. Our design approach looks at the navigational system, feeding controller and ground vehicle solution when making design choices based on the co-modelling. Our co-simulation based development approach to robot design is intended to determine a viable candidate solution for deployment in an actual platform.

### III. CO-MODEL DRIVEN DEVELOPMENT

The co-model was designed for a robot system to dispense mink food along a row of cages at predetermined locations. The robot co-model was evaluated according to the overall system performance demands for the different system configurations.

#### A. System Boundary Definition

The chosen robot is a four-wheeled vehicle with front wheel steering and the rear wheel differential driving. The robot receives sensory inputs from a laser-range scanner, radio frequency identification (RFID) tag reader, IMU, and rotary encoders on the back wheel and front wheel kingpins. Actuators control the vehicle steering, driving, and feeding system based on the sensory inputs. A feeder arm system mounted on the robot dispenses the food on the cages at the predetermined locations. RFID tags are placed along the animal cage rows, to provide fixed reference locations. Fused sensory data based on the sensor input are utilised to determine the current location and enable the robot to perform actions in the environment.

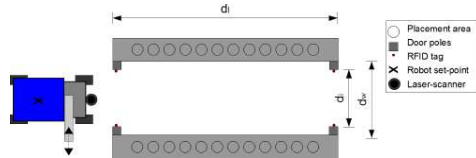


Fig. 2. Sketch of example robot vehicle and feeding area inside a mink farm house where the fodder must be placed at specific locations.

System performance demands defines what the robot must achieve to be perceived as a viable solution. The project stakeholder for the system performance were as follows:

- Maximum vehicle speed of  $0.25 \frac{\text{m}}{\text{s}}$  (conforming to ISO-10218 [11]).

<sup>3</sup>See [www.lely.com](http://www.lely.com) for the Lely Vector.

- Feeding with a precision of  $\pm 0.05\text{m}$  inside the placement areas.
- No collisions with the surroundings (see Figure 2).

Note that the performance demands are non-domain specific and focus on the overall response of the robot in action. Based on experience the standard length of row of mink farm houses  $d_1$  can be from  $30\text{m}$  to several hundred metres. The widths of the entrance and exit  $d_2$  were  $1.2\text{--}1.55\text{m}$  and are the narrowest parts the robot must pass. The number of mink farm houses can differ from farm to farm, and they tend to be aligned in parallel. A lack of collision means that neither the vehicle nor feeding arm collide with the surroundings.

#### B. Collaborative Modelling Framework

Crescendo combines discrete event (DE) modelling of a digital controller and continuous time (CT) modelling of the plant/environment for a co-simulation. The Overture tool and the Vienna development method (VDM) formalism [8], [16] were used to model the DE controller and 20-sim was used for the CT components. The Crescendo co-simulation engine coordinates the simulation between 20-sim and the VDM tool through a protocol for time-step synchronisation between the tools. Crescendo binds the domain models together using the Crescendo contract and is responsible for exchanging information between the tools. The contract contains the parameters and variables that CT and DE developers need to be aware of when developing a combined model.

Crescendo contains a functionality enabling the developer to carry out DSE of a co-model [22]. DSE can be used to test and evaluate different system configurations like actuator, controller or sensor combinations in the design space that the developers plans to explore.

#### C. Co-model Driven Development

We looked at different feeding arm solutions using co-modelling and co-simulation to determine a viable solution. We considered solutions with single- and double-sided feeding arm outputs with two either prismatic or revolute joints. The goal of this analysis was to determine the most viable candidate for development into an actual system. Double-sided feeding was considered based on an idea of better utilisation of the feeding robot. Feeding with both sides would double the output placement of fodder at the same vehicle speed. Shifting the arms half a cage length would allow the use of the same pump system for both sides while still allowing individual fodder amounts to be output.

The DSE functionality was used to evaluate each co-simulation robot system based on collision checking and placement of the mink fodder. For collision checking purposes, the robot's 2D bounding box was two rectangles: one for the vehicle body and one for the feeding arm system. If any bounding box comes within the range of the stored obstacles, the robot's pose is invalid. We utilised the method described in [6] to performed the collision checking.

Evaluating the feeding output requires information on the placement of each fodder dispensed in the operational environment. When a co-simulation was run, the dispensed

fodder from the robot was logged in a 2D XY grid with 0.01m intervals covering the mink cages. The logged fodder positions were used in the 3D visualisation like that portrayed in Figure 1 and processed afterwards to determine if the placement was a success. The execution was only run for a single house of mink-cages because the task would just be repeated for multiple houses without providing further insight when using co-simulation. We also limited the co-simulation to the first four meters of a mink farm house because we did not expect the remaining part to provide any new insight. Throughout model development, we ran the same scenarios using DSE on the four different candidate solutions. The DSE results were used to determine when the co-model was working as intended and to allow the project stakeholders to compare the solutions.

The Crescendo contract in table I defines the parameters and variables to be exchanged during co-simulation. Shared

	Name	Type	Parameter symbol
<b>sdp</b>	Initial.Position	array	$[x_{init}, y_{init}, \theta_{init}]$
<b>controlled</b>	Wheel.Angle	real	$\delta_{fo}$
<b>controlled</b>	Feeder.arm_pos	array	$[y_{arm}, z_{arm}]$
<b>controlled</b>	Feeder.out	real	$p_o$
<b>controlled</b>	Speed.out	real	$u_o$
<b>monitored</b>	Local.Pose	array	$[x_s, y_s, \theta_s]$
<b>monitored</b>	IMU	real	$r_s$
<b>monitored</b>	Encoder.Back	real	$V_s$
<b>monitored</b>	Encoder.Front	real	$\delta_{fs}$

TABLE I  
CRESCENDO CO-MODEL CONTRACT

design parameters are defined using the **sdp** keyword, variables operated by the CT side are defined by the **monitored** keyword and variables controlled by the DE side are defined by the **controlled** keyword. Shared design parameters represent values for which the developers want to explore the effect.  $x_{init}, y_{init}, \theta_{init}$  define the starting position of the robot in the global coordinate frame. The crescendo DSE functionality was used to start the robot at different initial positions and evaluate if the co-model conforms to the project stakeholder demands. The controlled variables were the input to robot movement and the feeding arm. The robot movement input was transmitted to the drive motor  $u_o$  and front wheel steering actuator  $\delta_{fo}$ . The feeding arm transmitted the desired arm position  $y_{arm}, z_{arm}$  and current feeding output  $p_o$  in kilograms to the CT model. Local.Pose is the abstraction of the fused sensor input into a estimated position  $x_s, y_s, \theta_s$  in the global reference coordinate frame. The abstraction of the fused sensor system is a general strength of modelling and simulation because this component did not need to be develop yet, so we were able to focus development efforts on steering and feeding control. IMU was also only represented by a single rotational variable rotated in the world frame, whereas the actual sensor may contain acceleration and rotation sensors for all three dimensions.

#### D. Discrete Event Modelling

The robot controller consists of a steering controller that can follow a pre-determined path and a feeding controller

system to place fodder at the pre-selected positions. The steering controller steers the robot along the predetermined path, which is defined by a sequence of waypoints. The steering controller utilises the modal mode concept illustrated in Figure 3. The current modal controller mode is dependent on movement inside or outside the feeding area because two different operational strategies are used. The RFID tags at the entry and exit of the mink farm house determine the steering current mode and when the feeding arm should be deployed.

A combination of feedforward and feedback control is used to set the steering angle of the front wheels. The feedforward response is based on the kinematic bicycle model where  $L$  is the length of the wheelbase and  $V_s$  is the speed measured by the wheel encoders.

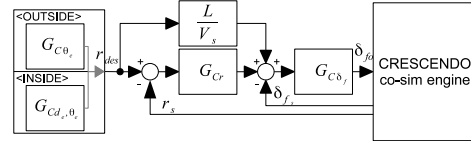


Fig. 3. Block diagram structure of modal steering controller.

Inside the mink farm house, the robot needs to move along the cages in straight lines and to ensure that the feeding arms are held straight over the cages. Correct operation is ensured by maintaining a fixed distance and orientation to the sides of the mink cages. The control law employed by [19], [20], which is given by Equation (1), was chosen for inside operation. The robot rotational angle speed  $r_{des}$  was set to be proportional to the errors in distance  $d_e$  and orientation  $\theta_e$ :

$$r_{des} = \begin{bmatrix} K_{11} & 0 \\ 0 & K_{22} \end{bmatrix} \begin{bmatrix} d_e \\ \theta_e \end{bmatrix} \quad (1)$$

The controller parameter is tuned by the Ziegler-Nichols closed loop method. The parameter  $K_{22}$  is determined first and tuned to diminish the angle error  $\theta_e$ . The procedure is then repeated for the  $K_{11}$  parameter for the distance error  $d_e$ . When the robot moves outside from the feeding area, the heading error  $\theta_e$  in relation to the predetermined path of the robot is selected as the steering concept. A classic PD controller is used to steer the robot outside the mink farm houses, based on the method described in [1].

When the robot moves into the feeding area, it stops to deploy the feeding arm system to the preselected position by updating  $y_{arm}, z_{arm}$ . Robot movement cannot continue before the feeding arm system has been completely moved in or out when the robot is entering or exiting a mink farm house. The robot has a feed map in the form of a sequence of amounts and positions of fodder to be placed. The feeding arm system starts the feeding process using the output  $p_o$  when the next position in the map is reached.

#### E. Continuous Time Modelling

The 20-sim block diagram in Figure 4 represents the steering wheel actuator and mechanical setup to operate

the front-wheel orientation  $\delta_f$ . The input and output signals

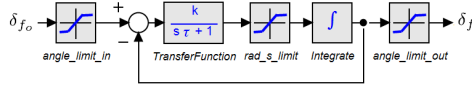


Fig. 4. Model of steering wheel system based on method described in [1]

from the steering wheel are controlled using limiter function blocks to model operational range. The closed loop inner system represents the steering angle rate response to the requested steering angle  $\delta_{f_o}$ .

The model of the robot vehicle utilises the bicycle approach meaning that lateral forces in the left and right wheels are assumed to be equal and summed together. This assumption holds for typical agricultural vehicle operation velocities ( $< 7.5 \frac{m}{s}$ ) [15]. The bicycle structure, is also known as a half-vehicle (Figure 5). The model allows for yaw and lateral motions with the steering of the front wheel angle  $\delta_f$ .

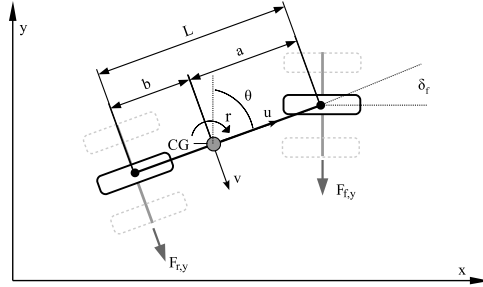


Fig. 5. Dynamic bicycle model of the vehicle part of the robot system.

The velocities  $u, v$  are at the center of gravity of the vehicle.  $L$  is the wheelbase where  $a$  is the longitudinal distance to the front wheel and  $b$  is the longitudinal distance to the rear wheel. For a constant forward velocity, the vehicle motion is given by

$$m(\dot{v} + ur) = F_{f,y} \cos(\delta_f) + F_{r,y} \quad (2)$$

where  $r$  is the angular rate about the yaw axis. Similarly, the vehicle yaw motion is expressed by

$$I_{zz}\dot{r} = aF_{f,y} \cos(\delta_f) - bF_{r,y} \quad (3)$$

where  $I_{zz}$  is the moment of inertia along the yaw axis.

We only considered the sideways force of the tire surface interaction because it provides the influence on the vehicle dynamics. The four factors which influence the lateral force are the normal force  $N$ , cornering stiffness  $C_\alpha$ , rolling angle  $\alpha$  and friction factor  $\mu$ . Formula (4) and (5) are used to calculate the roll angles of the back and front wheel, respectively. The main difference is that (4) also considers the angle of the steering wheel.

$$\alpha_f = \frac{v + ar}{u} - \delta_f \quad (4)$$

$$\alpha_r = \frac{v - br}{u} \quad (5)$$

The sideways force is expressed for the linear and nonlinear cases by a piecewise-defined function.

$$F(\alpha) = \begin{cases} -C_\alpha \tan(\alpha), & \text{if } |C_\alpha \alpha| < \frac{\mu N}{2} \\ -\mu N \frac{\alpha}{|\alpha|} (1 - \varrho(\alpha)), & \text{if } |C_\alpha \alpha| \geq \frac{\mu N}{2} \end{cases} \quad (6)$$

The linear case is used when the sideways stress in the contact patch upholds  $|C_\alpha \alpha| < \frac{\mu N}{2}$ . The function  $\varrho(\alpha)$  is defined by

$$\varrho(\alpha) = \frac{\mu N}{4C_\alpha |\tan(\alpha)|} \quad (7)$$

The output from the fodder outlet is modelled by standard first order differential describing output flow rate. When the fodder leaves the outlet their movement onto the cages are modelled using mass and earth gravity.

#### IV. RESULTS

##### A. Design Space Exploration

Each solution was modelled to conform to the given system performance requirements and evaluated based on the DSE co-simulation response. Running DSE co-simulation scenarios throughout the development of the robot allows us to determine that the key obstacle is the mode change between outside and inside. The safe start/stop procedure

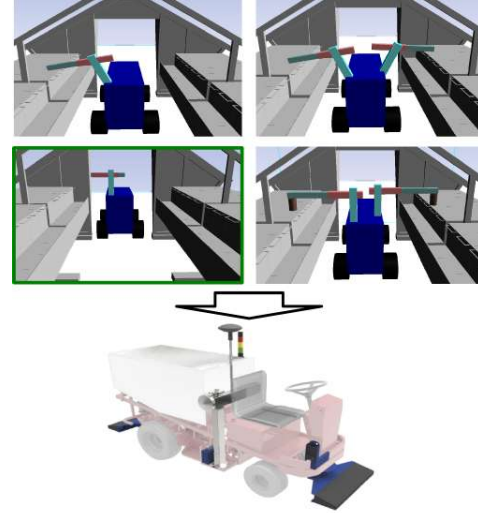


Fig. 6. Feeding arm candidate solutions that was experimented with to determine a viable candidate solution.

when the robot needs to retract and deploy the feeding arm is the major factor that influences successful feeding. For the double sided candidate solutions, the number of start/stop procedures was doubled because the arms needed to be operated individually owing to the placement difference. Placing

the fodder at the correct position mainly depends on accurate position information and can be achieved by increasing the number of RFID tags used at reference positions along the cages. In the final version, all four candidate solutions were able to fulfil the stakeholder demands. The four candidate solutions for the four different arm and feeding systems are illustrated in Figure 6.

The single sided solution with prismatic joints was selected for feed-arm operation. Because feeding is generally performed at the same height for each row of cages, a prismatic joint solution was deemed to have better functionality and move with ease between positions. The prismatic solution was also deemed simpler to operate manually should this be needed. The single-side solution was chosen over a double sided solution because the stakeholders deemed it to be a better first prototype design for the actual robot. The double sided solution can easily be used to upgrade the same prototype platform later because no major software upgrades would be needed.

#### B. Experimental Results

To test the candidate solution, it was deployed into a vehicle solution as illustrated in Figure 7. The DE model was rewritten as a solution in the robot operating system (ROS) ecosystem [24]. The ROS distribution Hydro Medusa was used in combination with ROS components from the Frobo-mind platform [12]. The robot solution was implemented on a Norcar Minkomatic 660 DLA mink-feeding vehicle normally used for human operated feeding. The current



Fig. 7. Robotic mink feeding system based on Norcar Minkomatic vehicle.

version of the robot system is intended as an add-on function to a standard vehicle platform. The solution also allows the operator to manually control the vehicle if necessary.

To evaluate the envisioned system, testing was performed at an outdoor mink farm in Denmark. Movement outside the mink farm houses is based on localisation using a reference map. The outside map provided in Figure 8 was created using OpenSlam's Gmapping ROS node. One part for each entry to the mink farm houses. Localisation with the created map was performed using an *acml* ROS node. Both *gmapping* and *acml* are part of the ROS navigation stack. The path the robot must follow to move between houses was pre-planned

based on the houses the robot was planned to cover in the current run.

Indoor operation was performed as defined in III-D. Input to the steering controller was based on laser-range scanner measurements from a SICK TiM551. The laser-range scanner measurement was processed using RANSAC [7] to determine the robot's relative position to side of cages in terms of angle and distance. The robot's relative position was compared against the chosen reference for the robot to stay at.

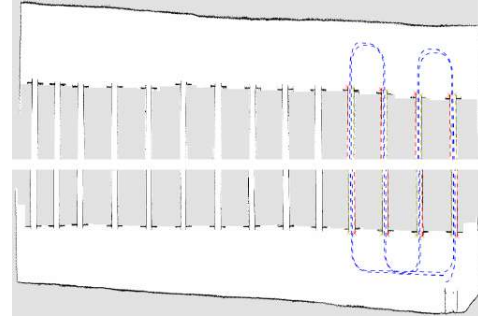


Fig. 8. Local map of mink farm used in localisation and navigation outside. A combined version is shown in this picture, for both entrances to the mink farm houses. The blue line represents an example path that the robot can take between the mink farm houses. The farm is surrounded by a fence as indicated by the black border. The area the robot has lacks information on are marked in grey.

#### V. DISCUSSION

There is still more work to be done on the feeding robot system before a first version is completed. This paper illustrates how co-modelling and co-simulation can be used in robotic development. DSE was used to provide an overview of the candidate system configurations of mink arm feeding systems. Factors such as material, development, implementation and maintenance cost can influence the selection of a candidate configuration. Developers can use the DSE results to select a configuration to develop into an actual robot vehicle solution. DSE will not guarantee optimal solutions, but is a tool assisting with tradeoff analysis with multiple candidate solutions and allows the project stakeholders to get an overview. The overview of the multiple feeding arm system solutions illustrates the DSE functionalities in *Crescendo* and shows that the method can support the selection of viable candidate solutions. The design overview approach would be an asset in the development of other robotic system where new aspects needs to be explored.

A similar simulation analysis could also have been developed directly in ROS, but the solution would lack the multi-disciplinary tool based collaboration and development. Based on the results, we deemed that the co-modelling concepts can be used as a supplementary feature in robotics development tools like ROS and Microsoft Developer Robotic Studio. Other tool combinations can be used for co-model driven



development of agricultural and field robotic systems. The development tools should depend on the developer team's preferences and problems faced by the robot must.

## VI. CONCLUSIONS

Developing a robotic system to conform to the overall system requirements is essential. In this article, we described the concept of co-modelling and co-simulation as a robotic design approach. We showed how co-simulation using DSE can provide an overview of cross-disciplinary design candidates in robotic development. The model of the feeding robot combines modelling in VDM and 20-sim into a complete co-model to allow developers to utilise tools specific to their discipline. We believe that co-modelling and co-simulation combined with DSE can be utilised as an early stage development approach to analyse and compare design candidates from different domains.

In the future, a new European research project called INTO-CPS<sup>4</sup> will work on further improving the Crescendo technology. Efforts will include covering requirements for heterogeneous models and realisations of both controllers as well as physical components.

## ACKNOWLEDGMENT

The work presented here is partially supported by the INTO-CPS project funded by the European Commission's Horizon 2020 programme under grant agreement number 664047. Thanks also go to Kompleks Innovation for their collaboration on the mink feeding case study and to Minkpapi A/S for providing the prototype platform. We also acknowledge Nick Battle for giving invaluable feedback on drafts of this paper.

## REFERENCES

- [1] David M. Bevly. *GNSS for Vehicle Control*. Artech House, 1 edition, 2009.
- [2] T. Brezina, Z. Hadas, and J. Vetiska. Using of Co-simulation ADAMS-SIMULINK for development of mechatronic systems. *14th International Conference Mechatronika*, pages 59–64, June 2011.
- [3] Jan F. Broenink and Y. Ni. Model-Driven Robot-Software Design using Integrated Models and Co-Simulation. In J. McAllister and S. Bhattacharyya, editors, *Proceedings of SAMOS XII*, pages 339 – 344, jul 2012.
- [4] Jan F. Broenink, Yunyun Ni, and Marcel A. Groothuis. On model-driven design of robot software using co-simulation. In E. Menegatti, editor, *Proceedings of SIMPAR 2010 Workshops International Conference on Simulation, Modeling, and Programming for Autonomous Robots*, pages 659–668, Darmstadt, Germany, November 2010. TU Darmstadt.
- [5] Martin Peter Christiansen, Morten Larsen, and Rasmus Nyholm Jørgensen. Collaborative model based development of adaptive controller settings for a load-carrying vehicle with changing loads. In Dionysis D. Bochtis and Claus Aage Gørn Sørensen, editors, *CIOSTA XXXV Conference*, July 2013.
- [6] Charbel Fares and Yskandar Hamam. Collision detection for rigid bodies: A state of the art review. *GraphiCon 2005*, 2005.
- [7] Martin A Fischler and Robert C Bolles. Random sample consensus: a paradigm for model fitting with applications to image analysis and automated cartography. *Communications of the ACM*, 24(6):381–395, 1981.
- [8] John Fitzgerald, Peter Gorm Larsen, Paul Mukherjee, Nico Plat, and Marcel Verhoef. *Validated Designs for Object-oriented Systems*. Springer, New York, 2005.
- [9] John Fitzgerald, Peter Gorm Larsen, and Marcel Verhoef, editors. *Collaborative Design for Embedded Systems – Co-modelling and Co-simulation*. Springer, 2014.
- [10] Adam Harris and James M. Conrad. Survey of popular robotics simulators, frameworks, and toolkits. In *2011 Proceedings of IEEE Southeastcon*, pages 243–249. IEEE, March 2011.
- [11] Robots for industrial environments - safety requirements - part 1: Robot. Technical report, The International Organization for Standardization and the International Electrotechnical Commission, 2013.
- [12] Kjeld Jensen, Morten Larsen, Sren H. Nielsen, Leon B. Larsen, Kent S. Olsen, and Rasmus N. Jrgensen. Towards an open software platform for field robots in precision agriculture. *Robotics*, 3(2):207–234, 2014.
- [13] Rasmus Nyholm Jørgensen, Claus G. Sørensen, Helle Frank Jensen, Bent Hindrup Andersen, Erik Fløjgaard Kristensen, Kjeld Jensen, Jørgen Maagaard, and Alastair Persson. FeederAnt2 - An autonomous mobile unit feeding outdoor pigs. In *ASABE Annual International Meeting*, volume 0300. ASABE, 2007.
- [14] Wang Jun, Zhou Zhou, and Du Xiaodong. Design and co-simulation for tomato harvesting robots. In *Control Conference (CCC), 2012 31st Chinese*, pages 5105–5108. IEEE, 2012.
- [15] Manoj Karkee and Brian L. Steward. Study of the open and closed loop characteristics of a tractor and a single axle towed implement system. *Journal of Terramechanics*, 47(6):379–393, December 2010.
- [16] Peter Gorm Larsen, Nick Battle, Miguel Ferreira, John Fitzgerald, Kenneth Lausdahl, and Marcel Verhoef. The Overture Initiative – Integrating Tools for VDM. *SIGSOFT Softw. Eng. Notes*, 35(1):1–6, January 2010.
- [17] Domenico Longo and Giovanni Muscato. Design and Simulation of Two Robotic Systems for Automatic Artichoke Harvesting. *Robotics*, 2(4):217–230, December 2013.
- [18] S. Murata, E. Yoshida, K. Tomita, H. Kurokawa, a. Kamimura, and S. Kokaji. Hardware design of modular robotic system. *Proceedings. 2000 IEEE/RSJ International Conference on Intelligent Robots and Systems (IROS 2000) (Cat. No.00CH37113)*, 3:2210–2217, 2000.
- [19] Yoshisada Nagasaka, Naonobu Umeda, Yutaka Kanetai, Ken Taniwaki, and Yasuhiro Sasaki. Autonomous guidance for rice transplanting using global positioning and gyroscopes. *Computers and Electronics in Agriculture*, 43:223–234, 2004.
- [20] N. Noguchi, K. Ishii, and H. Terao. Development of an Agricultural Mobile Robot using a Geomagnetic Direction Sensor and Image Sensors. *Journal of Agricultural Engineering Research*, 67:1–15, 1997.
- [21] N. Pannaga, N. Ganesh, and R. Gupta. Mechatronics – an introduction to mechatronics. *International Journal of Engineering*, 2(8):128–134, 2013.
- [22] Ken Piece, John Fitzgerald, Carl Gamble, Yunyun Ni, and Jan F. Broenink. Collaborative Modelling and Simulation — Guidelines for Engineering Using the DESTECs Tools and Methods. Technical report, The DESTECs Project (INFO-ICT-248134), September 2012.
- [23] K. G. Pierce, C. J. Gamble, Y. Ni, and J. F. Broenink. Collaborative Modelling and Co-Simulation with DESTECs: A Pilot Study. In *3rd IEEE track on Collaborative Modelling and Simulation, in WETICE 2012*. IEEE-CS, June 2012.
- [24] Morgan Quigley, Ken Conley, Brian Gerkey, Josh Faust, Tully Foote, Jeremy Leibs, Rob Wheeler, and Andrew Y Ng. Ros: an open-source robot operating system. In *ICRA workshop on open source software*, volume 3, page 5, 2009.
- [25] CL Tan, Za Kan, MJ Zeng, and Jing-bin LI. Rfid technology used in cow-feeding robots. *Journal of Agricultural Mechanization Research*, 2:169–171, 2007.
- [26] Feng-lei TIAN and Rong-lei SUN. The Flexible Robot Arm Simulation System Based on ADAMS and Simulink. *Machinery & Electronics*, 10:020, 2006.

<sup>4</sup>This is an acronym for “Integrated Tool Chain for Model-based Design of Cyber-Physical Systems”, see <http://into-cps.au.dk/>.



## 6

---

### **Robotic design choice overview using Co-simulation and Design Space Exploration**

---

The paper presented in this chapter has been submitted to MDPI Robotics

[P22] Martin Peter Christiansen, Peter Gorm Larsen, and Rasmus Nyholm Jørgensen. Robotic Design Choice Overview using Co-simulation and Design Space Exploration. *Robotics*, pages 398–421, October 2015

Submitted to *Robotics*. Pages 1 - 20.

OPEN ACCESS

*Article***Robotic Design Choice Overview using Co-simulation and Design Space Exploration****Martin Peter Christiansen<sup>1,\*</sup>, Peter Gorm Larsen<sup>1</sup> and Rasmus Nyholm Jørgensen<sup>1</sup>**<sup>1</sup> Department of Engineering, Aarhus University, Finlandsgade 22, 8200 Aarhus N, Denmark

\* Author to whom correspondence should be addressed; Email: mpc@eng.au.dk; Tel.: +4540420617

*Version June 16, 2015 submitted to Robotics. Typeset by L<sup>A</sup>T<sub>E</sub>X using class file mdpi.cls*


---

**Abstract:** Rapid robotic system development has created a demand for multi-disciplinary methods and tools to explore and compare design alternatives. In this paper, we present a collaborative modelling technique that combines discrete-event models of controller software with continuous-time models of physical robot components. The proposed co-modelling method utilises Vienna Development Method (VDM) and Matlab for discrete-event modelling and 20-sim for continuous-time modelling. The model-based development of a mobile robot mink feeding system is used to illustrate the collaborative modelling method. Simulations are used to evaluate the robot model output response in relation to operational demands. An example of a load carrying challenge in relation to the feeding robot is presented and a design space is defined with candidate solutions in both the mechanical and software domains. Simulation results are analysed using Design Space Exploration (DSE) that evaluates candidate solutions in relation to preselected optimisation criteria. The result of the analysis provides developers with an overview of the impacts of each solution instance in the chosen design space. Based on this overview of solution impacts the developers can select viable candidates for deployment and testing with the actual robot.

**Keywords:** Animal feeding, Crescendo, Collaborative modelling, Sensor-fusion

---

**1. Introduction**

The general goal an automatic robotic system development is to enable a robot to perform the desired tasks within the context of overall system requirements [1], and modelling and simulation are gradually being adopted as an integral part of the developmental process [2–4].

Modelling enables developers to explore hardware and software solutions before developing the actual component. In conjunction with simulation, it also enables the automatic evaluation of a much larger potential design space compared to a manual trial and error approach. The alternative approach to developing a robotic system involves time-intensive ad-hoc trial-and-error testing to achieve a usable configuration of the physical system. One drawback of this approach is that developers may spend valuable time determining the optimal solution to some aspect of the system, only for such effort to show little impact on the overall desired outcome.

The primary challenge of the modelling and simulation approach is that knowledge of many complementary disciplines such as electrical, mechanical, software, and embedded systems engineering and signal processing is required to determine viable solutions [5–7]. These disciplines have different cultures, tools, and methodologies, which may prove to be an impediment to cross-disciplinary projects. In this paper, we propose a collaborative modelling approach known as co-modelling that enables the combination of models from different disciplines. Co-operative simulations, or co-simulations, allow developers to examine different aspects of a system to explore design alternatives. They utilise models describe the different aspects of the robotic system.

The aim of the present study is the analysis of cross-disciplinary robotic design alternatives using co-simulation. The co-model robot design is based on a mink feeding vehicle used in agricultural farming applications, as illustrated in Figure 1. The co-modelling and co-simulation were accomplished by a combination of the Crescendo technology produced by the European DESTECs FP7 project<sup>1</sup> [8] and a MATLAB extension.

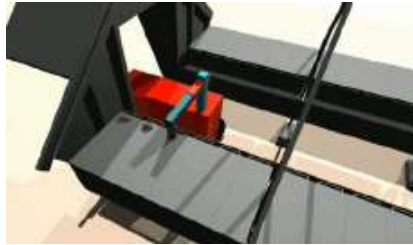


**Figure 1.** Three-dimensional visualisation of a co-simulated load-carrying robot dispensing mink fodder.

The remainder of the paper is organised as follows. Section 2 describes the co-modelling technologies utilised for coupling the Crescendo technology with MATLAB. Section 3 introduces the robotic design challenge of the mink feeding ground vehicle as a system boundary definition consisting of a problem area and modelling case. Section 4 describes the co-modelling of the developed vehicle, design exploration, and evaluated simulation conditions. The domain-specific modelling methods applied to the robot and its environment are documented in Section 5.

---

<sup>1</sup> See <http://destecs.org/>

Section 6 describes the signal processing and control. Section 7 presents the results of the simulations and an overview of the candidate solutions. Section 8 discusses the simulation results and setups that are considered to be capable of ensuring the expected performance under the required conditions. Finally, concluding remarks are made in Section 9.

## 2. Co-modelling Technologies

Co-modelling enables the modelling of system components using different developmental tools as well as facilitating simultaneous co-simulation [9,10]. Co-modelling involves the combination of separate domain specific models to create a complete model of the intended system by collaborative exchange of information between the utilised tools. The exchanged information comprises the simulation parameters, control signals, and system events.

### 2.1. Crescendo technology

The Crescendo technology enables modelling using different specialised tools. It combines the Discrete Event (DE) modelling of a digital controller and the Continuous Time (CT) modelling of the plant/environment for the purpose of co-simulation. The Overture tool and Vienna Development Method (VDM) formalism are used for the DE modelling and the 20-sim tool was used for the CT modelling. The 20-sim tool models multi-disciplinary dynamic systems, such as the combined mechanical, electrical, and hydraulic systems [11]. VDM Real Time (VDM-RT) [12] is the dialect used for the Crescendo co-model, which is capable of describing real-time, asynchronous, object-oriented software systems.

The Crescendo co-simulation engine coordinates the 20-sim and VDM simulations by implementing a protocol for time-step synchronisation between the tools. Crescendo binds the domain models together with a Crescendo contract and is responsible for the exchange of information between the tools. The Crescendo contract contains the parameters and variables that the CT and DE developers require for the development of a combined model. Crescendo has a feature known as Automated Co-model Analysis (ACA) that can be used for the Design Space Exploration (DSE) of a co-model [13]. ACA enables the testing of different system configurations by running all the combinations chosen by a user. The system configurations comprise different combinations of the actuators, controllers, filters, platforms, and sensors of the candidate systems in the design space that the developers intend to explore.

### 2.2. MATLAB extension

We have extended the current Crescendo technology to the two-tool DE co-modelling solution illustrated in Figure 2. The DE side was constructed so that actions sent to the CT side are determined by VDM and the sensory signal processing and sensor-fusion are performed in MATLAB. MATLAB is a well-known for signal processing and sensor fusion [14,15]. VDM utilises MATLAB as an extension to obtain a combined position estimate to input into the VDM controllers.

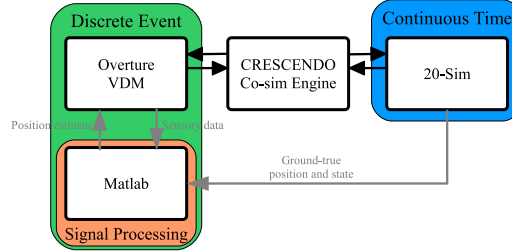


**Figure 2.** The Crescendo technology with a Matlab extension to allow for signal processing development.

84 Providing a ground position and system state reference is a well-known method for evaluating  
 85 sensor-fusion precision [16,17]. The 20-sim model provides these ground-truth position and system  
 86 state values to The MATLAB tool for evaluation of both the signal processing and overall intended  
 87 system response. Because MATLAB is implemented as an extension interface, the time-step  
 88 synchronisation of the overall model is kept intact without the need to change the co-simulation  
 89 engine structure.

### 90 3. System Boundary Definition

#### 91 3.1. Problem area definition

92 Identification tags such as Radio Frequency Identification (RFID) tags have been used for the  
 93 last decade to provide local and global positioning information about a vehicle [18–20]. RFID  
 94 tags with known positions are placed along the vehicle’s path to provide fixed position references  
 95 (landmarks). Using an a priori map of the identification tag locations, the vehicle is able to  
 96 obtain absolute positioning estimates in relation to the soundings. Positioning estimates from  
 97 the identification tags are provided to the vehicle when the tag is within the detection zone  
 98 of the tag reader. Using sensory information from other sensor sources can be used to lower  
 99 the number of RFID tags required. By combining the RFID tag locations with other on-board  
 100 positioning sensors, for example, wheel rotary encoders and an Inertial Measurement Unit (IMU),  
 101 the vehicle can continually update its current position estimate [21]. The allowable distance  
 102 between identification tags is dependent on the required position accuracy and available data  
 103 from other sensor sources.

When a wheel rotary encoder is used to estimate travelled distance, one normally assumes that the estimated effective radius  $R_{ee}$  of the tyre is known a priori. By measuring the tyre rotational speed using a wheel rotary encoder, the vehicle computer can provide an estimate of the tyre speed:

$$u_{wek} = R_{ee}\omega_w \approx R_{ee} \frac{2\pi G_k}{T_k G_n} \quad (1)$$

where  $\omega_w$  is the wheel rotational speed, obtained from the sample time  $T_k$  at the  $k$ th interval, the count value of encoder  $G_k$  at the  $k$ th interval, and encoder count per revolution  $G_n$ . The relative tyre wheel travelled distance can then be calculated using numeric integration.

In agriculture, load-carrying vehicles are used for tasks such as spraying plants and dispensing animal fodder. The change in load affects the weight distribution of the vehicle and consequently tyre compression. A load-carrying robotic vehicle provided with sensory information obtained from tyre-mounted rotary encoders, may over- or under-estimate current vehicle speed and position as a result of its tyre compression. If the effective radius is compressed 0.01 m compared to expected conditions, it would, according to Equation 1 result in an estimate difference of 0.0628 m each revolution, not accounting for other influencing factors.

These estimation problems require cross-disciplinary analyses because multiple factors affect the outcomes and possible solutions can be found in different engineering disciplines. Here, we analyse the estimation problems by modelling a load-carrying robot used for dispensing mink fodder at predetermined locations along rows of cages. Feeding mink is a high precision task compared to other domestic animals in livestock production. The farmer chooses the amount of fodder each cage gets based on personal experience and knowledge about demands for mink gender, age, and race. Based on feedback from mink-farmers, each mink cage, is given a portion of fodder in the range of 80–300 grams. In all cases of mink feeding, the total weight of the vehicle changes gradually throughout the feeding process. With vehicle fodder tanks able to transport loads of 500–2500 kg, a machine would theoretically be able to feed 1500–30 000 cages. Automatically placing the fodder at these specific areas requires an on-board localisation system that is able to determine the current vehicle position. The co-model of the robot is evaluated based on the



**Figure 3.** Robotic Mink Feeding system<sup>1</sup> mounted onto a manually operated vehicle.

required overall system performances obtained using solutions from different disciplines.

### 3.2. System configuration and performance demands

The chosen robot is a four-wheeled vehicle with front-wheel steering and rear-wheel drive equipped with a differential gearing. The mink feeding ground vehicle is able to transport a

<sup>1</sup> Source: Picture of a Minkpapr A/S vehicle solution, Kompleks Innovation.



130 maximum load  $M_{max}$  of 600 kg The robot receives sensory input from a vision system, RFID tag  
 131 reader, IMU, and rotary encoders installed on the back wheels and front wheel kingpins. The  
 132 vision system is used to detect the entrance to the feeding area when the robot still is outside.  
 133 The RFID tags are placed along the rows of mink cages to act as fixed location reference points,  
 134 as illustrated in Figure 4. Fused sensory data are used to determine the current location and  
 135 enable the robot to perform its required actions in the environment. A feeder arm mounted on  
 the robot is used to dispense the fodder on the cages (80 g) at the predetermined locations. When

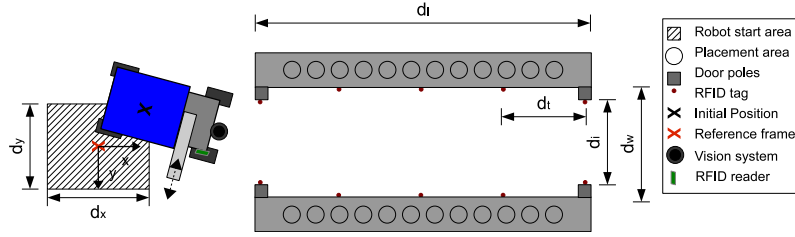


**Figure 4.** Sketch of the load-carrying feeding robot and the mink feeding area.

136 the robot moves into the feeding area, it stops to deploy the feeding arm and then begins the  
 137 feeding procedure.

139 The system performance requirements define what the robot must achieve to be considered  
 140 effective. The system performance required by the project stakeholders includes the following:

- 141 • Maximum vehicle speed of 0.25 m/s (conforming to ISO-10218 [22])
- 142 • No collisions with the surroundings, as laid out in Figure 4.
- 143 • Distance between the RFID tags  $d_t$  should be between 0.3–20 m.
- 144 • Feeding with a precision of  $\pm 0.08$  m inside the placement area.

145 It should be noted that the performance requirements are non-domain-specific and focus on the  
 146 overall performance of the robot. Here, the maximum distance between the RFID tags represents  
 147 the length of the feeding area and sets the limit for the minimum number of tags. The lower limit  
 148 for  $d_t$  is chosen based on the length of the mink cages used in the co-modelling, resulting in one  
 149 RFID tag for each cage.

### 150 3.3. Modelling cases

151 The co-model describes the vehicle and its sensor, actuator, steering controller, feeding system,  
 152 and sensor-fusion components. The goal was to achieve maximum distance between the RFID  
 153 tags without compromising the pre-set system constraints. The question here was whether the  
 154 loading of the vehicle should be accounted for by reducing the maximum compression of the tyre,  
 155 compensated for in the DE controller, or a combination of both approaches. The following DE  
 156 controller conditions were applied:

157 <**Static**> The estimated effective tyre radius was considered to be the mean of the values for  
 158 the unloaded and fully loaded robot. This is based on the assumption that the mean value  
 159 will produce the least overall error in the estimate.

160 <**Pre-calibration**> A pre-measured estimate of the current rear tyre wheel radius in relation to  
 161 the transported load is used in the DE part of the co-model. The estimates of the effective  
 162 radius were obtained through the MATLAB bridge and directly passed from 20-sim with an  
 163 accuracy of  $\pm 0.001$  m.

164 <**Estimator**> The input data obtained by the vision sensor were used to estimate the current  
 165 effective radius before entering the feeding area. This estimate was based on the distance  
 166 travelled between the updates, with an accuracy of  $-0.005$  m.

167 Rather than simulate a single scenario, the test set in Table 1 evaluates the expected  
 168 min-mean-max operational values. The DSE was used to evaluate the configuration solutions in  
 169 Table 1 in different development domains to account for the load-carrying effects. The operational  
 170 values represents the expected range of transported loads as well as the surface-tyre and initial  
 171 robot position conditions. The initial position was of interest in this case because a human operator  
 172 could inaccurately place the robot at its starting point. The models of the tyre radius on the CT  
 173 side are vary between low and fully loaded conditions. The tyre-surface friction is of interest here  
 174 since the vehicle will be stopping to deploy the feeding arm before starting the feeding process.

**Table 1.** Candidate solution sets used for the system evaluation and min-mean-max test set used for the DSE of the feeding robot.

<i>System configurations</i>		<i>Min-mean-max test set</i>		
Rear tyre radius change	Vehicle state estimate	Load mass	Surface-tyre $\mu$ friction	Initial Position $x_{init}, y_{init}, \psi_{init}$
0.001 m	<Static>	1% (6 kg)	0.3	$x_{init} = \{-0.5 \text{ m}, 0 \text{ m}, 0.5 \text{ m}\}$
0.02 m	<Pre-calibration>	50% (300 kg)	0.5	$y_{init} = \{-0.1 \text{ m}, 0 \text{ m}, 0.1 \text{ m}\}$
0.04 m	<Estimator>	100% (600 kg)	0.7	$\psi_{init} = \{-15^\circ, 0^\circ, 15^\circ\}$

#### 175 4. Co-modelling

176 The co-modelling perspective of the robot includes a contract between the DE and CT models  
 177 and the ACA specifications for a DSE using co-simulation. This contract represents the work  
 178 template between the developers, and the ACA specifications are the concrete requirements of the  
 179 stakeholder.

##### 180 4.1. Crescendo contract

181 The Crescendo contract in Table 2 defines the parameters and variables to be exchanged during  
 182 the simulation. The shared design parameters are defined by the **sdp** keyword, the variables  
 183 controlled by the CT side are defined by the **monitored** keyword, and the variables controlled

by the DE side are defined by the **controlled** keyword. The parameters in the contract provide the communication variables that both the DE and CT developers require for the development of a combined model. Compared to reality, these variables are abstractions and only provide information for current co-model development.

**Table 2.** Crescendo contract

	Name	Type	Parameter symbol
<b>sdp</b>	Initial_Position	array	$[x_{init}, y_{init}, \phi_{init}]$
<b>sdp</b>	Surface_Tyre	real	$\mu$
<b>sdp</b>	Load_Mass	real	$m_{L_p}$
<b>sdp</b>	Tag_dist	real	$d_t$
<b>controlled</b>	Speed_out	real	$u_o$
<b>controlled</b>	Steering_Wheel_Angle	real	$\delta_{f_o}$
<b>controlled</b>	Feeder_arm_pos	real	$y_{arm}$
<b>controlled</b>	Feeder_output	real	$p_o$
<b>monitored</b>	Vision	array	$[r_{s_1}, \theta_{s_1}, r_{s_2}, \theta_{s_2}, \theta_{s_e}, d_{s_e}]$
<b>monitored</b>	RFID	array	$[ID, RSSI]$
<b>monitored</b>	IMU	real	$\dot{\psi}_s$
<b>monitored</b>	Encoders_Back	array	$[\omega_{rrs}, \omega_{rls}]$
<b>monitored</b>	Encoder_Front	real	$\delta_{fs}$

In this co-model, the shared design parameters represent the values that developers should explore in terms of effect. Values  $x_{init}$ ,  $y_{init}$ , and  $\phi_{init}$  defines the starting position of the robot in the global coordinate frame, whereas  $m_{L_p}$  and  $\mu$  set the current operational parameters of the robot and its surroundings. Further,  $d_t$  is the factor to be increased while still achieving the system performance goals for each DSE candidate. The controlled variables are the input to the robot movement and the feeding arm. The input to the robot movement is transmitted to the drive motor and front wheel steering actuator, and the feeding arm transmits the desired arm position and current feeding output to the CT model. The monitored variables represent the sensory inputs to the DE side: vision, RFID, IMU, and encoders. In the case of vision, the full image or laser scan is not transmitted for processing; rather the processed input of the detected objects (e.g., the poles in illustrated in Figure 4) are transmitted when they are in view. When inside the feeding area, the vision system instead provides an estimate of vehicle orientation  $\theta_{s_e}$  and distance to the side-wall  $d_{s_e}$ . The IMU is also only represented by a single measurement value  $\dot{\psi}_s$  that is rotated into the global frame, where the actual sensor might contain acceleration and rotation sensors for all three dimensions. The RFID reader provides tag Identification Data (ID) and a Received Signal Strength Indicator (RSSI) value when in range of an RFID tag.

#### 4.2. Automatic co-model analysis

To select the value of parameter  $d_t$  that for the ACA co-simulation, an output cost-function is defined. The result of each co-simulation is evaluated based on the rate of success at placing the fodder at the correct positions between two tags.

$$f_{d_t} = -\frac{b_{suc}^2}{b_{tot}} \quad (2)$$

where  $b_{tot}$  is the total number of placement positions between two RFID-tags and  $b_{suc}$  is the number of successful fodder placements. The output of the cost-function ensures that the largest  $d_t$  with the highest number of successful fodder placements is the minimum for the searchable range. In mathematics, by convention, optimization problems are usually stated in terms of minimization, thus the minus sign. ACA uses the golden section search method [23, Chapter 7] in combination with the cost-function in Equation (2) to determine the best candidate within the design space. Golder-section search assumes that the cost-function is unimodal function, meaning that there is only a single local minimum.

Evaluation of each ACA run co-simulation is performed during the simulation or after the execution, as in post-processing. In-run co-simulation evaluation is based on readily available values such as the CT-simulated robot speed and position in the global coordinate frame. Evaluation of a running co-simulation allows for a direct exit from the execution, instead of having to run an already failed scenario to its end.

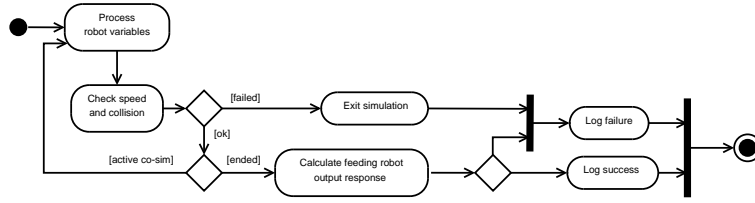


**Figure 5.** Activity diagram showing the evaluation of a co-simulation

The post-processing evaluation of an ACA co-simulation is based on the feeding output of the robot in its surroundings relative to the stakeholder requirements. Evaluating the feeding output requires information about the location of each food placement in the operational environment, and this significantly increases computation. By logging the types of failures that the co-simulation encounters, developers can order and rerun specific scenarios that are found to be relevant.

## 5. CT Modelling

The CT-model describes the sensors, actuators, robot vehicle, environment, and their interactions. The actuator output affects the robot movement and output response, which in turn affects the sensory responses. In the present study, vision and IMU sensors were modelled using known methods [24] that are not described in this paper.

## 228 5.1. Tyre modelling for encoder data

The wheel encoders provide inputs to the DE controller to control the drive speed and estimation of the current position. The data of the wheel encoders are based on rotational data obtained by a

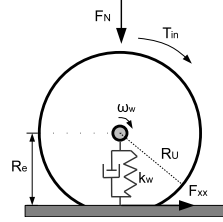


**Figure 6.** Forces in the longitudinal tyre model

dynamic tyre model that takes into consideration the vertical, lateral, and longitudinal dynamics of the tyre. The tyre model describes the rotational changes  $\dot{\omega}_w$  and the effects of the steering along the feed-area sidewall, braking, and wheel-surface conditions. The longitudinal tyre force  $F_{x_w}$  includes the effects of acceleration and braking:

$$J_w \dot{\omega}_w = T_{in} - F_{x_w} R_e \quad (3)$$

where  $J_w$  is the wheel moment of inertia,  $J_w$  is the acceleration or braking torque, and  $R_e$  is the effective rolling radius (a compression of the unloaded radius  $R_U$  based on the applied load  $F_N$ ). Radius  $R_e$  is modelled by a spring-damper system as follows:

$$R_e = R_U - F_N / k_w \quad (4)$$

Each tyre's  $R_e$  value changes dynamically depending on the load forces applied by the robot. The  $k_w$  factor represents the current tyre stiffness applied in the DSE and is based on the expected compression rate. The effect of the acceleration or braking of the tyre is calculated using a longitudinal slip equation and is reflected by the difference between the tyre rotational speed  $\omega_w$  and vehicle speed  $u$

$$s_x = \begin{cases} \frac{R_e \omega_w - u}{u} & \text{if } u > R_e \omega_w, u \neq 0 \\ \frac{R_e \omega_w - u}{R_e \omega_w} & \text{if } u < R_e \omega_w, \omega_w \neq 0 \end{cases} \quad (5)$$

Both empirical and analytical models have been developed to describe the generated lateral and longitudinal tyre forces [25–28]. In the present implementation of the tyre, the Fiala tyre model was used to calculate the resultant lateral and longitudinal tyre forces. This tyre model combines the lateral and longitudinal slips in the total slip  $s_{tot}$  of the tyre that is used to calculate the total tyre force  $F_w$ .

$$s_{tot} = \sqrt{s_x^2 + s_y^2} \quad (6)$$

Here,  $F_w$  includes the lateral and longitudinal tyre forces and is calculated using a parabolic pressure distribution, as follows:

$$\begin{bmatrix} F_{xw} \\ F_{yw} \end{bmatrix} = \begin{bmatrix} s_x \\ s_y \end{bmatrix} \frac{F_w}{s_{tot}}, F_w = \begin{cases} \mu F_N \left( 3p_w s_{tot} - \frac{(3p_w s_{tot})^2}{3} + \frac{(3p_w s_{tot})^3}{27} \right) & \text{if } s_{tot} < s_{max} \\ \mu F_N & \text{if } s_{tot} \geq s_{max} \end{cases} \quad (7)$$

where  $s_{max}$  is the maximum total tyre slip calculated using the current surface-tyre friction coefficient  $\mu$  and tyre cornering stiffness  $C_c$ :

$$s_{max} = \frac{1}{p_w} = \frac{3\mu F_N}{C_c} \quad (8)$$

## 5.2. Vehicle body dynamics

The generated tyre forces interact with the robot to produce the output response in the environment. To take the front steer angle into consideration, the CT-model rotates the front tyre forces into the coordinate system of the robot vehicle.

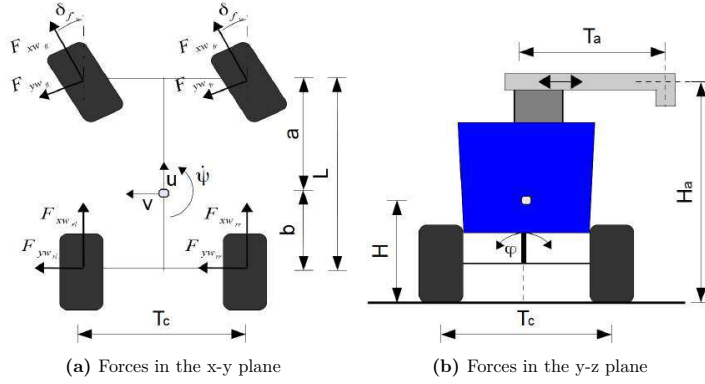


**Figure 7.** Free-body diagrams of the robot in the x-y and y-z planes

Based on the trigonometric relationships illustrated in Figure 7a, the steer angle was transformed using the rotation matrix at the front of the left-hand side of Equation (9) [29]. The robot utilises Trapezoid- steering, which produces equal steering angles on the right and left sides, making the transformation the same for both sides.

$$\begin{bmatrix} F_{xlf} \\ F_{ylf} \end{bmatrix} = \begin{bmatrix} \cos(\delta_f) & -\sin(\delta_f) \\ \sin(\delta_f) & \cos(\delta_f) \end{bmatrix} \begin{bmatrix} F_{xwlf} \\ F_{ywlf} \end{bmatrix} \quad (9)$$

The CT side models the dynamic yaw  $\psi$ , pitch  $\phi$ , lateral  $u$  and longitudinal  $v$  motion responses of the robot vehicle. The yaw motion is modelled by Equation (10). Variables  $a$  and  $b$  are respectively

the longitudinal distances from the front and rear wheels to the CG,  $I_{zz}$  is the yaw moment of inertia, and  $T_c$  is the tyre base track width.

$$I_{zz}\ddot{\phi} = a(F_{yfl} + F_{yrf}) - b(F_{yrl} + F_{yrr}) + \frac{T_c}{2}(F_{xlf} - F_{xrf} + F_{xlr} - F_{xrr}) \quad (10)$$

Similarly, the roll motion of the robot is expressed by the following equation (11), where  $K_r$  and  $C_r$  represent the combined rotational spring-damper based on the tyre spring-damper values.

$$I_{xx}\ddot{\psi} = -(H \sum F_y + (K_r - MgH)\psi + C_r\dot{\psi}) \quad (11)$$

Here,  $\sum F_y$  is the sum of the forces in the longitudinal direction,  $H$  is the current height of the CG above the ground,  $M$  is the current total mass of the robot and load, and  $g$  is gravitational acceleration.

The load shift from the right to the left of the robot is assumed to be proportional to the current pitch angle. The longitudinal motion output of the robot is given by

$$\sum F_y = M(\dot{u} - v\dot{\phi}) \quad (12)$$

The lateral motion of the feeder robot is determined by the sum of the lateral forces, roll acceleration, and longitudinal speed:

$$\sum F_x = M(\dot{v} + u\dot{\phi} + H\ddot{\psi}) \quad (13)$$

Roll angle  $\theta$ ,  $H$ ,  $a$ , and  $b$  were treated as in each simulation because the expected changes were assumed to be negligible and therefore only updated for each DSE case. The value of  $M$  was used to calculate the current values of  $a$  and  $b$ , which define the CG position:

$$M = M_{vehicle} + M_{lmax}m_{Lp} \quad (14)$$

$$a = a_u + \eta_x M_{lmax}m_{Lp} \quad (15)$$

where  $a_u$  and  $b_u$  are respectively the longitudinal distances of the front and rear wheels of the unloaded robot from its CG, and  $\eta_x$  is a constant because the change in the CG was assumed to be linear within the load limits  $[0, M_{lmax}]$ . Likewise,  $M$ ,  $a$ ,  $b$ , and the tyre spring values were used to calculate  $\psi$  and  $H$ , with  $H_U$  corresponding to the unloaded CG height.

### 5.3. RFID tag reader

An RFID reader has a zone in three dimensional space (the detection zone) in which a specific type of tag is detectable [30]. To model the detection zone, an ellipsoid with its centre at  $(x_{dz}, y_{dz}, z_{dz})$  and a semi-principal axis of length  $(r_1, r_2, r_3)$  was used to compare the RFID tag positions  $(x_{tg}, y_{tg}, z_{tg})$ , which were rotated into the coordinate frame of the reader to determine whether the tag was within range. An RFID reader is able to read a tag if the following equation (16) is satisfied.

$$\left( \frac{(x_{rf} - x_{tg})^2}{r_1^2} + \frac{(y_{rf} - y_{tg})^2}{r_2^2} + \frac{(z_{rf} - z_{tg})^2}{r_3^2} \right) \leq 1 \quad (16)$$

The actual distance  $d_{rf}$  is calculated using the global coordinates of the RFID reader  $(x_{rf}, y_{rf}, z_{rf})$  and the RFID tag.

$$d_{rf} = \sqrt{(x_{rf} - x_{tg})^2 + (y_{rf} - y_{tg})^2 + (z_{rf} - z_{tg})^2} \quad (17)$$

The mathematical relationship between the RSSI value and actual distance  $d_{rf}$  is as follows:

$$RSSI(d_{rf}) = \begin{cases} \frac{K_{rf}}{d_{rf}} & \text{if } \frac{K_{rf}}{d_{rf}} \geq RSSI_{min} \\ RSSI_{min} & \text{if } \frac{K_{rf}}{d_{rf}} < RSSI_{min} \end{cases} \quad (18)$$

where  $RSSI_{min}$  is the minimum value that the reader outputs to the DE side, and  $K_{rf}$  is a constant in the piece-wise function.

#### 5.4. CT setup

The CT parameters of the co-simulations for the intended DSE are documented in Table 3. In

**Table 3.** CT-parameters used for the co-simulations.

Sub-system	Parameter Values
Environment	$d_l = 20$ m, $d_w = 1.5$ m, $d_i = 1.34$ m, $d_x = 1$ m, $d_y = 0.2$ m
Vehicle body	$L = 2.1$ m, $a_U = 1.2$ m, $b_U = 0.9$ m, $H_U = 0.55$ m, $T_a = 0.65$ m, $T_c = 0.74$ m, $H_a = 1.2$ m, $M_{vehicle} = 800$ kg, $M_{I_{max}} = 600$ kg, $\eta_x = 5.83 \cdot 10^{-4} \frac{m}{kg}$ , $\eta_y = 1.33 \cdot 10^{-4} \frac{m}{kg}$ , $R_U = 0.3$ m, $k_{w,0.04} = 127250 \frac{N}{m}$ , $k_{w,0.02} = 254500 \frac{N}{m}$ , $k_{w,0.001} = 3100000 \frac{N}{m}$
Sensors	$RSSI_{min} = 4$ , $K_{rf} = 0.12$ m, $r_1 = 0.16$ m, $r_2 = r_3 = 0.12$ m Encoder-resolution = 13 bit, $r_{max} = 5$ m, $r_{min} = 0.01$ m, $r_\sigma = 0.005$ m $ \theta_{max}  = \frac{\pi}{2}$ , $\theta_\sigma = 0.5^\circ$

the co-simulation, the CT side utilised a variable step-size Ordinary Differential Equation (ODE) solver based on the Dormand–Prince method, a member of the Runge–Kutta family of ODE solvers. The ODE solver runs with a maximum step size of 1 kHz.

## 6. DE Modelling

### 6.1. Control

The robot controller consists of a steering controller that can follow a pre-determined path, and the feeding system is intended to place food at pre-selected positions. The steering controller steers the robot along the predetermined path, which is defined as a sequence of waypoints, utilising the modal mode concept illustrated in Figure 8. The current modal controller mode is dependent on movement inside or outside the feeding area.

The current waypoint determines the current mode and when the feeding arm is deployed.



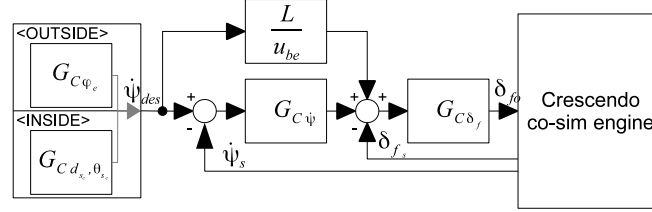


**Figure 8.** Block diagram of the modal steering controller

The feedforward response is based on the kinematic bicycle model where  $L$  is the length of the wheelbase and the estimated drive speed  $u_{be}$  by the rear wheels of the robot. The drive speed of the robot at time interval  $k$  is calculated as:

$$u_{be_k} = \frac{R_{ee} (\omega_{rl_s} + \omega_{rr_s})}{2} \quad (19)$$

where  $\omega_{rl_s}$  and  $\omega_{rr_s}$  are the sensory inputs of the left and right wheel encoders respectively.

When the robot is moving into and out of the feeding area, the estimated heading error  $\psi_e$  is the chosen steering concept. Inside the mink farm house, the robot needs to move along the cages in straight lines and ensure that the feeding arms are held straight over the cages. Correct operation is ensured by maintaining a fixed distance from and orientation to the sides of the mink cages. The control law employed by [31,32] was chosen for inside operation.

## 6.2. Sensor fusion

The idea of sensor fusion is that more accurate estimates of a physical phenomenon can be obtained by combining different sensor-data sources [33]. The combined sensor data can better accommodate uncertainty and noise in measurements [34]. The sensor fusion solution adopted in this study uses an Extended kalman filter (EKF) [24] to estimate the current position of the robot. The process is represented by the following velocity motion model:

$$f(\hat{x}_{k-1}, \mu_k, 0) = \begin{bmatrix} x_k \\ y_k \\ \psi_k \end{bmatrix} = \begin{bmatrix} x_{k-1} \\ y_{k-1} \\ \psi_{k-1} \end{bmatrix} + \begin{bmatrix} -\frac{u_{e_k}}{\dot{\psi}_{s_k}} (\sin(\psi_{k-1}) - \sin(\psi_{k-1} + \dot{\psi}_{s_k} T_k)) \\ \frac{u_{e_k}}{\dot{\psi}_{s_k}} (\cos(\psi_{k-1}) - \cos(\psi_{k-1} + \dot{\psi}_{s_k} T_k)) \\ \dot{\psi}_{s_k} T_k \end{bmatrix} \quad (20)$$

The process input  $\mu_k$  at interval  $k$  in time is used to predict the next state and is based on the monitored variables  $\dot{\phi}_s$ . Variables  $\omega_{rr_s}$  and  $\omega_{rl_s}$  obtained from the Crescendo contract. The value determined from  $\dot{\psi}_s$  is passed directly to the EKF and represents the current  $\psi_k$ .  $\omega_{rr_s}$  and  $\omega_{rl_s}$  represent the back wheel encoder measurements used to estimate the current robot speed:

$$u_{e_k} = \frac{R_{ee} (\omega_{rl_s} + \omega_{rr_s})}{2} \left( \sqrt{1 + \frac{4L^2 (\omega_{rl_s} - \omega_{rr_s})^2}{T_c^2 (\omega_{rl_s} + \omega_{rr_s})^2}} \right) \quad (21)$$

where  $R_{ee}$  is the estimated effective tyre radius used by the DE side, and  $L$  and  $T_c$  are respectively the length and width of the robot wheelbase. The square root part of Equation (21) is used to transpose the measurements to the chosen localization reference point.

The EKF utilises an event-based correction stage that is dependent on the inputs from the vision system and RFID. The vision system provides updates when the door poles of the entrance and exit are in view and compares them against a pole landmark map. The chosen landmark coordinates  $(m_{x,j}, m_{y,j})$  are converted into polar coordinates  $(r, \theta)$  to allow for direct comparison with the sensor input:

$$h_{vision_{out}}(x_{k,j}, 0) = \begin{bmatrix} r_{k,j} \\ \theta_{k,j} \end{bmatrix} = \begin{bmatrix} \sqrt{(m_{x,j} - x_k)^2 + (m_{y,j} - y_k)^2} \\ \arctan2(m_{y,j} - y_k, m_{x,j} - x_k) - \psi_k \end{bmatrix} \quad (22)$$

where  $(m_{x,j}, m_{y,j})$  is the position of the door-pole in the local map and  $(x_k, y_k, \psi_k)$  is the estimated position of the robot.

When the robot is moving inside the feeding area the vision input can be used to update the vehicle orientation and distance to the side wall [35].

$$h_{vision_{in}}(x_{k,j}, 0) = \begin{bmatrix} d_m \\ \theta_m \end{bmatrix} = \begin{bmatrix} \frac{A_m y_k + B_m x_k + C_m}{\sqrt{A_m^2 + B_m^2}} \\ \arctan2(A_m, B_m) - \psi_k \end{bmatrix} \quad (23)$$

where  $A_m$ ,  $B_m$  and  $C_m$  are the parameters for the general form of the line equation representing the mapped position of the side wall. The sensory update does not provide the robot with information about its current position along the side wall and, therefore, position correction is needed.

The positions of the RFID tags can also be seen as points along the sidewall  $(m_{x,i}, m_{y,i})$ . When the RFID tag reader first detects the tag we can use this to provide a position estimate  $(\Delta x_{e,i}, \Delta y_{e,i})$  relative to this tag by combining the detection event with input from the vision sensor. In these co-modelling scenarios, we assume it to be at the centre of the detection zone (i.e. at zero), making the relative position measurement output correspond the intersection point between the line (sidewall) and ellipse (detection zone). The landmark related to the RFID tag is then:

$$h_{rfid}(x_{k,j}, 0) = \begin{bmatrix} \Delta x_{k,i} \\ \Delta y_{k,i} \end{bmatrix} = \begin{bmatrix} m_{x,i} \cos(-\psi_k) - m_{y,i} \sin(-\psi_k) - x_k \\ m_{x,i} \sin(-\psi_k) + m_{y,i} \cos(-\psi_k) - y_k \end{bmatrix} \quad (24)$$

The Jacobian matrices utilised in the EKF localisation method is not presented in this paper, but can be calculated based on Equations (20), (22), (24) and (23).

## 7. Results

The result of the ACA is illustrated in Figure 9 using boxplots. In each boxplot, the central line marks the median, the edges of the box are the 25th and 75th percentiles and the whiskers marks to the two most extreme data points. A total of 12028 co-simulations was run, for the 2187 scenarios in the min-mean-max test set from Table 1. Each system configurations boxplot, represents the determined maximum RFID  $d_t$  distance values for each scenario.

## 8. Discussion

The results provide an overview of the candidate system configurations based on the estimated RFID tag distance. Developers can use the candidate overview to select configurations for testing

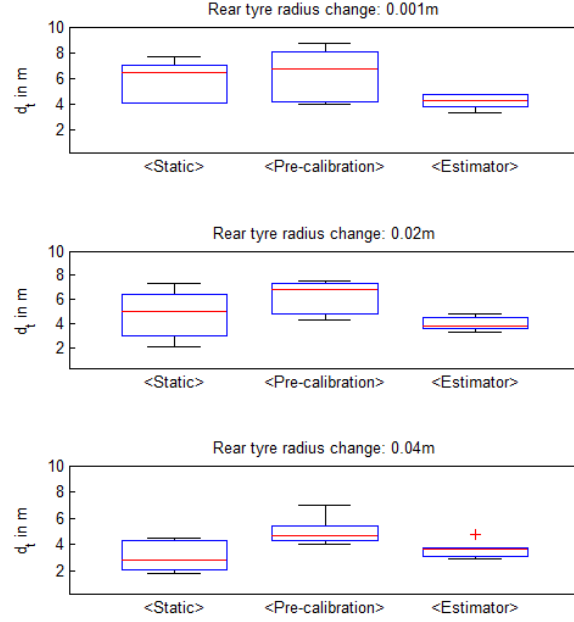


**Figure 9.** Result of the ACA run for the feeding farming co-model in terms of determined  $d_t$ , for the nine different system configurations in Table 1.

on the an actual platform. The intention here is to provide the stakeholders in the project with an overview of the different candidate solutions.

From the box plots, it can be seen that <Pre-calibration> method provides the best overall results for all tyre solutions. This is to be expected since the value  $R_{ee}$  used matches reality with a high degree of accuracy. The candidate with the best results in terms of largest overall  $d_t$  for all co-simulation cases is not necessarily the one that will be chosen for implementation on the actual robot. Factors such as material, development, implementation, and maintenance costs affect the final configuration selection. The 0.001 m tyre compression solution requires adjustment by an operator before start-up. The pre-calibrated solution must be updated periodically to account for changes in the robot setup. The vision solution is calibrated for a specific set of farm configurations and requires adjustments for new conditions. Nevertheless, this overview provides a means of evaluating the external costs with respect to the expected distance between the RFID tag and affords a more educated configuration selection.

Based on the co-simulation result approximately 300 hours are required to perform the analysis on the actual platform, excluding the time spent fixing the starting position and that taken up by mistakes during the test. Note, that the co-model can be reused to explore other aspects of

307 this robotic system. One could, for example, extend the co-model with another feeding arm to  
 308 provide feeding capabilities on both sides and redo a similar design analysis. The time saved by the  
 309 co-modelling and ACA could be invested in other areas of the project. The overview obtained by  
 310 ACA does not guarantee optimal solutions, but it does facilitate the analysis of multiple candidate  
 311 solutions.

312 A similar analysis could also be completely performed using MATLAB or a comparable tool.  
 313 However, developers would need to understand and work collaboratively using a single tool,  
 314 without the advantages of co-modelling and co-simulation using multiple domain-specific tools.

### 315 8.1. Related work

316 In Crescendo technology, DSE is used to select viable candidate sensor positions on an R2-G2P  
 317 line-following robot with a fixed controller setup [36]. Co-simulations performed using other  
 318 tools apart from Crescendo have also been documented. For example, the MODELISAR [37]  
 319 project developed the Functional Mock-up Interface, which enables co-simulation and model  
 320 exchange between different domain-specific simulation frameworks. The standard FMI can support  
 321 MATLAB/Simulink, Modelica, Python, and C/C++, among other tools.

322 Feeding robots used in animal husbandry have also been developed and documented. In [38],  
 323 a static feeding system was used in combination with an RFID reader to dispense food to cows  
 324 with the aid of an attached RFID tag.

325 A mobile feeding platform was also used for outdoor piglet feeding in [39]. The pig-feeding  
 326 robot was used to influence the behavioural pattern of the piglets to facilitate manure collection  
 327 by daily changing the feeding position in the field.

## 328 9. Concluding remarks

329 The development of a robotic system that conforms to overall system requirements is essential.  
 330 In this paper, we described the concept of co-modelling and co-simulation as an approach to robot  
 331 design. We also showed how co-simulation using DSE affords a cross-disciplinary overview of design  
 332 candidates for a proposed robot. This was exemplified by the case study of a load-carrying robot  
 333 for dispensing fodder. The cross-disciplinary DSE was used to determine the maximum distance  
 334 between the RFID tags for each design candidate. An alternative trial and error approach to  
 335 determining the best design candidate would normally require xxx hours.

336 The co-modelling and co-simulation of the feeding robot was used to illustrate tool-decoupled  
 337 development involving dynamic modelling, control, and signal processing. Overture, 20-sim,  
 338 and MATLAB were all used to create a complete co-model of the robot in the proposed design  
 339 approach, thereby allowing multi-disciplinary developers to utilise tools specific to their respective  
 340 disciplines. The effects of the carried load, surface conditions, and safety considerations were  
 341 considered in evaluating the different candidate designs in this study. It is our belief that the  
 342 combination of co-modelling and co-simulation with DSE can be used as a part of the development  
 343 to analyse and compare design candidates in different domains.

### Acknowledgements

The financial support of this study given by the Danish Ministry of Food, Agriculture, and Fisheries is gratefully acknowledged. The work presented here is partially supported by the INTO-CPS project funded by the European Commission's Horizon 2020 programme under grant agreement number 664047. Thanks also go to Kompleks Innovation for their collaboration on the mink feeding case study. We also acknowledge Morten Larsen for giving invaluable feedback on drafts of this paper.

### Conflict of Interest

The authors declare no conflict of interest.

### References

1. Sørensen, C.; Jørgensen, R.; Maagaard, J.; Bertelsen, K.; Dalgaard, L.; Nørremark, M. Conceptual and user-centric design guidelines for a plant nursing robot. *Biosystems Engineering* **2010**, *105*, 119–129.
2. Harris, A.; Conrad, J.M. Survey of popular robotics simulators, frameworks, and toolkits. 2011 Proceedings of IEEE Southeastcon. IEEE, 2011, pp. 243–249.
3. Staranowicz, A.; Mariottini, G.L. A survey and comparison of commercial and open-source robotic simulator software. *Proceedings of the 4th International Conference on Pervasive Technologies Related to Assistive Environments - PETRA '11* **2011**, pp. 121–128.
4. Longo, D.; Muscato, G. Design and Simulation of Two Robotic Systems for Automatic Artichoke Harvesting. *Robotics* **2013**, *2*, 217–230.
5. Murata, S.; Yoshida, E.; Tomita, K.; Kurokawa, H.; Kamimura, a.; Kokaji, S. Hardware design of modular robotic system. *Proceedings. 2000 IEEE/RSJ International Conference on Intelligent Robots and Systems (IROS 2000) (Cat. No.00CH37113)* **2000**, *3*, 2210–2217.
6. Baheti, R.; Gill, H. Cyber-Physical Systems. In *The Impact of Control Technology*; Samad, T.; Annaswamy, A., Eds.; IEEE Control Society, 2011; pp. 161–166. Available at [www.ieeecss.org](http://www.ieeecss.org).
7. Pannaga, N.; Ganesh, N.; Gupta, R. Mechatronics – An Introduction to Mechatronics. *International Journal of Engineering* **2013**, *2*, 128–134.
8. Fitzgerald, J.; Larsen, P.G.; Verhoef, M., Eds. *Collaborative Design for Embedded Systems – Co-modelling and Co-simulation*; Springer, 2014.
9. Nicolescu, G.; Boucheneb, H.; Gheorghe, L.; Bouchhima, F. Methodology for Efficient Design of Continuous / Discrete-Events Co-Simulation Tools. Proceedings of the 2007 Western Multiconference on Computer Simulation WMC 2007, San Diego; Anderson, J.; Huntsinger, R., Eds.; SCS, SCS, San Diego: San Diego, 2007.
10. Broenink, J.F.; Larsen, P.G.; Verhoef, M.; Kleijn, C.; Jovanovic, D.; Pierce, K.; F., W. Design Support and Tooling for Dependable Embedded Control Software. Proceedings of Serene 2010 International Workshop on Software Engineering for Resilient Systems. ACM, 2010, pp. 77–82.

- 382 11. Kleijn, C. Modelling and Simulation of Fluid Power Systems with 20-sim. *Intl. Journal of*  
383 *Fluid Power* **2006**, 7.
- 384 12. Verhoef, M.; Larsen, P.G. Enhancing VDM++ for Modeling Distributed Embedded  
385 Real-time Systems. Technical Report (to appear), Radboud University Nijmegen, 2006.  
386 A preliminary version of this report is available on-line at [http://www.cs.ru.nl/~marcelv/](http://www.cs.ru.nl/~marcelv/vdm/)  
387 [vdm/](http://www.cs.ru.nl/~marcelv/vdm/).
- 388 13. Piece, K.; Fitzgerald, J.; Gamble, C.; Ni, Y.; Broenink, J.F. Collaborative Modelling  
389 and Simulation — Guidelines for Engineering Using the DESTECs Tools and Methods.  
390 Technical report, The DESTECs Project (INFSO-ICT-248134), 2012.
- 391 14. Kim, J.; Kim, Y.; Kim, S. An accurate localization for mobile robot using extended Kalman  
392 filter and sensor fusion. *2008 IEEE International Joint Conference on Neural Networks*  
393 *(IEEE World Congress on Computational Intelligence)* **2008**, pp. 2928–2933.
- 394 15. Raol, J.R. *Multi-Sensor Data Fusion with MATLAB*, 1 ed.; CRC Press, 2009; p. 568.
- 395 16. Guivant, J.; Nebot, E.; Whyte, H.D. Simultaneous Localization and Map Building  
396 Using Natural features in Outdoor Environments. *Intelligent Autonomous Systems* **2000**,  
397 6, 581—586.
- 398 17. Wulf, O.; Nuchter, A.; Hertzberg, J.; Wagner, B. Ground truth evaluation of large urban  
399 6D SLAM. *2007 IEEE/RSJ International Conference on Intelligent Robots and Systems*  
400 **2007**, pp. 650–657.
- 401 18. Lin, H.h.; Tsai, C.c.; Chang, H.y. Global Posture Estimation of a Tour-guide Robot using  
402 REID and Laser Scanning Measurements **2007**. pp. 483–488.
- 403 19. Choi, B.s.; Lee, J.j. Mobile Robot Localization in Indoor Environment **2009**. pp.  
404 2039–2044.
- 405 20. Zhou, J.; Shi, J. A comprehensive multi-factor analysis on RFID localization capability.  
406 *Advanced Engineering Informatics* **2011**, 25, 32–40.
- 407 21. Marín, L.; Vallés, M.; Soriano, A.; Valera, A.; Albertos, P. Multi sensor fusion framework for  
408 indoor-outdoor localization of limited resource mobile robots. *Sensors (Basel, Switzerland)*  
409 **2013**, 13, 14133–60.
- 410 22. 2, I.S. Robots for industrial environments - Safety requirements - Part 1: Robot.  
411 Technical report, The International Organization for Standardization and the International  
412 Electrotechnical Commission, 2013.
- 413 23. Chong, E.K.; Zak, S.H. *An introduction to optimization*, 3 ed.; John Wiley & Sons, 2008;  
414 p. 608.
- 415 24. Thrun, S.; Burgard, W.; Fox, D. *Probabilistic robotics*; MIT press, 2005.
- 416 25. Dugoff, H.; Fancher, P.S.; SEGEL, L. TIRE PERFORMANCE CHARACTERISTICS  
417 AFFECTING VEHICLE RESPONSE TO STEERING AND BRAKING CONTROL  
418 INPUTS. Technical report, 1969.
- 419 26. Bakker, E.; Pacejka, H.B.; Lidner, L. A New Tire Model with an Application in Vehicle  
420 Dynamics Studies. Technical report, 1989.
- 421 27. Pacejka, H.B.; Bakker, E. Shear Force Development by Pneumatic Tyres in Steady State  
422 Conditions: A Review of Modelling Aspects. *Vehicle System Dynamics* **1991**, 20, 121–175.

- 423 28. Pacejka, H.B.; Bakker, E. THE MAGIC FORMULA TYRE MODEL. *Vehicle System*  
424 *Dynamics* **1992**, *21*, 1–18.
- 425 29. Bevy, D.M. *GNSS for Vehicle Control*, 1 ed.; Artech House, 2009; p. 247.
- 426 30. Marrocco, G.; Di Giampaolo, E.; Aliberti, R. Estimation of UHF RFID Reading Regions  
427 in Real Environments. *IEEE Antennas and Propagation Magazine* **2009**, *51*, 44–57.
- 428 31. Noguchi, N.; Ishii, K.; Terao, H. Development of an Agricultural Mobile Robot using a  
429 Geomagnetic Direction Sensor and Image Sensors. *Journal of Agricultural Engineering*  
430 *Research* **1997**, *67*, 1–15.
- 431 32. Nagasaka, Y.; Umeda, N.; Kanetai, Y.; Taniwaki, K.; Sasaki, Y. Autonomous guidance for  
432 rice transplanting using global positioning and gyroscopes. *Computers and Electronics in*  
433 *Agriculture* **2004**, *43*, 223–234.
- 434 33. Hall, D.; Llinas, J. An introduction to multisensor data fusion. *Proceedings of the IEEE*  
435 **1997**, *85*, 6–23.
- 436 34. Thrun, S. Is robotics going statistics? The field of probabilistic robotics. *Communications*  
437 *of the ACM* **2001**, pp. 1–8.
- 438 35. Hansen, S.; Bayramoglu, E.; Andersen, J.C.; Ravn, O.; Andersen, N.; Poulsen, N.K.  
439 Orchard navigation using derivative free Kalman filtering. American Control Conference  
440 (ACC), 2011. IEEE, 2011, pp. 4679–4684.
- 441 36. Pierce, K.G.; Gamble, C.J.; Ni, Y.; Broenink, J.F. Collaborative Modelling and  
442 Co-Simulation with DESTECs: A Pilot Study. 3rd IEEE track on Collaborative Modelling  
443 and Simulation, in WETICE 2012. IEEE-CS, 2012.
- 444 37. Abel, A.; Blochwitz, T.; Eichberger, A.; Hamann, P.; Rein, U. Functional Mock-up Interface  
445 in Mechatronic Gearshift Simulation for Commercial Vehicles. 9th International Modelica  
446 Conference. Munich, 2012.
- 447 38. Tan, C.; Kan, Z.; Zeng, M.; LI, J.b. RFID technology used in cow-feeding robots. *Journal*  
448 *of Agricultural Mechanization Research* **2007**, *2*, 169–171.
- 449 39. Jørgensen, R.N.; Sørensen, C.G.; Jensen, H.F.; Andersen, B.H.; Kristensen, E.F.; Jensen,  
450 K.; Maagaard, J.; Persson, A. FeederAnt2 - An autonomous mobile unit feeding outdoor  
451 pigs. ASABE Annual International Meeting. ASABE, 2007, 0300.

452 © June 16, 2015 by the authors; submitted to *Robotics* for possible open access  
453 publication under the terms and conditions of the Creative Commons Attribution license  
454 <http://creativecommons.org/licenses/by/4.0/>.